DEVELOPMENT OF A METHODOLOGY FOR THE QUANTIFICATION OF REAEROSOLIZATION OF A BIOLOGICAL CONTAMINATE SURROGATE PARTICLE FROM MILITARY UNIFORM FABRIC

THESIS

George D. Cooksey, Capt, USAF, BSC

AFIT-ENV-MS-22-M-187

DEPARTMENT OF THE AIR FORCE
AIR UNIVERSITY
AIR FORCE INSTITUTE OF TECHNOLOGY

Wright-Patterson Air Force Base, Ohio

AFIT-ENV-MS-22-M-187

DEVELOPMENT OF A METHODOLOGY FOR THE QUANTIFICATION OF REAEROSOLIZATION OF A BIOLOGICAL CONTAMINATE SURROGATE PARTICLE FROM MILITARY UNIFORM FABRIC

THESIS

Presented to the Faculty

Department of Systems Engineering and Management

Graduate School of Engineering and Management

Air Force Institute of Technology

Air University

Air Education and Training Command

In Partial Fulfillment of the Requirements for the

Degree of Master of Science in Industrial Hygiene

George D. Cooksey, BS

Captain, USAF, BSC

February 2022

DEVELOPMENT OF A METHODOLOGY FOR THE QUANTIFICATION OF REAEROSOLIZATION OF A BIOLOGICAL CONTAMINATE SURROGATE PARTICLE FROM MILITARY UNIFORM FABRIC

George D. Cooksey, BS

Captain, USAF, BSC

Committee Membership:

Dr. Jeremy Slagley
Chair

Lt Col Casey Cooper, PhD
Member

Dr. Douglas Lewis
Member

Abstract

During a mass casualty medical evacuation after a bioaerosol attack, a decontamination method is needed that is effective at both decontamination and preventing the secondary hazard of biological particles reaerosolizing from contaminated clothing. However, neither the efficacy of current decontamination methods nor the risk of biological particle reaerosolization is significantly explored in existing literature. The goals of this thesis were to develop a repeatable methodology to quantify the reaerosolization of a biological contaminate off Airman Battle Uniform (ABU) fabric swatches, and to test the efficacy of one decontamination method (high-volume, low-pressure water) using 1 μm polystyrene latex (PSL) spheres as a surrogate. Four major methodologies were developed: Contamination using a Collison Nebulizer; Reaerosolization using a laboratory mixer and collection using an air pump and inhalable air sampler with a polyvinyl chloride (PVC) filter; Decontamination using a gravity-fed water shower; and Quantification using ultraviolet (UV) microscopy techniques via both human eye and computer techniques. All results for control samples showed little to no presence of PSL sphere-like particles, while the experimental trials showed a ~73% reduction in reaerosolization before and after decontamination via water, at the 99% confidence level (p-value = 0.0081), along with a change in deposition patterns from aerosol-like (before decontamination) to droplet-like (after decontamination).

Acknowledgments

I would like to thank my research advisor, Dr. Jeremy Slagley, for the countless hours he has spent brainstorming, advising, editing, and guiding my work, and for the flexibility he has shown as the project developed from one target to another. I would also like to thank my committee members, Lt Col Casey Cooper and Dr. Douglas Lewis, for the feedback and guidance they have provided for both my methodology and my literature review. I would also like to thank all of members of the 711 HPW, AFIT, AFRL, and WPAFB community who took the time to lend their expertise on topics I was unfamiliar with. Lastly, I would like to thank my teammates, especially Ms. Alisha Helm, for all of the extra hours they spent making completing this thesis on time possible.

George D. Cooksey

Table of Contents

Page
Abstract v
Acknowledgments vi
Table of Contents vii
List of Figures ix
List of Tables xi
List of Equations xiii
I. Introduction 1
II. Literature Review 5
Chapter Overview 5
Bacillus anthracis (Anthrax) 5
Polystyrene Latex (PSL) Spheres as a Biological Surrogate 9
Reaerosolization of Biological Particles 13
U.S. Military Doctrine Regarding Biological Decontamination 15
Vibration Patterns During Medical Evacuations 20
Chapter Summary 23
III. Methodology 24
Chapter Overview 24
Experimental Design 24
Contaminating Fabric Swatches with Biological Surrogate 25
Reaerosolization of Biological Surrogate from Contaminated Fabric 32
Decontamination Method for Removing the Biological Surrogate from the Contaminated Fabric 36
Microscopy Techniques to Quantify 1 µm PSL Sphere Contamination 38
Experimental Sample Swatch Selection 51
Summary of Methodology 53
IV. Results 54
Chapter Overview 54
Contamination 54
Uncontaminated (Clean-Series) Results 56
Contaminated (Dirty-Series) Results 59
Decontaminated Clean (Water-Series) Results 61
Decontaminated Dirty (Post-decontamination-Series) Results 64

Statistical Comparison of Trials 67
Summary of Results 78
V. Conclusions and Recommendations 79
Chapter Overview 79
Research Objective #1: To develop a methodology to quantify the reaerosolization of a dry-biological surrogate aerosol from clothing during a medical evacuation. 79
Research Objective #2: To use the developed methodology to test the effectiveness of existing biological decontamination procedures in regards to bioaerosols. 80
Applicability of Results to Real-World Scenarios 81
Aerosol Versus Droplet Deposition Patterns Before and After Water Decontamination 83
Limitations and Recommendations for Future Research 84
Significance of Research 89
APPENDIX I 90
APPENDIX II: Additional Methodology Explored in the Development of this Thesis 100
Bibliography 104
REPORT DOCUMENTATION PAGE 108

List of Figures

Page

Figure 1: Steps in the Mass Casualty Response Process (Figure taken from source: ECBC, 2013) 20

Figure 2: Medical Evacuation Transport Vibration Analysis of AMBUS (A), C-130J (B), and C-130H (C) (Figures and images taken from source: Smith et al, 2019/ 2020/ 2021) 21

Figure 3: Overview of the Developed Methodologies 25

Figure 4: Collison Nebulizer with PSL Solution in Natural (A) and UV Light (B) 26

Figure 5: Undyed and Dyed ABU Fabric, Clean and Contaminated 27

Figure 6: Large Aerosol Test "MURPHEE" Chamber (Chapman, 2021) 28

Figure 7: Swatch Organization During Contamination Procedure 29

Figure 8: Graphical Representation of Contamination Process 29

Figure 9: Exterior View of Contamination Process 30

Figure 10: Graphical Representation of Reaerosolization Process 32

Figure 11: Vibration profile of Vortex Mixer (Frequency vs Acceleration) 33

Figure 12: PVC Filter with No (A), Light (B), Heavy (C), and TNTC (D) PSL Sphere Contamination 34

Figure 13: Overhead View of Reaerosolization Process 36

Figure 14: Graphical Representation of Decontamination Process 37

Figure 15: Decontamination Process Apparatus 38

Figure 16: Determination of Microscope Imaging Diameter Using a Calibration Slide 39

Figure 17: Graphical Representation of Marked Sample Filter 40

Figure 18: Contaminated Undyed ABU Fabric, Concentration TNTC 42

Figure 19: Quick-Guide on Counting PSL Spheres on PVC Filter Under UV Light 44
Figure 20: Steps in the Image-J Software Particle Counting Process, from Original Image (A), Converted into usable format (B), and Counted (C) 45
Figure 21: Side-by-Side of Human Eye (A) and Computer (B) Counting Techniques 46
Figure 22: When to Use Human Eye versus Computer Techniques when Counting 48
Figure 23: Predesignated Sample IDs Based on Contamination Placement 52
Figure 24: Representative Photographs of Clean-Series Trials 57
Figure 25: Representative Photographs of Dirty-Series Trials 59
Figure 26: Representative Photographs of Water-Series Trials 62
Figure 27: Representative Photographs of Post-Decontamination-Series Trials 65
Figure 28: Concentration of Reaerosolized 1 µm PSL Spheres Across Series with Standard Error Bars 67
Figure 29: Distribution Analysis of the Four Reaerosolization Series Trials 68
Figure 30: Distribution Analysis of the Four Reaerosolization Series Trials (Outliers Removed) 71
Figure 31: Concentration of Reaerosolized 1 µm PSL Spheres Across Series with Standard Error Bars (Outliers Removed) 72
Figure 33: Analysis of Concentration by Group (Outliers Removed) 77
Figure 34: Distribution of Results of Dirty-Series and Post-Decontamination-Series over Swatch Contamination Layout 85

List of Tables

Page

Table 1: Collected Characteristics of *Bacillus anthracis* 6

Table 2: Collected MIDs and LD50s of Various Biological Pathogens 9

Table 3: Preferred Methods of Skin Decontamination (from *most* to *least* preferred) 17

Table 4: File Naming Conventions 41

Table 5: Counting Rules for PSL Sphere Presenting Particles 43

Table 6: Side-by-Side of Human Eye (A and B) and Computer (C and D) Counting Techniques Under the Effects of Water Droplets. 47

Table 7: Swatch Contamination Confirmation 55

Table 8: Clean-series Fabric Reaerosolization Trials Filter Particle Counts 58

Table 9: Clean-Series Reaerosolization Concentrations of PSL Spheres 58

Table 10: Dirty-series Fabric Reaerosolization Trials Filter Particle Counts 60

Table 11: Dirty-Series Reaerosolization Concentrations of PSL Spheres 61

Table 12: Water-series Clean Fabric Reaerosolization Trials Filter Particle Counts 63

Table 13: Water-Series Reaerosolization Concentrations of PSL Spheres 63

Table 14: Post-Decontamination-series Fabric Reaerosolization Trials Filter Particle Counts ... 66

Table 15: Post-Decontamination-Series Reaerosolization Concentrations of PSL Spheres 66

Table 16: W-Test for Normality and D-Test for Lognormality Results for all Series 69

Table 17: Reaerosolization Concentrations of PSL Spheres Summary Statistics (Outliers Removed) 70

Table 18: W-Test for Normality and D-Test for Lognormality Results for all Series (Outliers Removed) 71

Table 19: Wilcoxon Rank Sums Test Comparing Control Group #1 (Clean) and Experimental Group #1 (Dirty) 73

Table 20: Wilcoxon Rank Sums Test Comparing Control Group #2 (Water) and Experimental Group #2 (Post-decontamination) 74

Table 21: Wilcoxon Rank Sums Test Comparing Experimental Group #1 (Dirty) and Experimental Group #2 (Post-decontamination) 74

Table 22: Two Directional t-Test for Difference of Means Between Dirty and Post-Decontamination Groups (Outliers Removed), 99% Confidence 77

List of Equations

Page

Equation 1: Calculation of Required PSL Sphere Diameter (Hinds, 1999) 12

Equation 2: Calculation of Settling Time for 1 µm PSL Spheres..... 31

Equation 3: Estimation of Particles per Filter..... 49

Equation 4: Calculation of Sample Volume 51

Equation 5: Calculation of Particle Concentration 51

Equation 6: Small-Sample Difference of Means for Dirty and Post-Decontamination Series..... 76

DEVELOPMENT OF A METHODOLOGY FOR THE QUANTIFICATION OF REAEROSOLIZATION OF A BIOLOGICAL CONTAMINATE SURROGATE PARTICLE FROM MILITARY UNIFORM FABRIC

I. Introduction

General Issue

In both a historical and modern context, biological warfare has been and continues to be a threat. This branch of warfare has existed since "before microbial pathogenesis" was understood, with early examples including the use of "cadavers, animal carcasses, plant-derived toxins, and filth" as biological warfare agents (BWAs) with the intent to spread disease. Within the last two centuries, biological warfare has advanced to focusing on the use of biological aerosol (or bioaerosol) attacks, which are biological organisms — usually a pathogenic agent such as smallpox, plague, anthrax, etc. — that have been dispersed as airborne particles to drastically increase the risk of inhalation of the organism by the target victim (Dembek, 2007).

The most well-known attack on U.S. soil involving a bioaerosol weapon was the 2001 anthrax attacks through the U.S. mail system, but the threat of biological weapons is ever present. One factor that makes biological aerosol weapons so effective in terrorist attacks is the fear factor associated with the "unseeable" nature of the particles, whose size are often smaller than 1 um. This fear factor is so effective that in the 1990s alone there were three separate strings of domestic terror incidents all involving "hoax" threats of anthrax poisoning (Keim & Kaufmann, 1999).

Problem Statement

Two major concerns that fuel the fear factor of bioaerosols stem from a lack of understanding of how bioaerosols behave in a physical environment, as well as a lack of confidence in the prescribed methods to decontaminate surfaces and personnel following a bioaerosol attack. To address the first concern, one must have an understanding of how biological particles "aerosolize" and "reaerosolize." Initial aerosolization patterns, resulting from initial dispersion of a biological weapon, are fairly characterized in literature. However, the risk of reaerosolization — secondary particles that have already settled, but then become re-aerosolized by a variety of means — has not been studied as deeply.

For example, in a hypothetical chemical-biological-radiological-nuclear (CBRN) attack, a group of victims may become covered by spores of a pathogenic agent. At the same time, the biological attack may or may not be accompanied by conventional weapon attack — such as an explosion — that may distract from the emergency response effort. The victims may exhibit no symptoms at the time, and may have other injuries that need to be addressed. Thus, they may be placed in a medical evacuation transport (such as an ambulance or transportation aircraft) without consideration for decontamination. This creates an unknown reaerosolization risk of the biological particles on the victims' clothing being resuspended in the transportation process, creating a potential secondary inhalation for not only the primary victims, but the medical staff on the transport as well.

Additionally, it is also important to develop confidence in the methods used to decontaminate surfaces, equipment, and personnel that may be contaminated by bioaerosols. These methods may include wiping down surfaces or equipment with bleach, or spraying personnel down with water and removing their clothing. Regardless of the method, it is

important to have a reliable method to quantify the efficacy of each method such that confidence may be placed in the practice.

Research Objectives

This thesis will take a look at *Bacillus anthracis* as a case study example of a potentially weaponized bioaerosol, if and how it reaerosolizes after an initial attack, as well current doctrine and studies regarding decontamination of bioaerosols. Additionally, from the major concerns presented above, the following two primary research objectives were established as the scientific aims of this study:

1. To develop a methodology to quantify the reaerosolization of a dry- biological surrogate aerosol from clothing during a medical evacuation.
2. To use the developed methodology to test the effectiveness of existing biological decontamination procedures in regards to bioaerosols.

Thesis Outline

This thesis is constructed of five major sections: Introduction, Literature Review, Methodology, Results, and Conclusions and Recommendations. Chapter I consists of the introduction and research objectives. Chapter II includes a literature review covering the field of biological aerosols, current decontamination procedures in medical evacuations, and the use of surrogates to model biological particles. Chapter III covers the broad experimental design methodology, as well as the development process for the four unique methodologies developed for this thesis. Chapter IV includes the quantitative and qualitative results of the reaerosolization experiments, as well as a statistical analysis of those results. Chapter V discusses how the research objectives were met, any significant observations of the research, significant limitations of the research, and recommendations for future work based on this thesis.

II. Literature Review

Chapter Overview

This chapter includes a comprehensive literature review of important background information for the development of this study.

Bacillus anthracis (Anthrax)

Anthrax as a disease is caused by *Bacillus anthracis*, which is a collection of spore-forming, Gram-positive, rod-shaped, and toxigenic bacteria (D'Amelio, 2015). As its spores are rod-shaped, it is important to note both its diameter as well as its mean length. Although there is some variation in nature, *B. anthracis* has been found to have a "mean diameter range" between 0.81 ± 0.08 μm and 0.86 ± 0.08 μm. Additionally, one study found "mean spore lengths" of *B. anthracis* to fall into two groups: 1.26 ± 0.13 um or shorter, and another group of strains with mean spore lengths between 1.49 and 1.67 um (Carrera, 2007). Furthermore, the wet density of *B. anthracis* spores was found to be in two groups between 1.162-1.165 g/ml and 1.174-1.186 g/mL; meanwhile, the dry density of *B. anthracis* spores was found to be consistently 1.41 ± 0.01 g/ml (Carrera et al, 2008). A summary of the features of *B. anthracis* may be seen below in Table 1.

Table 1: Collected Characteristics of *Bacillus anthracis*

Characteristic	Notes	Source
Spore Diameter	0.81 ± 0.08 μm & 0.86 ± 0.08 μm	Carrera et al, 2015
Spore Length	1.26 ± 0.13 μm or shorter & 1.49 - 1.67 μm	Carrera et al, 2015
Spore Density	1.162-1.165 g/ml & 1.41 ± 0.01 g/ml	Carrera et al, 2008
Settling Time (Settling Velocity)	6.6-7.9 hours to settle 1 m ($3.5*10^{-5}$ - $4.2*10^{-5}$ m/s)	(Derived) Hinds, 1999
Case-Fatality Rate	Untreated, inhalational anthrax fatality is >90%	ARMY ATP 4-02.84, 2019
Spore stability	"High spore stability, even for decades, risk from secondary dispersal"	D'Amelio et al, 2015 Pottage et al, 2014 Jończyk-Matysiak et al, 2014
Ease of Production	Easy to culture, able to be dried into spores, easy to store, cheap to produce	D'Amelio et al, 2015 Jończyk-Matysiak et al, 2014
Dispersal Methods	Spores can be weaponized to form "white powder," though more sophisticated techniques are required. The powder can be put in envelopes or any aerosol dispersal device, such as missiles, bomblets, artillery fires, point release, or airborne line release. Contamination of food and water may also be used.	D'Amelio et al, 2015 Pottage et al, 2014 ARMY ATP 4-02.84, 2019

Although 90 percent of all anthrax cases worldwide are cutaneous, weaponized anthrax tends to be inhalational (or pulmonary) anthrax (ARMY ATP 4-02.84, 2019). As an example, one of the most well-known employments of biological warfare in recent American history is the series of anthrax attacks conducted through the U.S. Mail in the fall of 2001. Prior to these attacks, anthrax was only rarely recorded in the United States, with the last inhalation case observed in 1976. During these attacks, "22 cases of anthrax," 11 inhalational, and 5 of which

were fatal, were recorded (Jernigan et al, 2002). The delivery method of the anthrax was through letters and envelopes filled with “white powder,” which was actually highly purified and dried-out anthrax spores (Jernigan et al, 2002; FBI, 2010). Additionally, there have been a number of unintentional biological incidents involving cases of anthrax, such as the 2008 “drumming” incidents involving contaminated goat skins, as well as the 2009/2010 outbreak associated with contaminated heroin in Europe (Pottage et al, 2014).

While many biological hazards can be spread by person-to-person contact, either through touch or respiration, this is not naturally the case for anthrax. Additionally, the “minimum infectious dose (MID)” can vary between different biological pathogens, with anthrax having a relatively high MID. A brief comparison of studied MIDs and LD50s for various known biological pathogens is presented in

Table 2. Although *B. anthracis* bioaerosols are the target to model in this study, it is important to note that other biological pathogens are capable of human to human infectious transfer at significantly lower doses.

Table 2: Collected MIDs and LD50s of Various Biological Pathogens

Pathogen	MID	Source
Bacillus anthracis	<600 spores for infectivity Est. 8,000-11,000 spores for lethal dose (alt. 2,500-55,000 spores)	D'Amelio et al, 2015 Keim & Kaufmann, 1999 Toth et al, 2013
Brucellosis	10-100 organisms	Stanek et al, 2020
Plague	500-15000 organisms	
Q-Fever	1-10 organisms	
Smallpox	Est. 1-100 organisms	
Tularemia	10-50 organisms	
Viral Hemorrhagic Fevers	10-10 organisms	

For both its history in use as a biological weapon and its characteristics that lend itself to reaerosolization, this study will focus on using *B. anthracis* as the target model for the biological surrogate PSL spheres.

Polystyrene Latex (PSL) Spheres as a Biological Surrogate

The scientific goals of this study aim to quantify the reaerosolization of biological agents, but aim to do so using the behavior of their physical properties, rather than the organisms themselves. This is because using a live biological agent in aerosolization studies comes with a number of added difficulties and potential sources of error. For example, to quantify a biological agent, the agent must be captured, plated, cultured, and then counted. This introduces many potential sources of error when developing a new methodology, as a negative result could be from either a mistake in the developed methodology, or simply a non-viable culture. To

minimize the effects of live agents on the reaerosolization studies, it was determined that a biological surrogate would be used.

Polystyrene Latex (PSL) spheres — also referred to as PSL beads or PSL microparticles in literature — are microscopic, inert rubber beads, that are generally sold in a water or oil solution, and are available in diameters from as low as 1 nm to as high as 15 μm and greater (ThermoFisher, 2021). PSL spheres have been used historically for a number of scientific testing purposes, usually as a surrogate for another agent, either chemical or biological, when the agent of concern is difficult/dangerous to use, or when it is difficult to obtain. For example, in one environmental study, 200 nm PSL spheres were used to model the behavior of black carbon in melting Antarctic glacier water, as access to black carbon was extremely limited (Ellis et al, 2015). Additionally, PSL spheres have also been used in practical medical applications; for example, "peptide-immobilized latex beads" are PSL spheres that have been coated with antibodies that can be used in immunoassays that are equally reliable, cheaper, and faster than traditional assay techniques (Deng et al, 2021). Of particular interest is the use of PSL spheres as a surrogate for bioaerosols, such as the use of radioisotope C-14 coated 225 nm PSL spheres to trace and model organic nanoparticle inhalation in mice (Parkhomchuck et al, 2016).

In the case of this study, the PSL spheres were chosen to use as a surrogate to model the behavior of *Bacillus anthracis* spores in still air. However, with a density of 1.05 g/ml, PSL sphere would appear to have neither the exact shape nor density of a standard ellipsoidal anthrax spore (ThermoFisher, 2012). Thus, calculations must be made to choose and test the correct diameter of PSL spheres used to model anthrax spores.

This target PSL sphere diameter can be determined first finding the "aerodynamic diameter" of the anthrax spore, which is defined as the "equivalent" spherical particle that has

the same settling velocity as an irregularly shaped particle — such as anthrax spores (Hinds, 1999). The calculation of the appropriate PSL sphere size was calculated using Equation 1 shown below. It is important to note that these equations are based solely on particle shape, density, gravity, and air viscosity. External factors, such as electrostatic forces, were not used in surrogate particle selection.

Equation 1: Calculation of Required PSL Sphere Diameter (Hinds, 1999)

First, the ellipsoid-shaped anthrax spore must be converted into its equivalent sphere:

$$V_{ellipsoid} = \frac{4}{3} * \pi * \left(\frac{d_p}{2}\right)^2 * \frac{L}{2}$$

$$V_{ellipsoid} = \frac{4}{3} * \pi * \left(\frac{0.81\ \mu m}{2}\right)^2 * \left(\frac{1.26\ \mu m}{2}\right) = 0.43\ \mu m^3$$

Where:

V = volume

d_p = diameter of ellipsoid particle = 0.81 µm for anthrax

L = length of ellipsoid particle = 1.26 µm for anthrax

Next, the equivalent sphere with the same density can be calculated:

$$V_{sphere} = \frac{4}{3} * \pi * r^3 = 0.43\ \mu m^3$$

Where:

r = radius of sphere = ½ of diameter of sphere

$$\rightarrow r_e = \sqrt[3]{V_{sphere} * \frac{3}{4\pi}} = 0.47\ \mu m$$

$$\rightarrow d_e = 2 * r_e = 0.94\ \mu m$$

Finally, the target diameter of the PSL sphere can be calculated:

$$v_{TS} = \frac{\rho_p * d_e^2 * g}{18 * \eta * \chi} = \frac{\rho_t * d_t^2 * g}{18 * \eta}$$

Where:

v_{ts} = equivalent diameter terminal velocity equation

ρ_p = density of anthrax = 1163 kg/m^3

ρ_t = density of PSL sphere = 1050 kg/m^3

d_t = target diameter of PSL sphere

g = acceleration due to gravity

η = viscosity of air

χ = dynamic shape factor of anthrax = 1.09 (Hinds, 1999, Table 3.2)
(from axial ratio = Ld=1.260.81=1.56 2)

$$\rightarrow d_t = \sqrt{d_e^2 * \left(\frac{\rho_p}{\rho_t * \chi}\right)} = 0.94\ \mu m \approx 1\ \mu m$$

Thus, from the above equation it can be seen that as the equivalent diameters of a 1.163 g/ml density ellipsoidal anthrax spore and a 1.05 g/ml density PSL sphere are equal, then 1 µm PSL spheres are an appropriate physical surrogate for *Bacillus anthracis* spores.

Reaerosolization of Biological Particles

Resuspension, reentrainment, or reaerosolization, all refer to particles being reintroduced into the atmosphere following previous deposition and settling (Layshock et al, 2012). While the resuspension of large particles such as dusts and radiological particles has been largely characterized, the reaerosolization of biological particles is still "poorly understood" (Brown et al, 2011). In fact, at this time, according to U.S. military doctrine, although the threat of reaerosolization hazards is recognized, the "operational impact" of reaerosolized biological warfare (BW) agents "cannot be measured" (ARMY ATP 4-02.84, 2019).

Regardless, a number of experiments - particularly after the Hart Senate Office Building anthrax incident - have indicated that *B. anthracis* spores are capable of reaerosolization (Layshock et al, 2012). In outdoor studies, past experiments have included *Bacillus* spores deposited onto animal carcasses and then subjected to natural weather, and spores deposited onto grassy patches and then subjected to "troop activity," such as marching and digging. In both of the studies involving troops, the respiratory hazard to individuals wearing "grossly contaminated" clothing was found to be "an order of magnitude higher" than the hazard to those wearing less contaminated clothing (Davids and Lejeune, 1981). Further outdoor studies conducted in 1970 and 1998 experimented with "vehicle induced" reaerosolization, again showing *Bacillus* spores capable of reaerosolization in the respirable particle-size range (Layshock et al, 2012).

Indoor, or laboratory setting, studies involving reaerosolization of *Bacillus* spores have included reaerosolization off of contaminated sand agitated by air bursts, reaerosolization off of metal via a model jet engine, and reaerosolization in an ambient breeze tunnel following "human activity" (Layshock et al, 2012). In the ambient breeze tunnel test, "human activity" was defined as a technician performing maintenance work on a biological sampler, taking readings, making notes, and other mundane tasks. The technician was found to have caused a reaerosolization rate of up to "73 CFU/L_{air}" from an average initial airborne concentration of "25,000 CFU/L_{air}," which could pose "serious risks" for a population. Furthermore, the technician's clothing was found to be a significant contributor to secondary transportation of biological particles, even for areas of clothing that did not come in direct contact with the sampler - indicating reaerosolization contamination (Byers et al, 2013).

Similar to the outdoor study involving troops on grass, an indoor study was conducted in 2015 to quantity reaerosolization of microorganisms off of industrial carpet and polyvinyl-chloride (PVC) floor coverings by human foot-traffic. Samples of carpet and PVC flooring were contaminated with *Bacillus* spores via an airbrush filled with a solution of "10^6 spores/ml" applied at 30 cm distance with an air pressure of "30 lb/in^2", placed in an environmental chamber, and then walked upon via a consistent path and footwork. Results were expressed as "reaerosolization factors" based on "surface samples" taken during contamination and "air concentrations" taken during reaerosolization trials. This study found that reaerosolization off of carpet was actually significantly higher than that of the PVC flooring, capable of "reaching breathing height" in the respirable particle-size range, and in concentrations that exceeded the infectious dose for *B. anthracis* when accounting for worker breathing rate and exposure time (Paton et al, 2015). This is particularly relevant to reaerosolization of particles off of a patient,

because whereas PVC flooring is a smooth, flat surface, carpet flooring is made up of many layers of interwoven synthetic fibers, which is much closer in structure to clothing that is also constructed of interwoven fibers.

Another study evaluated the reaerosolization of deposited genetic material (DNA) on "clothing, pillowcases, and towels." In this study, the contaminated object was subjected to "gentle shaking agitation" above a secondary surface, which was then analyzed for genetic material. In 87% of trials, the secondary surface showed some degree of contamination fitting the genetic profile of the person-of-interest (Thornbury et al, 2021). This study further highlights the potential for deposited biological particles (in this case, DNA) on clothing to be reaerosolized following agitation.

U.S. Military Doctrine Regarding Biological Decontamination

The majority of current U.S. military doctrine and standard operating procedures (SOPs) regarding decontamination following a chemical, biological, radiological, or nuclear (CBRN) contamination event largely draws from a 2013 report published by the Edgewood Chemical Biological Center (ECBC) (Titus et al, 2019). As a guiding principle, this report considers the key to successful mass casualty decontamination to be "the fastest approach that will cause the least harm and do the most good for the majority of the people" (ECBC, 2013). It is important to note that in a "mass casualty" event, which is defined as "any large number of casualties produced in a relatively short period of time [...] that exceeds local logistic support capabilities," "life- or limb-saving care" takes precedence over patient decontamination, which may result in increased risk of biological warfare agent (BWA) spread. As this is the most critical phase in a medical evacuation, this paper will focus only on "immediate" decontamination, as opposed to

"operational" or "thorough" decontamination which happens at a much later phase after a CBRN incident (ARMY ATP 4-02.7, 2016; ARMY ATP 4-02.84, 2019).

Decontamination of patients who have been potentially exposed to a BWA is not a strictly defined procedure (ECBC, 2013). Per this report, the number one principle behind mass casualty decontamination is the "immediate removal of clothing" for suspected contaminated victims and processing said victims through a "high-volume, low-pressure water shower" (specified as ~50-60 psi, no specified volume); this report estimates this process "may aid" in the removal of 80-90% of physical contamination (ECBC, 2013). However, in some cases, patients may not be decontaminated at all, as they may not report for medical treatment for an extended period of time due to the time delay between BWA exposure and the onset of symptoms. As another example, because certain BWAs, such as anthrax, are not transmissible from person to person, it is currently standard accepted procedure to evacuate patients with anthrax alongside other categories of patients. However, this only accounts for patients with anthrax the disease, not patients who may be coated in *B. anthracis* spores (ARMY ATP 4-02.84, 2019).

When establishing control of patients, contacts, and treatment areas, to decontaminate equipment and surfaces, it is recommended that a "five percent hypochlorite" solution be used. Additionally, equipment can be "autoclaved" or "steam sterilized" for complete eradication of spores. However, these techniques are all hazardous to human skin and are not feasible for casualty decontamination (ARMY ATP 4-02.84, 2019).

For both individual and mass casualty decontamination, "physical removal" of the contaminants is the primary method and top priority. This includes washing and wiping, but falls short of scrubbing as to avoid damaging the patient's skin (ATP 4-02.84, 2019). For skin

decontamination, the preferred methods are summarized in Table 3 in order of most preferred to least preferred.

Table 3: Preferred Methods of Skin Decontamination (from *most* to *least* preferred)

Method	Notes	Source
Liquid Soap and Water	Most preferred. Mix fat-based soaps with water. Collect runoff as BWA is not killed. Use lukewarm water as hot water can open up pores of skin.	ATP 4-02.84, 2019 Koenig et al, 2007
Water	Next preferred. Same application instructions as above apply, but use copious amounts of water in the absence of soap.	
Misc. Absorbent Material	Any material that can absorb a liquid then be "brushed or scraped" without abrading the skin. Examples: soft towel, baby wipes, clay, dirt, baking powder. Abrasive materials, such as sand, are not recommended.	
Reactive Skin Decon. Lotion	A specialized liquid decontaminant dispensed on a sponge. Approved for use on intact skin and only against T-2 mycotoxin, but not recommended due to risk of irritating wounds or eyes.	
Hypochlorite Solution	0.5% hypochlorite solution is *not* recommended for skin decontamination of BWAs due to risk of skin irritation and opening skin pores.	

Current BWA decontamination doctrine removes external clothing as a first step, before washing, as "disrobing" is claimed to be "an order of magnitude more effective" than water decontamination (Koenig et al, 2007; ATP-02.84, 2019; ECBC, 2013). However, in the case of a dry-particle contamination — such as contaminated dusts or spore bioaerosols such as *B. anthracis* — the aggressive human activity involved in removing clothing may greatly increase the risk of reaerosolization and secondary contamination; for instance, this behavior was shown in one study where a "statistically significant amount of re-aerosolization" was observed during removal of clothing contaminated with settled dense particles (Chapman, 2021). The issue of

reaerosolization during disrobing is well documented in large fiber asbestos removals; for example, in one study documenting asbestos reaerosolization during asbestos remediation, the decontamination procedures for workers involved five steps, each in a separate airlock: storage of polluted tools, shower with overalls and respirator still on, storage of overalls and respirator, body shower, and dressing in a bathrobe (Villa et al, 1994). However, asbestos remediation decontamination procedures assume that the individual being decontaminated is wearing a filtering-facepiece respirator and disrobes in a contained space, and thus is not at as much risk to themselves or others. This assumption cannot be made for decontamination during a mass casualty incident.

Thus, in order to reduce the risk of additional contamination or reaerosolization, victims are recommended to have their clothes removed via being cut off or a similar method to avoid being pulled directly overhead (Chilcott et al, 2019; ECBC, 2013). However, it is also standard practice that in the case that clothing is "difficult to remove," or if any victim is "unwilling to disrobe," then decontamination may be conducted without removing any clothing (Chilcott & Amlôt, 2015).

Decontamination in a "mass casualty" setup is structured in a similar manner to individual decontamination. In a traditional setup, multiple fire trucks parked parallel to each other provide a pathway through which a "high-volume, low-pressure" shower line may be established. Again, current doctrine recommends that clothing is removed prior to entering the decontamination shower line; however, as the ultimate priority is processing as many casualties as possible, if victims do not desire to remove clothing this is not enforced. Shower times are recommended to be greater than 30 seconds, but less than 3 minutes, as excess water can actually increase risk of exposure to some agents. In cold and freezing environments, a "dry"

decontamination alternative may be used, which involves blotting the full body with a paper towel, then providing a warm shower indoors once facilities are available (ECBC, 2013).

Figure 1 illustrates the mass casualty decontamination and medical evacuation process as defined by the ECBC guidelines described above. Step 1 is where victims are evacuated from the immediate "hazard area" and enter the response line. Step 2 is where first responders perform "decontamination triage" and direct victims to either a waiting area or the decontamination line; this is particularly concerning during a bioaerosol attack, as a contaminated victim may have no visible signs of contamination, leading to them being directed to a waiting area *without* undergoing decontamination. Step 3 depicts an example mass casualty decontamination line using "high volume, low pressure water." Step 4 designates the waiting area for decontaminated victims as well as victims that were determined to not require decontamination; again, the same concern as in Step 2 arises that false-negative victims (those that are contaminated with bioaerosols but appear not to be) are placed in the same space as decontaminated victims. Step 5 represents the point where victims that require additional medical care are loaded into vehicle transportation — such as an ambulance — and transferred to a medical facility. Finally, Step 6 marks where victims are released from the decontamination/ medical evacuation line as directed.

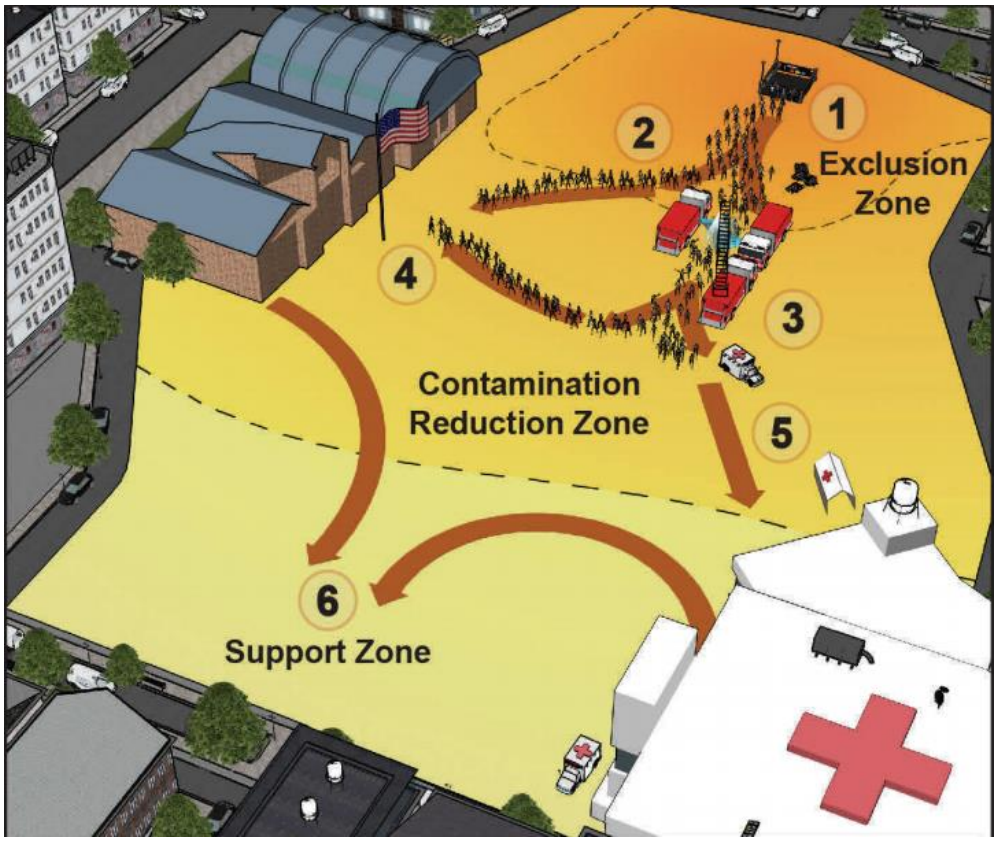

Figure 1: Steps in the Mass Casualty Response Process (Figure taken from source: ECBC, 2013)

Vibration Patterns During Medical Evacuations

As this study is particularly centered on potential reaerosolization during a medical evacuation, it must be understood what potential sources for reaerosolization exist during the evacuation process. For example, as previously stated, any "human activity" has the potential to cause reaerosolization, which can include running, undergoing triage, or riding in a vibrating vehicle. For the sake of repeatability, this experiment focused on the risk of reaerosolization off of a stationary patient — such as one sitting still or placed on a litter — while riding in a military medical transport.

Vibration is generally measured through two attributes: frequency and acceleration. As reaerosolization of particles across the spectra of frequency vibrations is not significantly

characterized in scientific literature, for this experiment, identifying an appropriate frequency to model a military transport was prioritized. Furthermore, the three chosen military medical transports to model were a medical ambulance-bus (AMBUS), and both the C-130J and C-130H models of the C-130 aircraft. Each measurement was taken at the "pelvis interface" or "pan interface," which is the horizontal surface of a seat. Worst-case vibrations for each transport were evaluated, and presented below in Figure 2. The AMBUS (Figure 2.A) showed highest vibrations at a frequency of about 3 Hz; the C-130J (Figure 2.B) showed highest vibrations at a frequency of 100 Hz; and the C-130H (Figure 2.C) showed highest vibrations at a frequency of 68 Hz. Thus, frequencies that a human body might be subjected to under medical transport range from 1-100 Hz, with an average among these three transports of 56 Hz (Smith et al, 2019; Smith & Dooley, 2020; Smith et al, 2021).

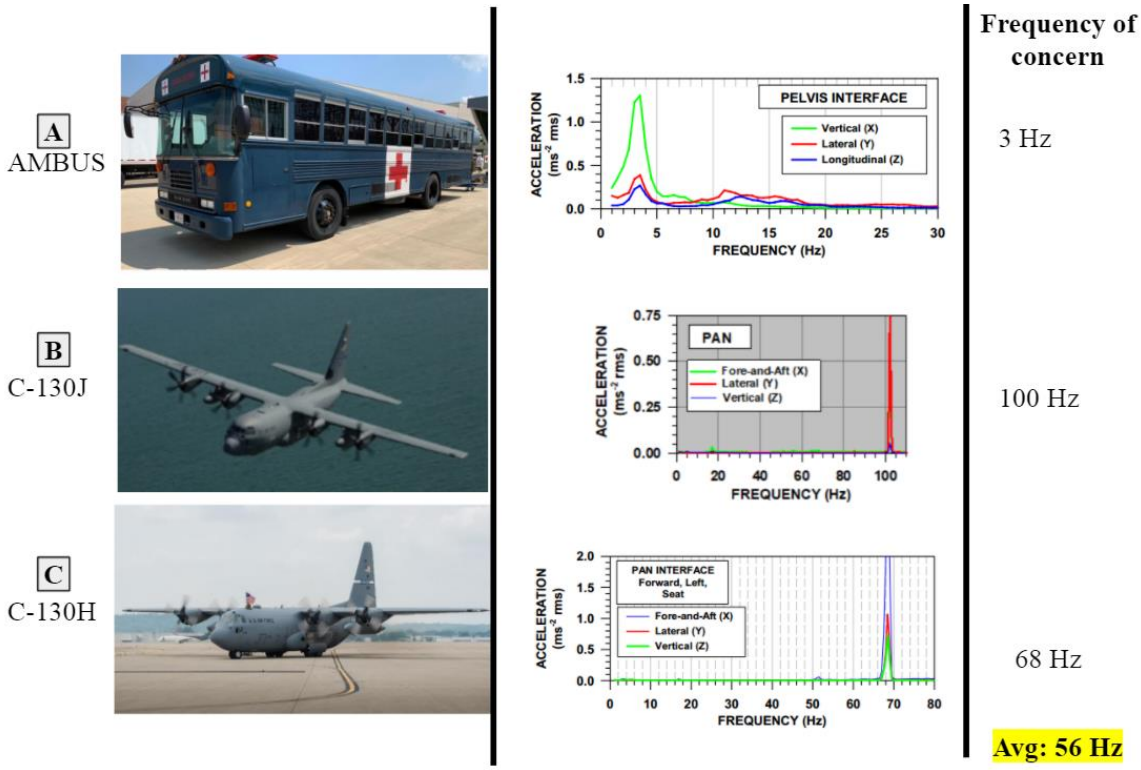

Figure 2: Medical Evacuation Transport Vibration Analysis of AMBUS (A), C-130J (B), and C-130H (C) (Figures and images taken from source: Smith et al, 2019/ 2020/ 2021)

It should be noted again that there are many other factors that may cause additional or greater reaerosolization during a medical evacuation, such as turbulent air from aircraft propellers, shaking, or running. However, these sources are not as easily controlled for in a repeatable manner. Additionally, although there is some degree of variation of vibration between the three transports, for the sake of repeatability, this experiment will focus on reaerosolization occurring at the average of 56 Hz.

Chapter Summary

Bioaerosols, such as spore-forming *Bacillus anthracis,* are a present and future threat through their use as bioweapons. Not only is there precedent for biological weapons to be dispersed as bioaerosols, but the potential exists for them to be reaerosolized after settling following initial contamination. Thus, having an effective means of decontamination for surfaces, equipment, and people is critical. Current methodologies call for a use of water and soap administered via high-volume, low-pressure flow to remove contamination from personnel. However, the actual efficacy of this methodology has not been extensively tested.

III. Methodology

Chapter Overview

This chapter includes a description of the experimental design of this study, as well as the four primary methodologies developed for the quantification of reaerosolized biological surrogate particles.

Experimental Design

The overall goal of this experiment was to develop a repeatable methodology to quantify the reaerosolization of a biological surrogate off of fabric. To this end, there are four major methodologies that were explored: contaminating fabric swatches with the biological surrogate; reaerosolizing the biological surrogate off of the contaminated fabric; a repeatable decontamination method for removing the biological surrogate from the contaminated fabric; microscopy techniques to quantify biological surrogate contamination.

This section will describe each of the four methodologies in sequential order; materials will be described in the order in which they appear. A graphical representation of the four developed methodologies is shown below in Figure 3.

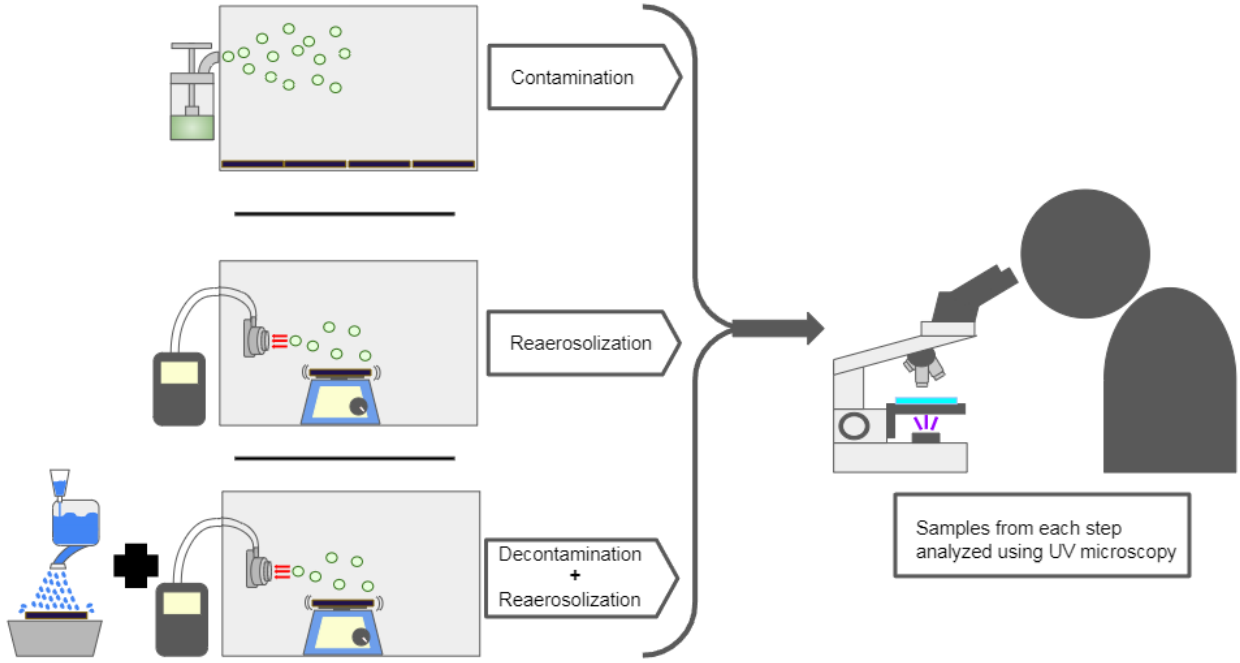

Figure 3: Overview of the Developed Methodologies

Contaminating Fabric Swatches with Biological Surrogate

As this report is focused on the *reaerosolization* of bioaerosols off of fabric, the fabric must undergo primary contamination first. This step is intended to model the experience of being the direct target of a biological weapon attack (such as opening up an envelope filled with anthrax spores), so the goal is to inundate the fabric swatches with PSL spheres. The basic structure of this step is to place a large number of fabric swatches evenly spread throughout a small, enclosed aerosol chamber, saturate the box with aerosolized 1 µm fluorescent PSL spheres, and allow an appropriate amount of time for the spheres to settle and adhere to the fabric.

First, the PSL sphere solution was prepared. During this experiment, "1 µm (1±0.098 µm), yellow-green, 2.5% by volume" PSL stock solution (Magsphere Inc., Pasadena, CA) was

used. The stock was then diluted with deionized (DI) water into a 2 mL PSL stock / 10 mL solution ratio. Following mixing, the 10 mL of PSL solution were poured into a six-jet Collison nebulizer (CH Technologies, Westwood, NJ). The fluorescent stock solution in the nebulizer as seen under both natural and ultra-violet (UV) light is shown in Figure 4.

A: Natural Light B: UV Light

Figure 4: Collison Nebulizer with PSL Solution in Natural (A) and UV Light (B)

Next, the fabric was cut into 10 cm x 10 cm (4" x 4") squares to prepare the sample fabric swatches. All trials were tested with summer-weight, rip-stop, "Airman Battle Uniform (ABU)" fabric. This is a cotton/nylon blend fabric that was chosen due to its prevalence of use in a military environment, as this is the fabric that potential casualties in a biological attack will most likely be wearing. During pilot studies, it was observed that the naturally green fibers of ABU fabric fluoresce brightly under the UV microscope. To correct for this, the fabric was

darkened with black dye (Rit, Indianapolis, IN) in order to make the PSL spheres more visible against the fabric fibers. This phenomena may be seen in Figure 5 below, where "A" is a photograph of clean, undyed fabric, "B" is clean, dyed fabric, and "C" is dyed fabric that has been contaminated with fluorescent PSL spheres. In the "contaminated" image, the spheres can be seen as many small, green dots that were not present in any "clean" fabric images.

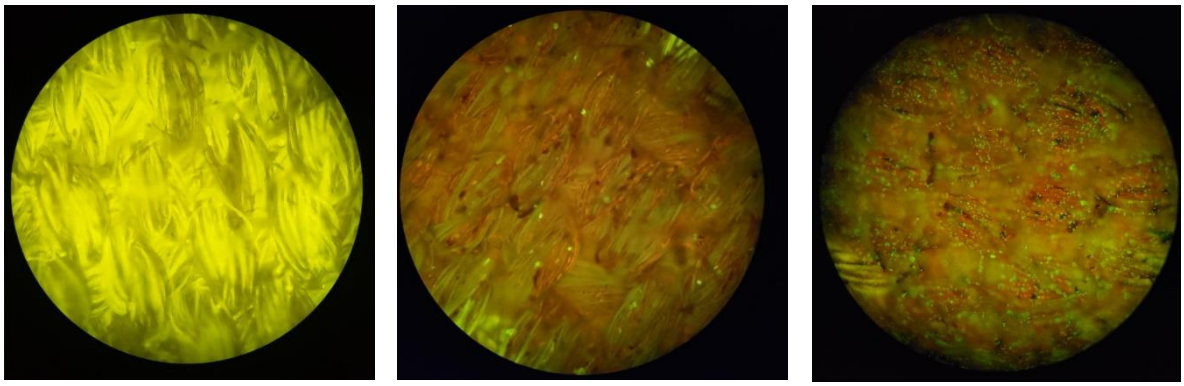

A. Undyed ABU B. Dyed ABU C. Dyed ABU (Contaminated)

Figure 5: Undyed and Dyed ABU Fabric, Clean and Contaminated

Both the "contamination" process and all "reaerosolization" processes were conducted in an enclosed 0.61 x 0.61 x 0.91 meter (2 x 2 x 3 ft) plexiglass chamber, which itself was placed in a larger Multi-Use for Research for Particulate Hazards and Environmental Exposures (MURPHEE) aerosol test chamber, with dimensions of 0.91 x 0.91 x 6.40 meters (3 x 3 x 20 ft) During reaerosolization trials and fabric contamination, the small aerosol chamber was enclosed, with all holes for tubing and wires sealed with tape. Additionally, during trials the door to the MURPHEE chamber was closed as well. However, it should be noted that while the chamber was enclosed, it was not air tight, nor was it climate controlled. The atmospheric conditions inside the chamber varied greatly depending on the day, and both temperature and relative humidity were recorded before each trial. Neither factor appeared to have any

qualitative correlation with results. In between trials, while the chamber was being cleaned with deionized water and wipes, the MURPHEE chamber's exhaust fan would be activated to evacuate any lingering airborne particles from the previous trial through high-efficiency particulate absorbing (HEPA) filters to prevent cross-contamination into the laboratory. A graphical representation of the MURPHEE chamber is presented in Figure 6.

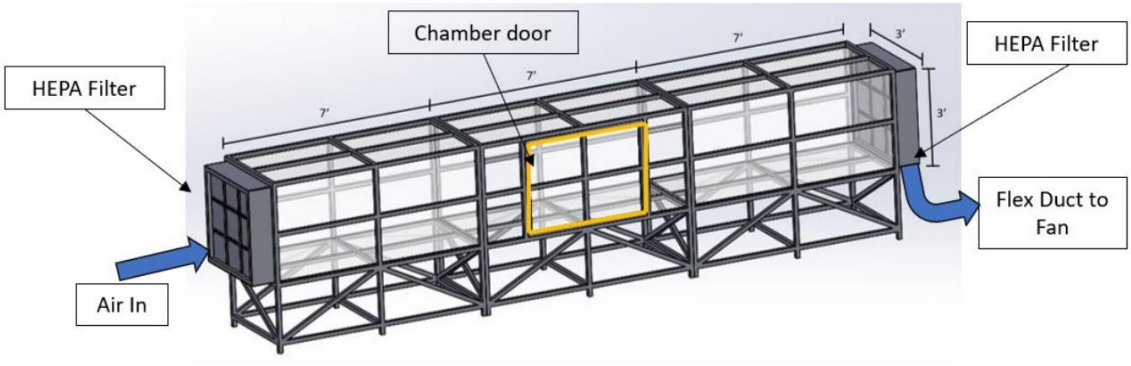

Figure 6: Large Aerosol Test "MURPHEE" Chamber (Chapman, 2021)

Once all materials were prepared, the fabric swatches were numbered and arranged throughout the aerosol chamber, annotating whether they were in the "near", "middle," or "far" region from the Collison nebulizer's spraying point, as shown in Figure 7. The Collison nebulizer was attached outside the box to spray into an opening located at the center-point of the side of the aerosol chamber (at location 0.30 m (1 ft) height and depth).

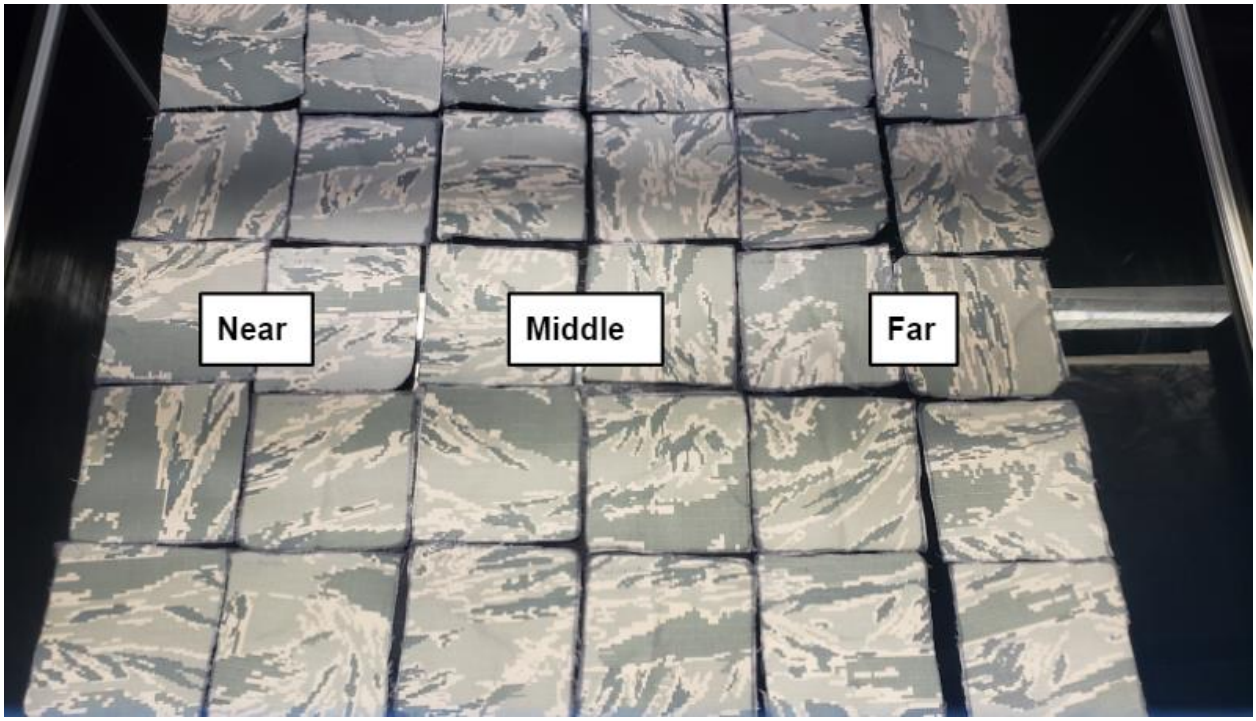

Figure 7: Swatch Organization During Contamination Procedure

To initiate the contamination, the Collison nebulizer was supplied with 20 pounds-per-square-inch (PSI) air, which activates the jets, lofting the 1 µm PSL spheres into the chamber. A graphical representation of the contamination process may be seen in Figure 8.

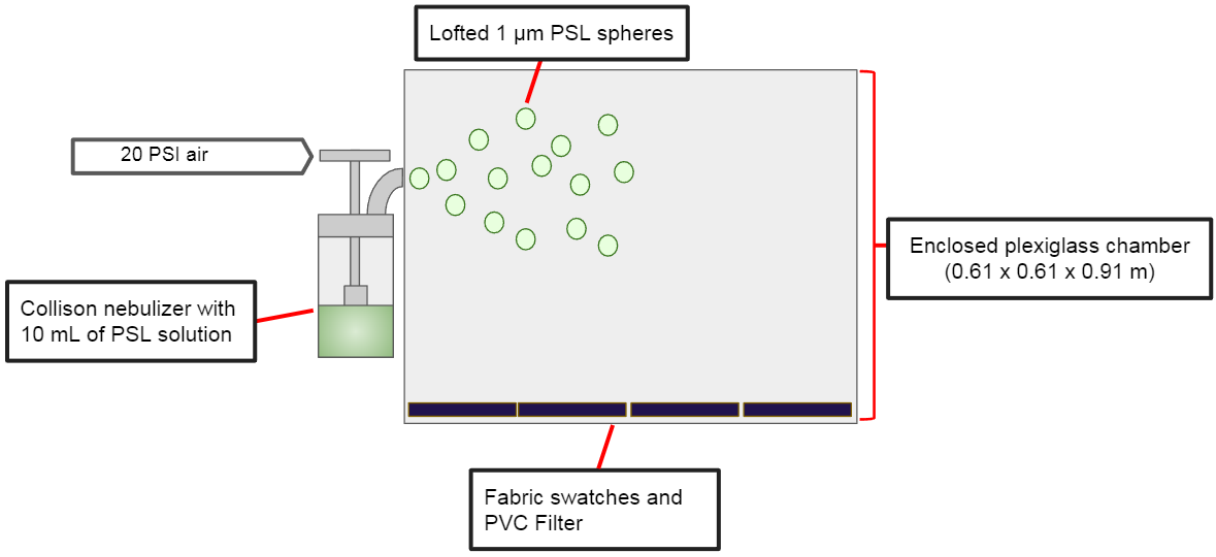

Figure 8: Graphical Representation of Contamination Process

Additionally, an optical particle counter (OPC) (Model: Handheld 8506-30, Particles Plus, Stoughton, MA) was used to monitor the airborne concentration of 1 µm particles in the chamber during the contamination process in real time. It was attached to a hole centered on the front of the chamber (location 0.30 m (1 ft) height and 0.45 m (1.5 ft) from side). The OPC was set to collect 1 minute samples repeatedly at 2.82 L/minute. The Collison nebulizer was then continuously supplied with air until the OPC read 1,000,000 particles per minute (sampled at a flow rate of 2.82 L/min) in the "1 µm diameter" bucket. Then, the OPC was removed, its hole in the chamber was sealed with tape, and a timer was set for 15 minutes to allow the system to continue to run. At the end of the 15 minutes, the air supply was shut off, and the box was sealed. A photograph of the contamination setup with the OPC may be seen in Figure 9.

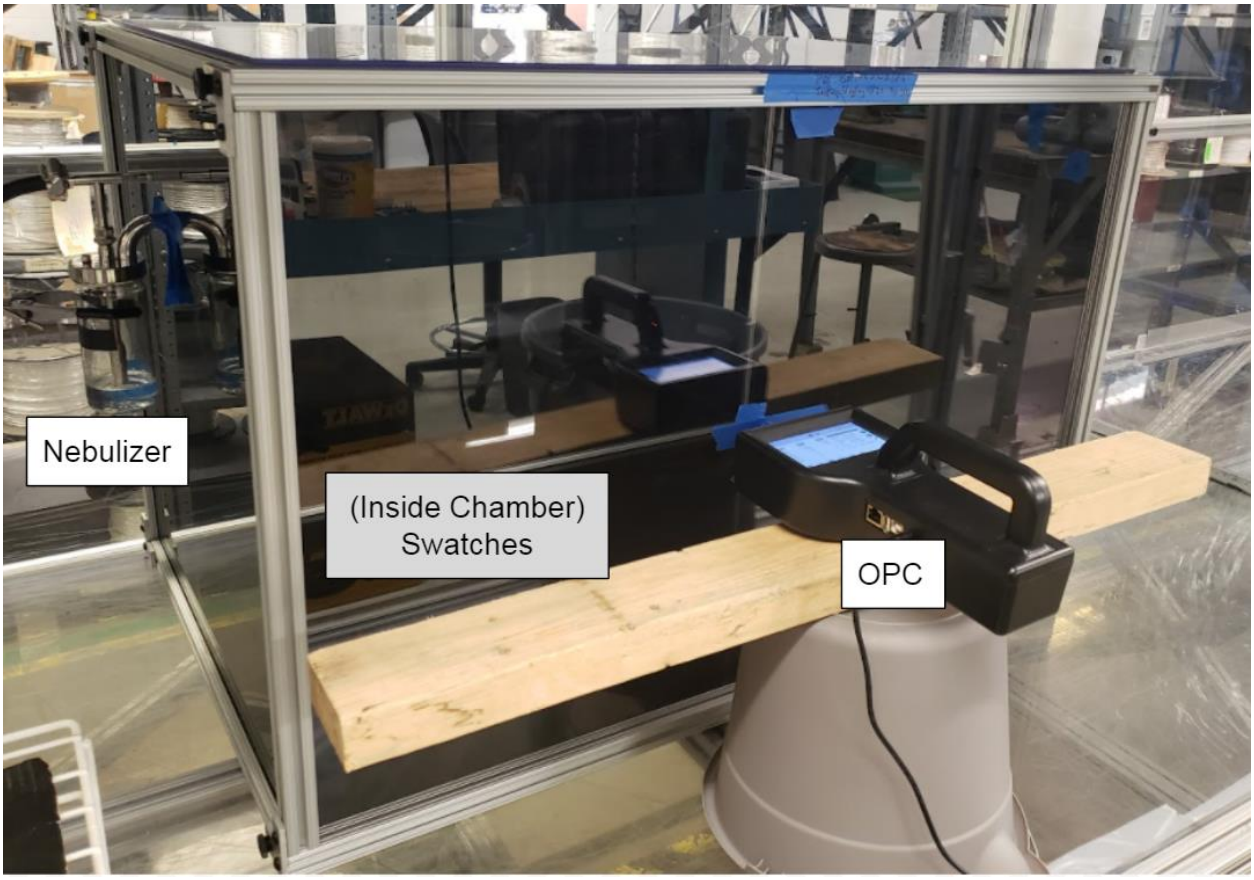

Figure 9: Exterior View of Contamination Process

Lastly, an adequate amount of time needed to be allowed for the 1 µm particles to settle. The minimum amount of time necessary for the 1 µm particles to settle out of the chamber was calculated to be 5.8 hours, using the terminal settling velocity equation, seen in Equation 2 (Hinds, 1999). As the particles are incredibly susceptible to air mixing, the chamber was completely sealed for the entire settling duration so that the air in the chamber would be completely stagnant.

Equation 2: Calculation of Settling Time for 1 µm PSL Spheres

$$v_{TS} = \frac{\rho_p * d_e^2 * g}{18 * \eta} \quad (1)$$

Where:

V_{ts} = Settling Velocity (m/s)
p = Particle Density (kg/m^3) = 1.05*10^3 kg/m^3
d = Particle Diameter (m) = 1*10^{-6} m
g = Acceleration due to gravity (m/s^2) = 9.81 m/s^2
η = Viscosity of air (kg/m*s^2) = 1.81*10^{-5} kg/m*s^2

$$V_{ts} = \frac{\left(1.05 * \frac{10^3 kg}{m^3}\right) * (1 * 10^{-6} m)^2 * \left(9.81 \frac{m}{s^2}\right)}{18 * \left(1.81 * \frac{10^{-5} kg}{m * s^2}\right)} = 3.16 * 10^{-5} \frac{m}{s}$$

$$t = \frac{H}{V_{TS}} \quad (2)$$

Where:

t = time to settle (seconds)
Vts = Settling Velocity (m/s) = 3.16*10^{-5} m/s
H = height of aerosol chamber (m) = 0.66 m

$$t = \frac{0.66\ m}{3.16 * 10^{-6} \frac{m}{s}} = 2.09 * 10^5 \text{ seconds} = 5.8 \text{ hours}$$

After the chamber was allowed to settle, the fabric swatches were carefully stored, and inspected under a UV microscope per the UV microscopy procedure to ensure that all swatches had PSL spheres present.

Reaerosolization of Biological Surrogate from Contaminated Fabric

Once the fabric swatches were verified to be contaminated with PSL spheres, the next step was to *reaerosolize* the spheres back off of the fabric via vibration, and to capture those spheres using active air sampling. The basic apparatus for this procedure involved securing the fabric swatches to a laboratory vortex mixer (Model: Vortex-Genie 2, Scientific Industries, Bohemia, NY) inside the small aerosol chamber, vibrating the swatch at 50 Hz for 30 minutes, and sampling the air above the swatch using an Institute of Occupational Medicine (IOM) air sampler (SKC Inc, Eighty Four, PA) equipped with a 5 µm PVC filter. A graphical representation of the reaerosolization process is shown below in Figure 10.

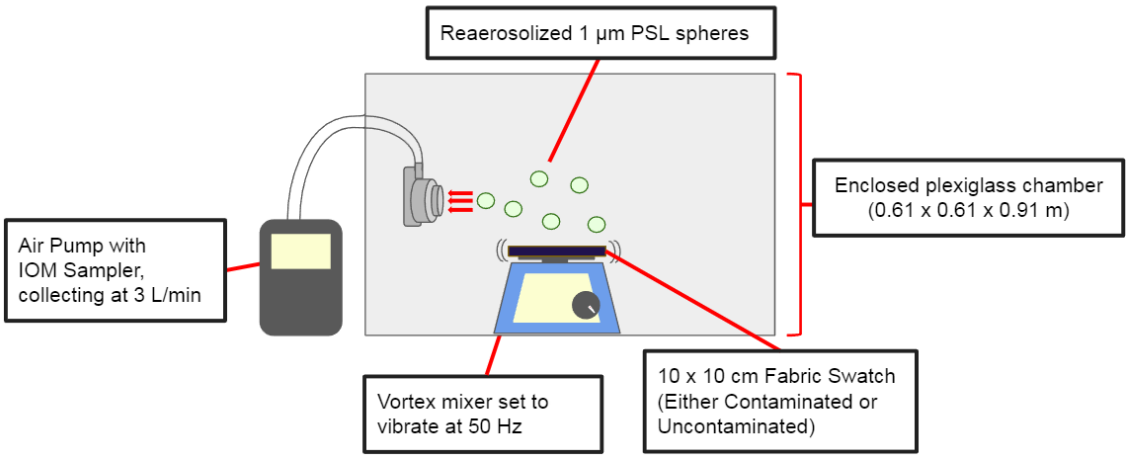

Figure 10: Graphical Representation of Reaerosolization Process

The primary method used to loft, or reaerosolize, the PSL spheres from the fabric swatches was vibration via the Vortex-Genie 2 mixer, set to vibrate in the Z-axis at 50 Hz, with moderate vibration also present in the X-axis and Y-axis directions. An accelerometer was used to verify the vibration profile of the mixer, confirming its predominant frequency of 50 Hz, shown in Figure 11 below.

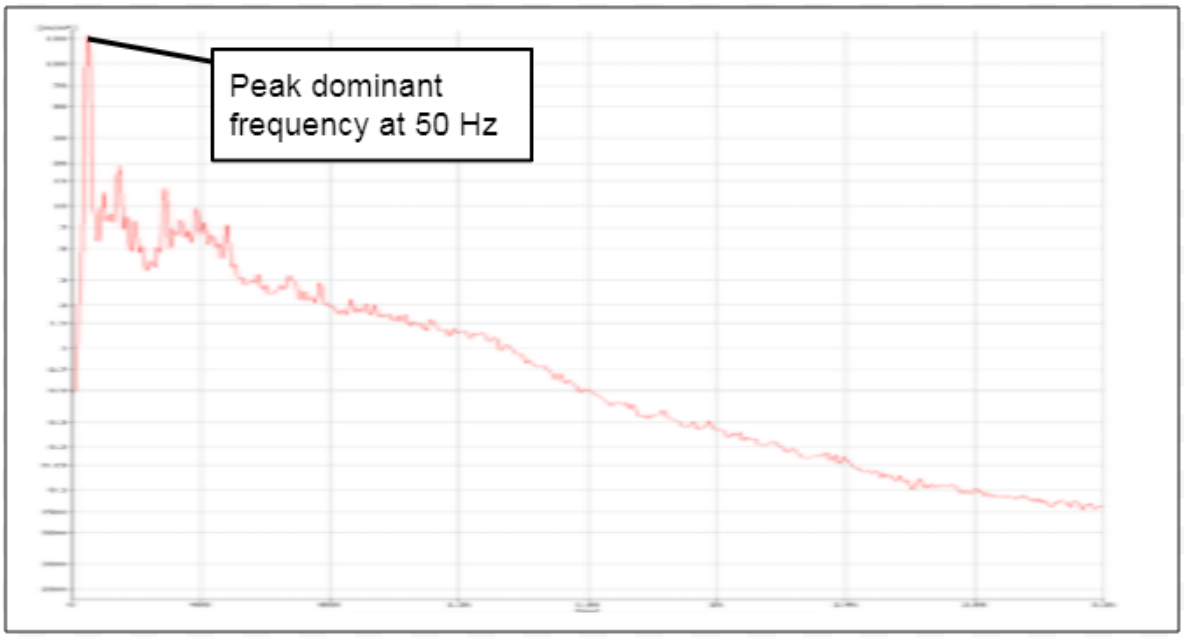

Figure 11: Vibration profile of Vortex Mixer (Frequency vs Acceleration)

In order to capture the greatest number of particles that were reaerosolized off of the ABU fabric, an air pump with a capture filter was used. The air pump was an SKC Airchek 2000 (SKC Inc, Eighty Four, PA), calibrated using a DryCal Defender 510 (Mesa Labs, Lakewood, CO). At the beginning and end of each day of trials, the air pump was pre-calibrated and post-calibrated, respectively; the average between the two flow rates would then be considered the official flow rate for that day. Typically, the pre-calibration would be set as close to 3 L/min as possible (with an average of 3.01 L/min), and the post-calibration would be just below that (with an average of 2.97 L/min), leading to an official flow rate average of 2.99

L/min. The air pump was then fitted with a 0.6 m (2 ft) length tygon tube connected to a metal IOM Multidust sampler, using a 25 mm diameter, 5 µm, polyvinyl chloride (PVC) filter (Cat. No. 225-5-25, SKC Inc, Eighty Four, PA). The 5 µm PVC filter was chosen for its consistent appearance underneath a UV microscope, able to easily distinguish between no contamination, light, heavy, and too-numerous-to-count (TNTC) contamination of PSL spheres, shown in Figure 12 below. As a note, "A" is a clean PVC filter, "B" and "C" are from reaerosolization trials, and "D" is a PVC filter placed in the aerosol chamber during initial contamination.

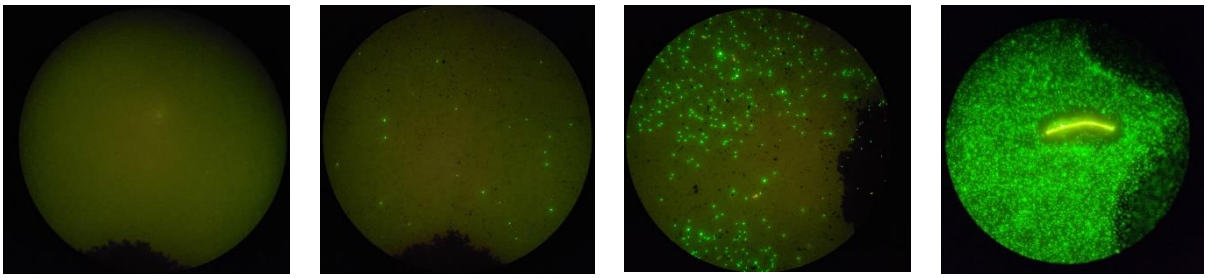

A. None B. Light C. Heavy D. TNTC

Figure 12: PVC Filter with No (A), Light (B), Heavy (C), and TNTC (D) PSL Sphere Contamination

For the experiment itself, first the fabric swatch was fixed to the vortex mixer using clips. Next, the IOM sampler was set up within a 0.3 m (1 ft) radius from the fabric swatch, with the sampler calibrated to capture air at a rate of 3 L/min. The chamber was then sealed, the mixer and pump both turned on, and a timer was set for 30 minutes. This length of time was chosen to better model the effects of a patient being transported during a medical evacuation, either on an AMBUS or a short flight.

Each 30 minute trial was alternated between using uncontaminated fabric and contaminated fabric, with all other experimental procedures held constant. For clarity,

"uncontaminated, clean," fabric swatches are ones that were *not* treated with PSL spheres, whereas "contaminated, dirty," fabric swatches are those that *were* treated with PSL spheres. These swatches will be referred to as "uncontaminated" and "contaminated" samples, respectively.

The reason for alternating uncontaminated and contaminated trials was two-fold. First, as Aim 1 of this study was to determine if 1 µm particles reaerosolize at all, a significant sample size testing the reaerosolization off of a control group (the *uncontaminated* fabric) was required. Secondarily, as sampling was not conducted outside of the aerosol chamber, once the background reaerosolization off of uncontaminated fabric was established, the uncontaminated fabric trials served to ensure that the aerosol chamber was adequately cleaned and evacuated between trials. If a trial using uncontaminated fabric was analyzed to have significant quantities of 1 µm fluorescent spheres, then the adjacent trials must also be thrown out due to the potential for cross-trial contamination in the chamber.

An overhead photograph of the setup for this process is shown below in Figure 13.

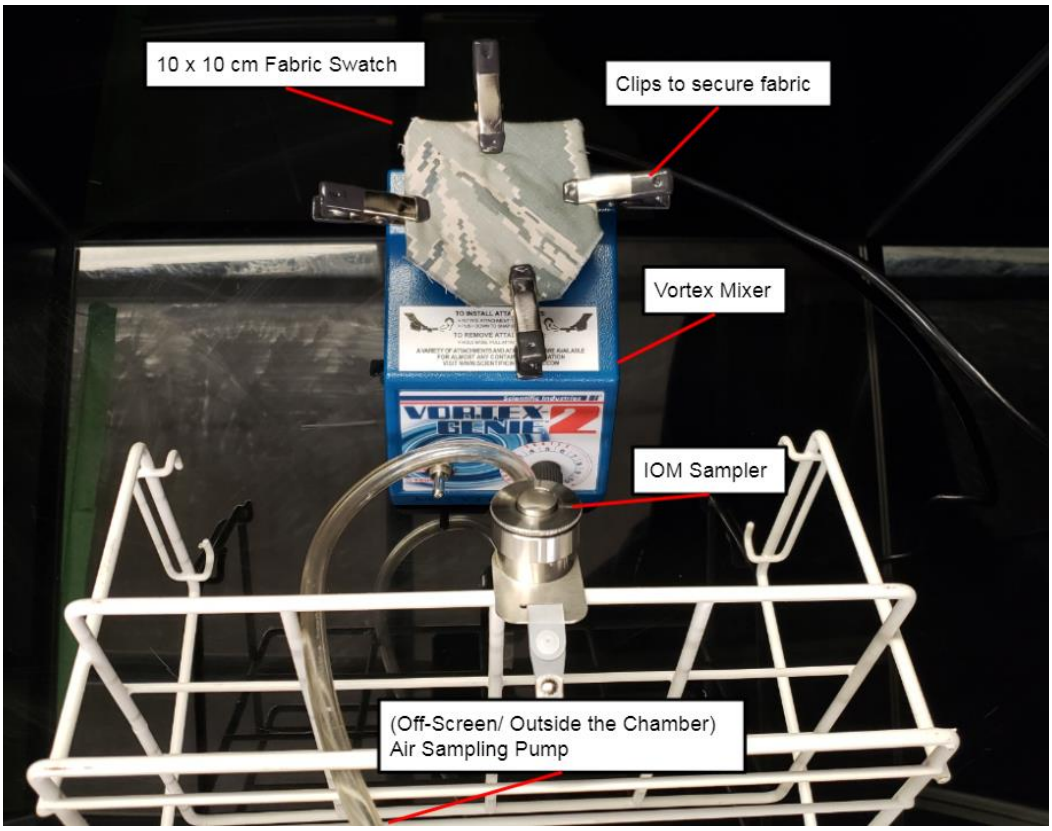

Figure 13: Overhead View of Reaerosolization Process

Decontamination Method for Removing the Biological Surrogate from the Contaminated Fabric

After testing the reaerosolization of 1 µm fluorescent spheres off of uncontaminated fabric and contaminated fabric, the next step was to apply a *decontamination* procedure to the contaminated fabric to observe its effect on reaerosolization. There are a number of options present in the literature for decontamination procedures, but for this study, a "high volume, low-pressure" water shower was chosen. For this experiment, 0.35 L of DI water was poured through a funnel into a gravity-fed shower head that would channel the water directly onto the contaminated 10 x 10 cm fabric swatch, soaking it. The water-soaked swatch would then be placed directly onto the vortex mixer, and the sample would be vibrated again using the

reaerosolization procedure. A graphical representation of the decontamination apparatus is shown in Figure 14.

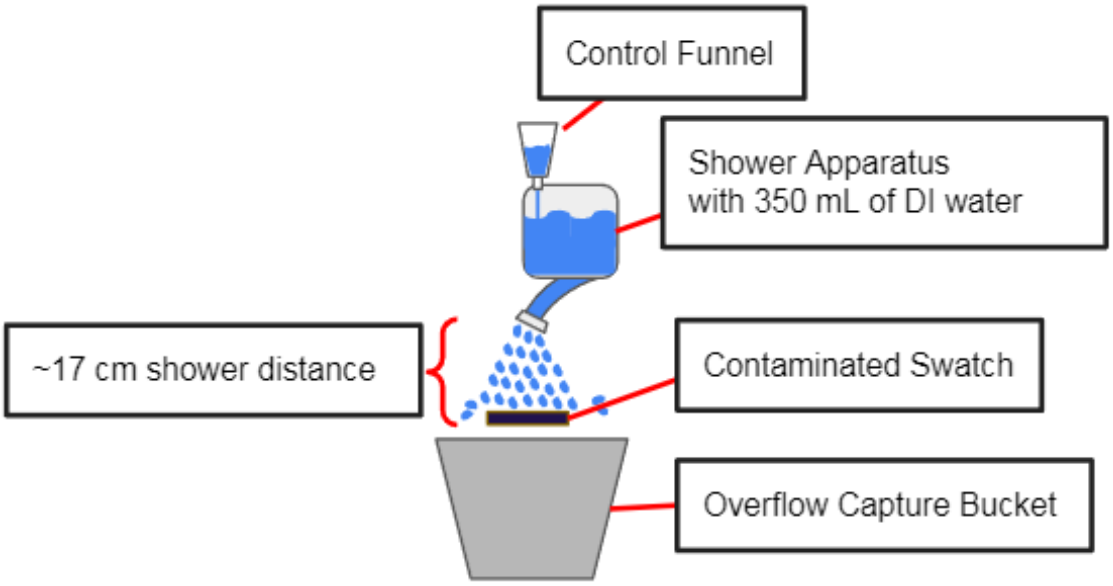

Figure 14: Graphical Representation of Decontamination Process

The decontamination apparatus consisted of an over-the-counter garden bucket with a curved shower head nozzle, fixed in place above a plate with clamps to hold the contaminated fabric swatch, above a large bucket to capture run-off. A funnel was attached at the top of the shower-bucket such that the flow of water into the apparatus was consistent between trials. It should be noted that due to gravity-fed nature of the system, the flow of water out of the shower nozzle was not perfectly consistent, and would typically follow a "ramp-up," "steady-flow," and "wind-down" pattern of flow. During the "ramp-up" and "wind-down," the shower would mildly overshoot and undershoot the fabric swatch, respectively. Nevertheless, following the decontamination procedure the fabric swatch could be qualitatively described as "soaked." Additionally, because only a 10 x 10 cm fabric square was being decontaminated, as opposed to

an entire human body, the amount of water was scaled down. Thus, 350 mL of water was used for the decontamination, which flowed out from the shower at a rate of 24.5 mL/sec. A photograph of the full decontamination process is shown in Figure 15.

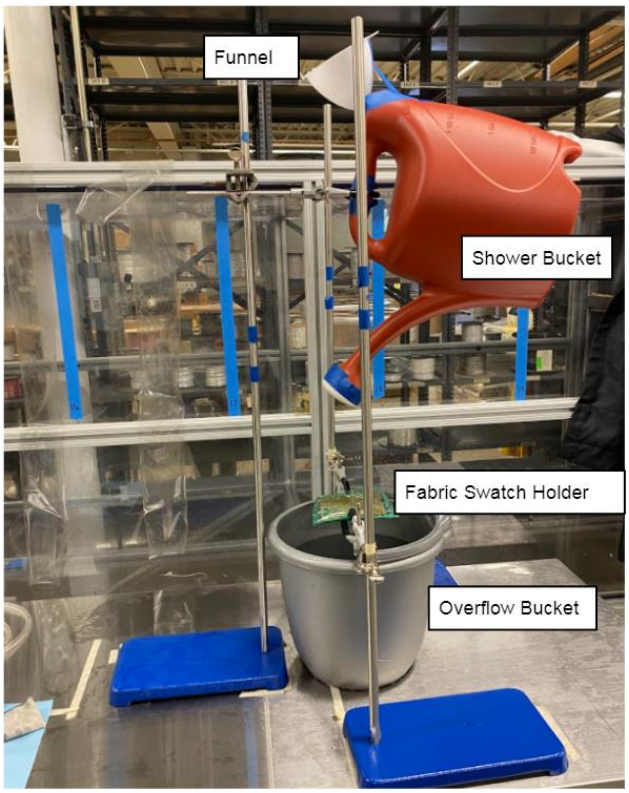

Figure 15: Decontamination Process Apparatus

Microscopy Techniques to Quantify 1 µm PSL Sphere Contamination

At each stage of the experiment, for each of the above procedures, it is imperative to be able to verify the presence of the 1 µm PSL spheres on the surface of concern. However, due to the microscopic size of the spheres, they are not visible to the naked eye. Thus, microscopic techniques must be utilized. This procedure involves analyzing samples from the contamination and reaerosolization trials under an ultraviolet microscope, and counting using both visual and computer-assisted techniques.

All samples were analyzed under a fluorescent microscope (Model: CKX41, Olympus Corp., Tokyo, Japan), set to an objective of 10x. Photographs of all samples were collected using a 12 MP camera (Samsung, Seoul, South Korea) through the view scope of the microscope. To calibrate the objective, zoom, and focus on the UV microscope, a calibration slide was used. The millimeter divisions were viewed under natural and UV light, and it was determined the diameter of any photo taken through the view scope under a 10x objective was exactly 2 mm. Photographs from this calibration are shown below in Figure 16, with "A" being an unmagnified photograph of the glass calibration slide, marking each division as 0.1 mm. Images "B" and "C" represent the slide under 10x magnification, where twenty divisions can be counted in both images, representing 2 millimeters.

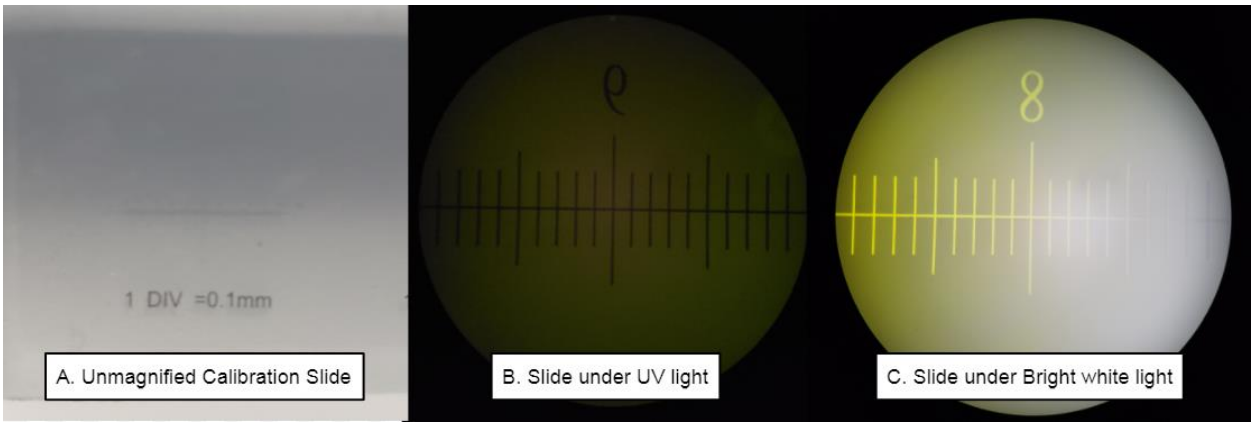

Figure 16: Determination of Microscope Imaging Diameter Using a Calibration Slide

To ensure a consistent approach was used to image and count each sample, a standardized analysis procedure was established. As it was infeasible to fully and consistently analyze the entirety of every sample, each 25 mm diameter PVC filter was marked using a fine-tip marker with five points, shown below in Figure 17.

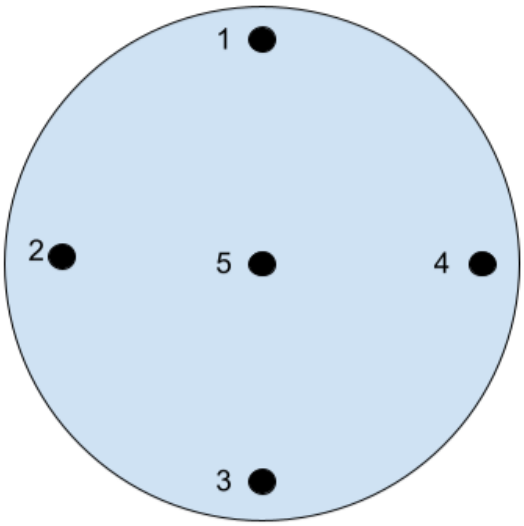

Figure 17: Graphical Representation of Marked Sample Filter

Starting at the marked position 1, a photograph would be taken just inside the position marker such that black spot would be barely visible. This was repeated for positions 2 through 4; for position 5, the photograph would be taken on the side of the mark which appeared to have the highest visible contamination. While the method for choosing position 5 introduces a small amount of sampling bias, this method was chosen in order to better model "worst-case" reaerosolization. As the scientific aim of this study was to quantify reaerosolization for risk analysis, it was determined to be better to inadvertently overestimate the risk, than inadvertently underestimate the risk. Ultimately, this methodology balances out consistency with designated locations on positions 1-4, with a focus on "worst-case" conditions with position 5. As a note, as PSL distribution was consistent across the filters for the clean, dirty, and water series, the selection method for position 5 did not introduce bias to the data set. However, for a single sample in the post-decontamination series, the selection of position 5 did cause an outlier sample due to a large droplet (this is expanded upon in the Discussion section of this report).

All images were saved as a JPEG file type, and named using a standardized convention, based on their sample ID. The basic file naming convention followed the format: MMDDT#L#, explained in Table 4 below.

Table 4: File Naming Conventions

MM	**DD**	**T#**	**L#**
Month (i.e. 11)	Day (i.e. 04)	Sample Type and Trial Number C = "Clean" Fabric D = "Dirty" Fabric W = "water" or decontaminated "Clean" fabric P = "Post-decontamination" of "Dirty" fabric	Location Number
Example: File named "1117P2L4" represents the second post-decontamination trial on date November 17th, at Location #4 under the microscope.			

Quantifying contamination was treated in two different ways for fabric swatch initial contamination verification and for reaerosolization filter analysis. After the fabric swatch contamination procedure, it was important to visually verify that the swatches were in fact contaminated before testing them for reaerosolization. However, due to the many-layered nature of fabric fibers as well as the TNTC concentration of PSL spheres, it was infeasible to attempt to make an accurate count of PSL sphere contamination. As a note, it is for this same reason that PVC filters were used during reaerosolization trials instead of fabric swatches, as the PVC filters only have a single-layered surface, making quantification feasible.

Instead, each fabric swatch was carefully checked under the UV microscope for a qualitative, binary presence/ absence of PSL spheres. Using this method, it was determined that all fabric swatches in the aerosol chamber during contamination were contaminated; however, if some swatches exhibited higher levels of contamination, it was not captured using this

method. An example of a contaminated, undyed segment of ABU fabric is shown in Figure 18.

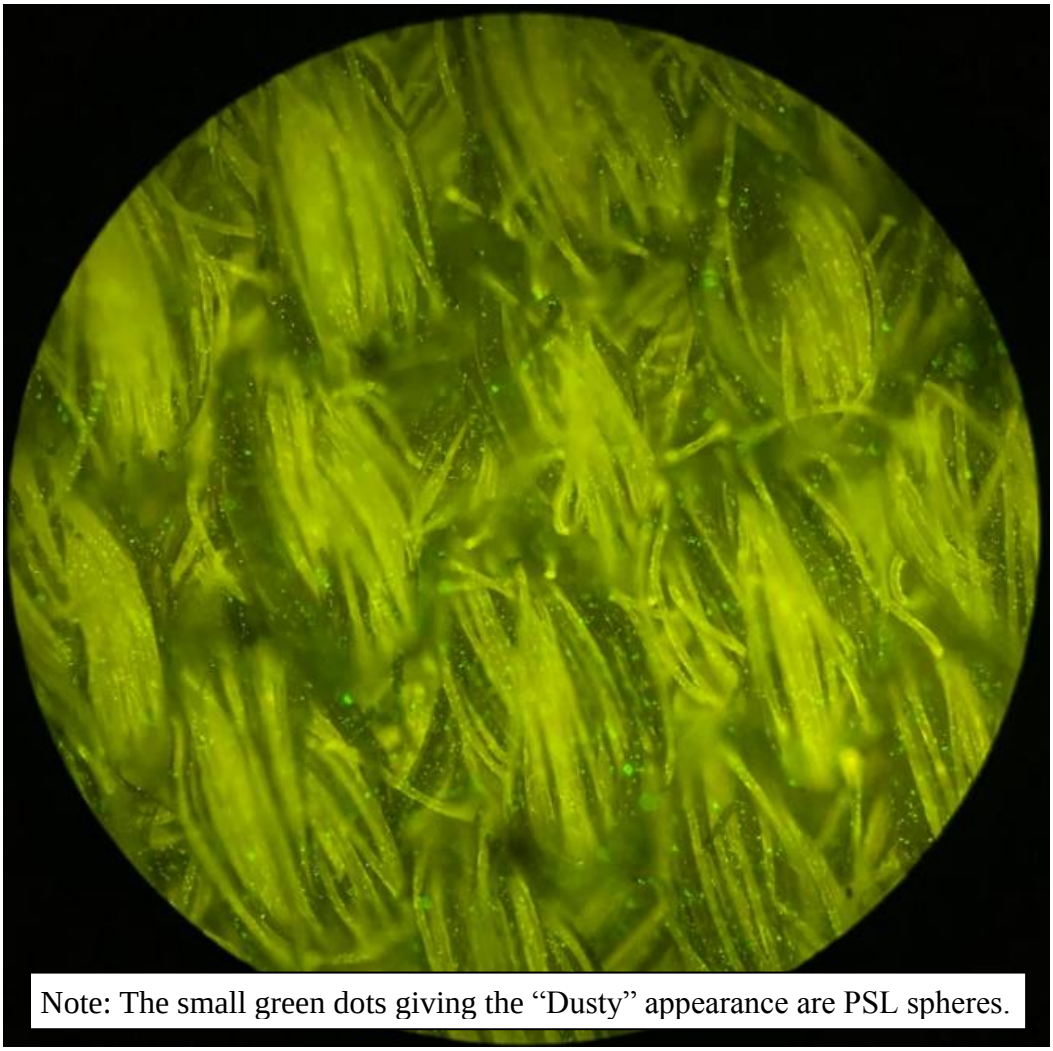

Figure 18: Contaminated Undyed ABU Fabric, Concentration TNTC

For the reaerosolization trials, both visual and computer techniques were used to quantify filter contamination. In the visual method, the observer took each of the five photographs for each filter, and counted the number of bright green-fluorescent 1 µm sphere-like particles present in each image. As the PSL spheres were designed to fluoresce bright green under ultraviolet light, they were relatively easily picked apart from other dusts that may have been collected on the sample filters. The guiding principles for counting particles are presented below in Table 5.

Table 5: Counting Rules for PSL Sphere Presenting Particles

Counting Rules:

A. Particle must be round
    a. Aspect ratio cannot exceed 1.5:1
    b. Fibers and irregularly shaped particles not counted
B. Particle must be small
    a. Cannot exceed ~1.5 µm diameter
C. Particle must be the proper color
    a. Must fluoresce under UV light as a distinctly bright green
    b. Color guide:

Bright Green	Dull Green	Yellow	Orange/other
YES	NO	NO	NO

Nevertheless, because the photographs were analyzed via a human eye, there is still room for human error in counting and determining what is and is not a PSL sphere. Some examples of what was counted and not counted are presented below in Figure 19.

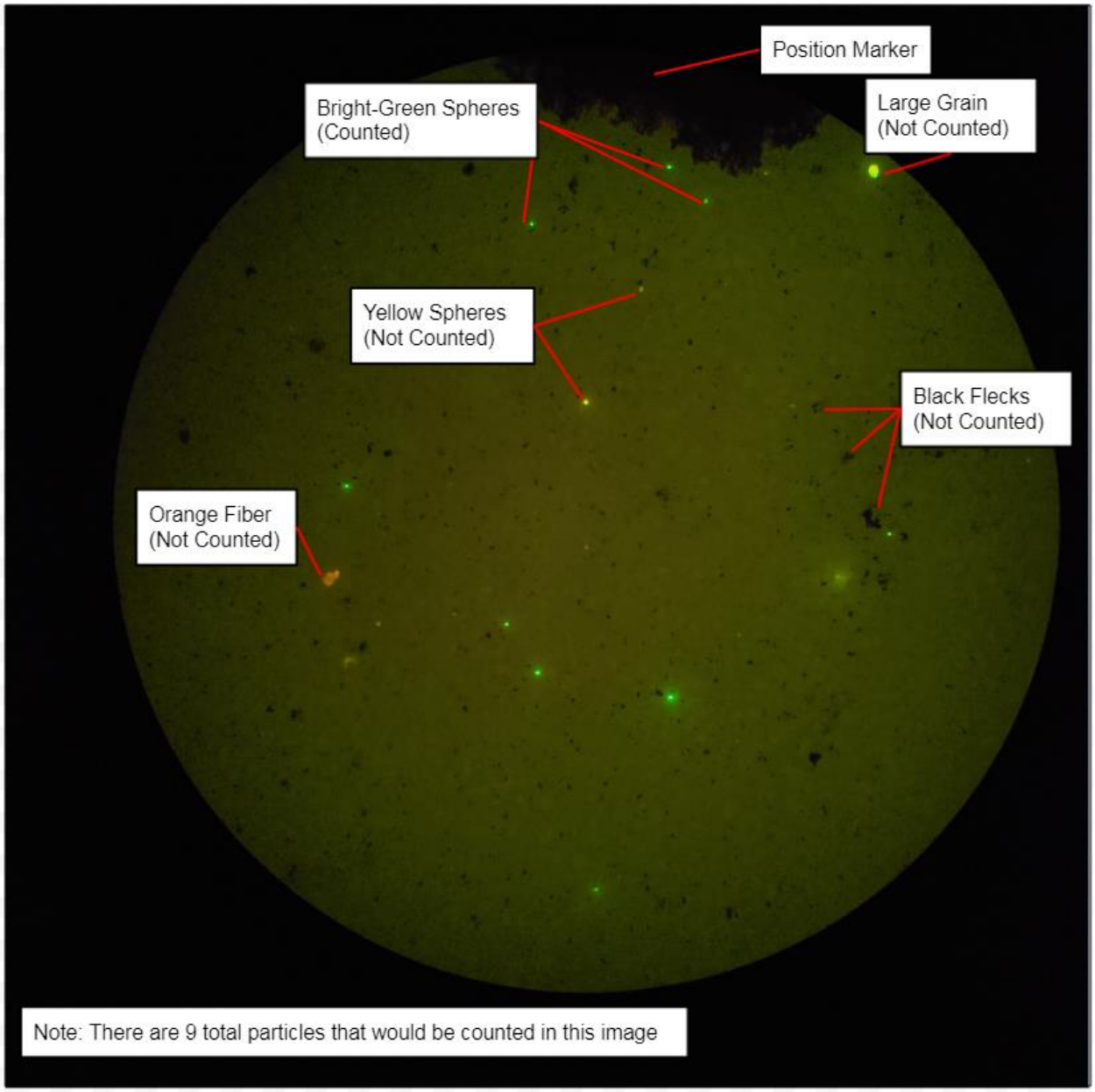

Figure 19: Quick-Guide on Counting PSL Spheres on PVC Filter Under UV Light

While the human eye method works well for filters with only low to mild contamination, it is not feasible for repeated samples with high to near-TNTC concentration. Thus, a repeatable computer method was also established using the public software program Image J. Image J is an open-source software specifically designed to count bacteria on sample slides, and was able to be translated to counting fluorescent PSL spheres. To use this program, each photograph

needed to be converted to an “8-bit” black and white image, the background subtracted, and a threshold applied to instruct the software on how to identify the particles to count. The parameters given to the computer matched the human-eye counting rules for particle size and roundness, but used brightness instead of color due to the 8-bit black and white image requirement. A macro was developed to ensure these parameters were consistent between analyzing multiple photographs, as well as consistent with the “Counting Rules” established for the human eye method. For example, an errant fiber would not be counted by the program due being filter out for a non-circular shape, too-large size, and incorrect brightness. In developing the computer method, several photographs were also counted by hand to ensure counts were consistent between both methods. A timeline of the computer image process is shown in Figure 20, where the original image “A” is converted into a black and white 8-bit image “B”, and then counted and annotated by the software “C”.

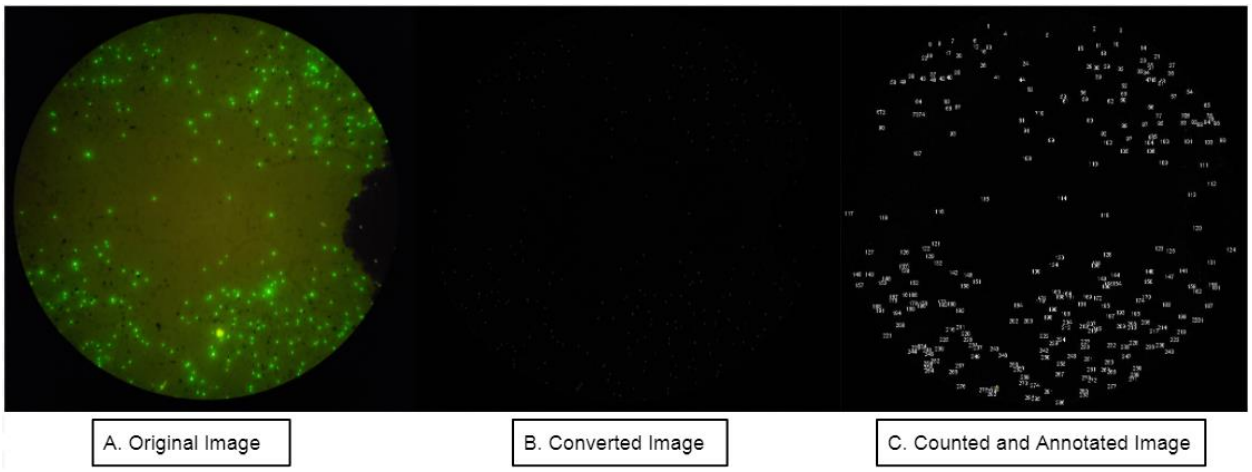

Figure 20: Steps in the Image-J Software Particle Counting Process, from Original Image (A), Converted into usable format (B), and Counted (C)

Additionally, there was concern that after converting each original image to an 8-bit black and white image, the computer would not be able to tell the difference between a green particle and a yellow particle of similar fluorescence. For this reason, a sample of images were selected to be counted via both human eye and computer techniques to "calibrate" the computer method. A side-by-side comparison between the human method "A" and computer method "B" is shown in Figure 21.

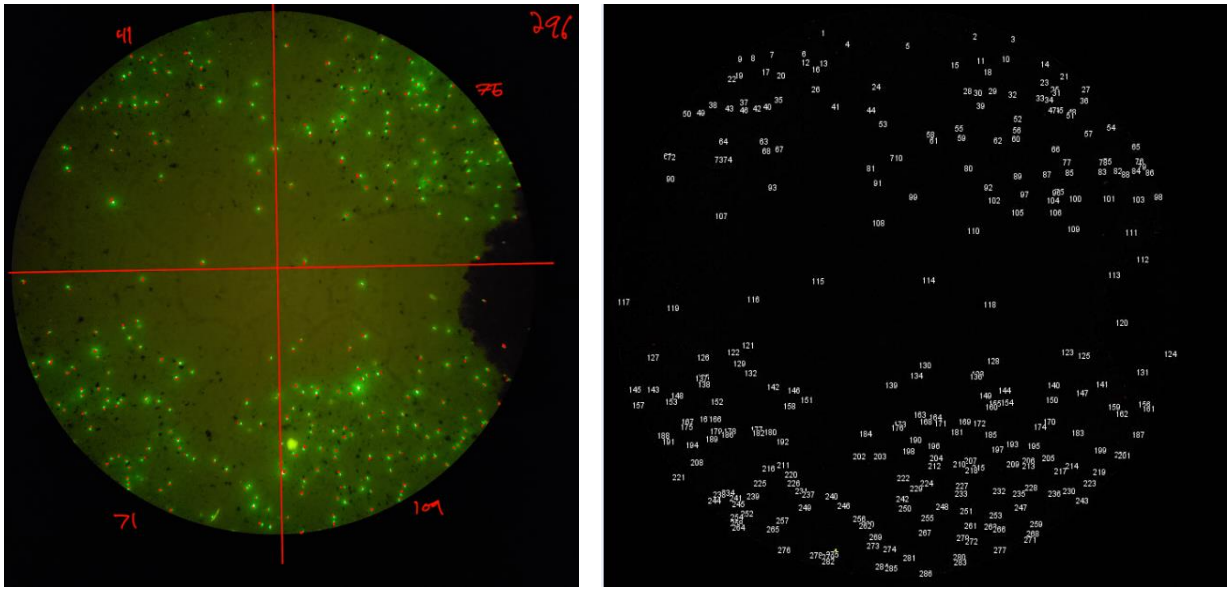

A. Human Eye **B. Computer**

Figure 21: Side-by-Side of Human Eye (A) and Computer (B) Counting Techniques (296 particles vs 286 particles [~3.5% difference])

Additionally, there was an increased concern that the visible yellow circles produced by the water droplets in the decontamination trials (water and post-decontamination series) would inhibit Image J's ability to count PSL spheres. When tested, this concern seemed to be true with low-concentration images, but not with high-concentration images. Using the same standardized macro written for the dirty series tests, the decontamination trials produced very similar counts to the human eye counts for the same images for images with many PSL spheres

(as shown in Table 6.A and C); however, without the presence of a large number of PSL spheres, the program is unable to establish a strong background, leading to significant computer error (as shown in Table 6.B and D). Thus, Image J is an effective tool for counting particles even under the effects of water droplets only when the image is confirmed to have PSL spheres prior to counting. The validation process used is shown below in Table 6.

Table 6: Side-by-Side of Human Eye (A and B) and Computer (C and D) Counting Techniques Under the Effects of Water Droplets.

Human Eye	**Computer**
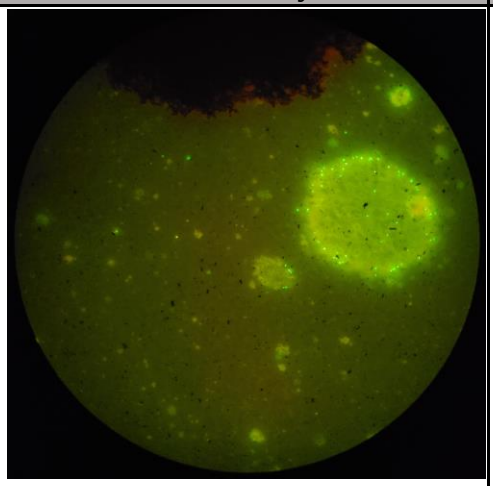 **A:** Count: 71 particles	 **C:** Count: 74 particles (~4% difference)
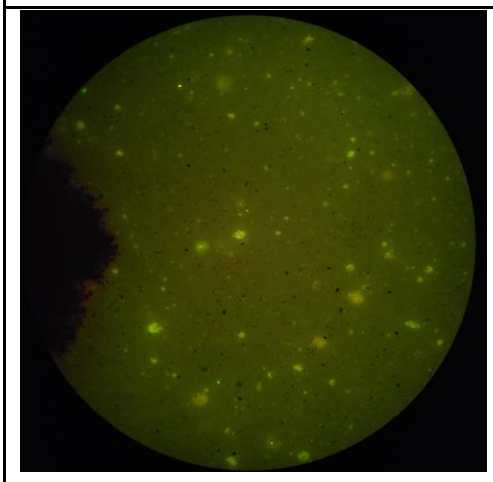 **B:** Count: 2 particles	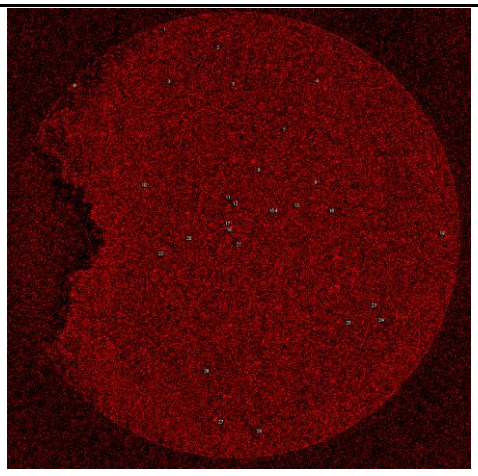 **D:** Count: 28 particles (1,300% difference – significant computer error)

Ultimately, it was determined that both human eye and computer techniques were viable methodologies, depending on the scenario. For samples with little to no presence of particles, the human eye method was both faster and more reliable. For heavily contaminated samples, while both methods proved accurate, the computer technique was significantly faster (~2 minutes per image versus ~15 minutes per image for human eye counting). However, at extremely high contamination levels (>10,000 particles per image) counting became infeasible per both techniques, and the image would be considered too-numerous-to-count (TNTC). A guide for when to use which technique is presented below in Figure 22.

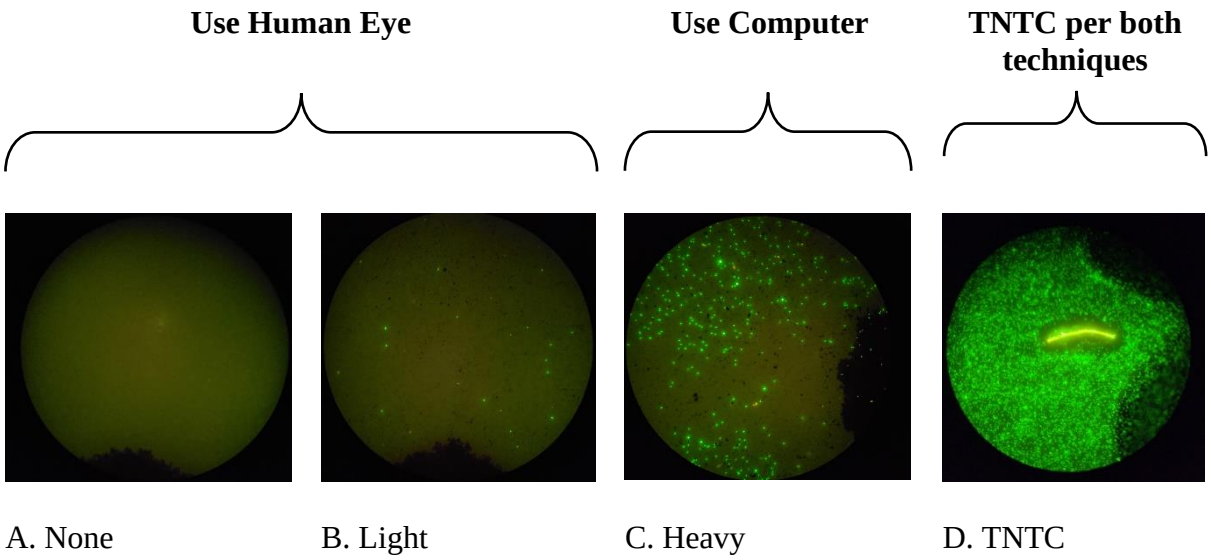

Figure 22: When to Use Human Eye versus Computer Techniques when Counting

At this point, the number of particles counted in each photograph represented "the number of green-fluorescent spheres per 2 mm diameter circular section." In order to convert this number into a concentration, several transformations must be applied. First, the sum of the

number of particles over the five photographed areas was linearly scaled up via the ratio between total area of the photographs, and the total area of a 25 mm diameter filter, shown in Equation 3.

Equation 3: Estimation of Particles per Filter

$$n_{filter} = \sum(n_{photo}) * \left(\frac{A_{filter}}{\sum A_{photo}}\right) \quad \textbf{(1)}$$

Where:

n_{filter} = Number of particles per filter
Σn_{photo} = Sum of counter particles per five photographs
A_{filter} = Area of entire filter
ΣA_{photo} = Sum of Areas per five photographs

And, $\sum A_{photo} = 5 * \frac{\pi}{4} * d^2$ **(2)**

Where:

A_{photo} = Area of photographed section (m^2)
d = Diameter (m) = 2 mm = $2*10^{-3}$ m

The resulting number from the above equation estimates the total number of particles per filter; however, for the reaerosolization trials it was of particular interest to view these values in units of airborne concentration, or particles per volume of air. To perform this transformation, the total number of particles per filter was divided by total volume of air captured per trial, to give a concentration in units of particles/m^3. In order to find the total volume for each trial, the length of time (in minutes) for each trial was multiplied by the flow rate during the trial (in liters/minutes), and then converted into units of meters-cubed (m^3). These transformations are shown below in

Equation 4 and Equation 5.

Equation 4: Calculation of Sample Volume

(1)

$$V = Q * t * \frac{1\ m^3}{1000\ L}$$

Where:

V = Total sample volume (m^3)
Q = Sample flow rate (L/min)
t = Sample time (min)

Equation 5: Calculation of Particle Concentration

(1)

$$C = \left(\frac{n_{filter}}{V}\right)$$

Where:

C = Sample concentration (particles/m^3)
n_{filter} = Number of particles per filter
V = Total sample volume (m^3)

It should be noted that each of these transformations from particles per photograph into concentration are linear scaling, and thus makes no difference in regards to comparing results. However, by putting units of results into units of concentration, they become more useful for consideration as a biological surrogate that has been reaerosolized.

Experimental Sample Swatch Selection

For the two types of "control" groups (dry fabric and wet, "decontaminated" fabric), clean 10 x 10 cm ABU swatches were kept in a sealed container, and a fresh swatch would be pulled out for each new trial. For the experimental groups, "contaminated" swatches were required for two separate types of trials: direct reaerosolization, and reaerosolization following

decontamination procedures. While all fabric swatches that were contaminated during the contamination process were determined to have TNTC amounts of PSL spheres, extra steps were taken to remove selection bias from the sampling procedure. As previously mentioned, during the contamination process, the fabric swatches were numbered by column and annotated as being in the near, middle, or far region of the aerosol chamber. Using this layout as a guide, swatches were carefully pre-designated for use in "direct reaerosolization" or "post-decontamination" trials to ensure a balanced sample size across all points in the aerosol chamber during contamination. The layout of the fabric swatches, annotated with their predesignated sample ID for trials, is shown in Figure 23.

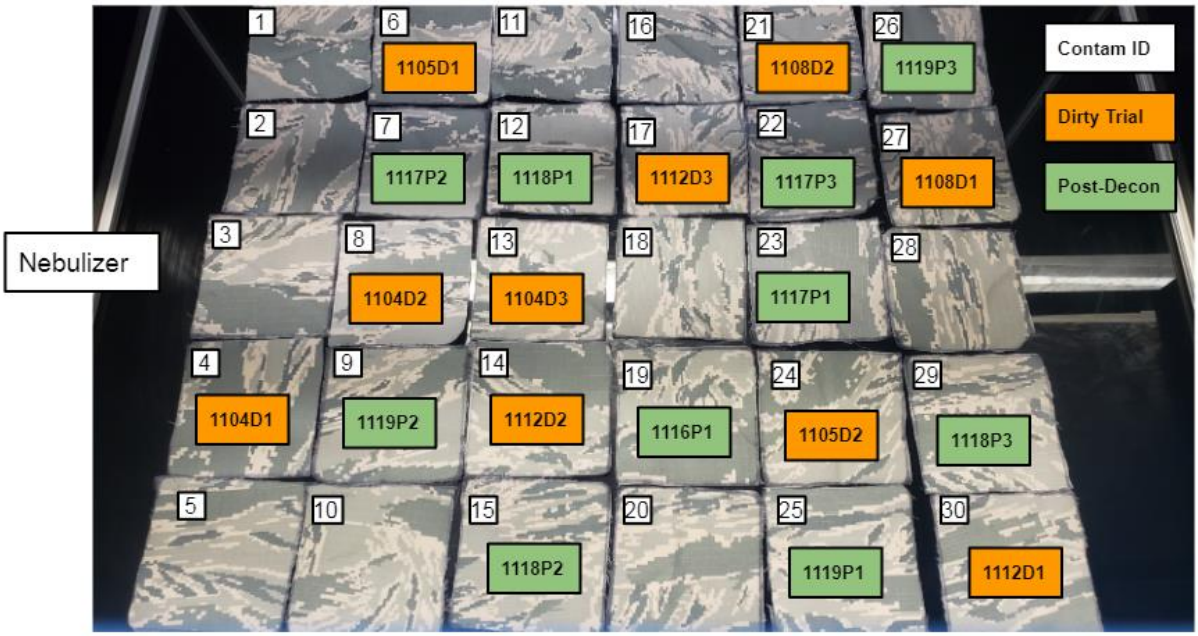

Figure 23: Predesignated Sample IDs Based on Contamination Placement

Summary of Methodology

This chapter included a description of the experimental design of this study, as well as the four primary methodologies developed for the quantification of reaerosolized biological surrogate particles: Contamination using a Collison Nebulizer; Reaerosolization using a laboratory mixer and collection using an air pump and inhalable air sampler with a polyvinyl chloride (PVC) filter; Decontamination using a gravity-fed water shower; and Quantification using ultraviolet (UV) microscopy techniques via both human eye and computer techniques.

IV. Results

Chapter Overview

This chapter includes the experimental results from the study using methodology described above, as well as a statistical analysis of those results.

Contamination

To ensure that the PSL spheres successfully deposited onto the 10 x 10 cm ABU fabric swatches, each swatch was analyzed under a UV microscope for contamination. As it was not deemed feasible to obtain an accurate count for each swatch, they were instead analyzed qualitatively as “contaminated” or “not contaminated.” The results for the analysis of the initial contamination phase are presented in Table 7.

Table 7: Swatch Contamination Confirmation

Contamination ID	Region of Chamber	Presence of PSL Sphere Contamination (Y/N)				
		Location 1	Location 2	Location 3	Location 4	Location 5
1	Near-side	Y	Y	Y	Y	Y
2	Near-side	Y	Y	Y	Y	Y
3	Near-side	Y	Y	Y	Y	Y
4	Near-side	Y	Y	Y	Y	Y
5	Near-side	Y	Y	Y	Y	Y
6	Near-side	Y	Y	Y	Y	Y
7	Near-side	Y	Y	Y	Y	Y
8	Near-side	Y	Y	Y	Y	Y
9	Near-side	Y	Y	Y	Y	Y
10	Near-side	Y	Y	Y	Y	Y
11	Middle	Y	Y	Y	Y	Y
12	Middle	Y	Y	Y	Y	Y
13	Middle	Y	Y	Y	Y	Y
14	Middle	Y	Y	Y	Y	Y
15	Middle	Y	Y	Y	Y	Y
16	Middle	Y	Y	Y	Y	Y
17	Middle	Y	Y	Y	Y	Y
18	Middle	Y	Y	Y	Y	Y
19	Middle	Y	Y	Y	Y	Y
20	Middle	Y	Y	Y	Y	Y
21	Far-side	Y	Y	Y	Y	Y
22	Far-side	Y	Y	Y	Y	Y
23	Far-side	Y	Y	Y	Y	Y
24	Far-side	Y	Y	Y	Y	Y
25	Far-side	Y	Y	Y	Y	Y
26	Far-side	Y	Y	Y	Y	Y
27	Far-side	Y	Y	Y	Y	Y
28	Far-side	Y	Y	Y	Y	Y
29	Far-side	Y	Y	Y	Y	Y
30	Far-side	Y	Y	Y	Y	Y

Uncontaminated (Clean-Series) Results

After confirming contamination of the sample swatches, reaerosolization trials began. Trials were conducted in the alternating order of "clean, dirty, clean, dirty, etc." for the duel purpose of establishing a baseline background, and to ensure chamber decontamination procedures between trials was effective. After sampling, filters were analyzed under the UV microscope. The raw counts were then averaged over the full filter surface area, and divided by sample volume to achieve a particle concentration in units of particles per meter cubed.

A small selection of representative photographs taken from the analysis of the uncontaminated (clean-series) filters is presented in Figure 24. It should be noted that with the exception of rare 1 μm green-fluorescent round particles, there were little to no particles that appeared to be PSL spheres on any of the samples of the clean-series trials (shown in Figure 24.A). Occasionally it was noticed that a number of fluorescent particles would be on the sample filter; however, these would either be the incorrect shape, color, or size to be counted as a PSL sphere. For example, in Figure 24.B in the middle photograph, there were two small particles that were distinctly a specific shade of green, small, and circular. Thus, even though the image at a distance has many visual "specks," only two fit the criteria for a "PSL sphere representing particle." The rightmost image in Figure 24.C shows an auto-fluorescing fiber on the sample filter. This was not counted as a PSL sphere, and was most likely present on the PVC filter even before being used in the experiment. As a note, errant fibers were not solely limited to appearing in the clean-series trials; they occasionally showed up at all stages of experimentation, but were never counted as a form of contamination.

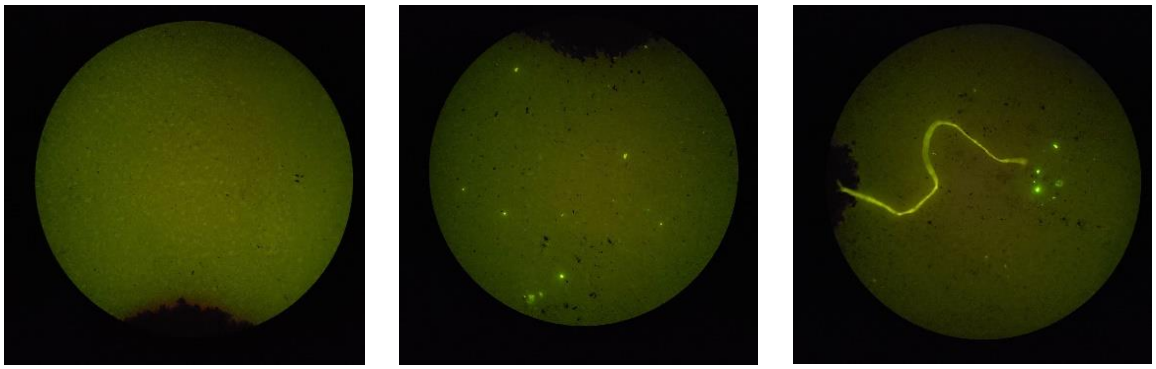

A. No Particles (most common)

B. Auto-flourescent yellow particles (not PSL spheres)

C. Errant Fiber

Figure 24: Representative Photographs of Clean-Series Trials

The average particle counts for each sample in the uncontaminated (clean-series) trials is presented in Table 8. As a note, the average count per filter was calculated using Equation 3, and the average airborne concentration was calculated using Equation 5. The highest number of PSL-representing particles on any single image was 2 particles, with the most common number being zero particles per image.

Table 8: Clean-series Fabric Reaerosolization Trials Filter Particle Counts

Sample ID	Average Count per 5 Images (part/image)	Average Count per Whole Filter (part/filter)	Average Concentration of Reaerosolized PSL Spheres (part/m^3)
1104C1	1	156.25	$1.74*10^3$
1104C2	0.4	62.5	$6.97*10^2$
1104C3	0.2	31.25	$3.48*10^2$
1105C1	0.4	62.5	$6.97*10^2$
1105C2	0.2	31.25	$3.48*10^2$
1105C3	0.6	93.75	$1.04*10^3$
1108C1	0.6	93.75	$1.04*10^3$
1108C2	0.6	93.75	$1.04*10^3$
1112C1	0.6	93.75	$1.04*10^3$
1112C2	0.6	93.75	$1.04*10^3$
1112C3	0.6	93.75	$1.04*10^3$
Average	0.53	82.38	$9.18*10^2$

Additionally, standard descriptive statistics results for the clean-series reaerosolization trials are presented in Table 9.

Table 9: Clean-Series Reaerosolization Concentrations of PSL Spheres

Attribute	Value (particles/m^3)
Average (x)	$9.18*10^2$
Sample Size (n)	11
Standard Deviation (s)	$3.9*10^2$
Minimum	$3.48*10^2$
Median	$1.04*10^3$
Maximum	$1.74*10^3$

Contaminated (Dirty-Series) Results

Next, a small selection of representative photographs taken from the analysis of the contaminated (dirty-series) filters is presented in Figure 25. All ten of the dirty-series trials showed the presence of PSL sphere-appearing particles, typically spread fairly evenly (or randomly) across the filter. Particle concentrations were generally consistent across the five analyzed locations on a single sample filter; however, there was significant variation in concentrations between different samples. For example, a sample with "low concentration" as shown by the leftmost image of Figure 25.A consistently showed 5-9 particles per image at any given location on the sample filter. Likewise, the sample with "high concentration" in Figure 25.B, and the sample with "very high concentration" as shown by the rightmost image of Figure 25.C also showed very consistent contamination at all locations across that sample.

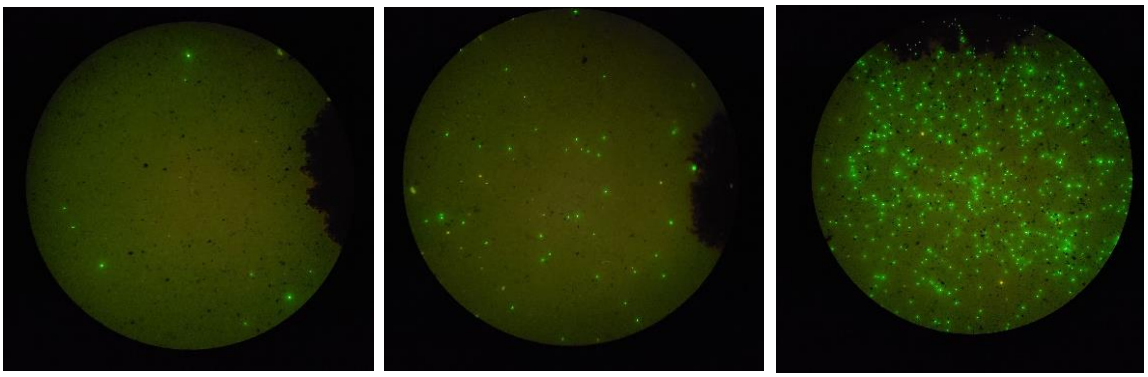

A. Low Concentration B. High Concentration C. Very High Concentration

Figure 25: Representative Photographs of Dirty-Series Trials

The average particle counts for each sample in the contaminated (dirty-series) trials is also presented in Table 10, with the average count per filter calculated using Equation 3, and the average airborne concentration calculated using Equation 5. In this table it can be seen again that samples tended to fall into the low (below 10), high (10-100), or very high (>100) categories. Of

particular note is sample 1108D2, which showed an average concentration of greater than ten-times the next highest sample.

Table 10: Dirty-series Fabric Reaerosolization Trials Filter Particle Counts

Sample ID	Average Count per 5 Images (part/image)	Average Count per Whole Filter (part/filter)	Average Concentration of Reaerosolized PSL Spheres (part/m^3)
1104D1	6.4	1000	$1.11*10^4$
1104D2	15.8	2468.75	$2.75*10^4$
1104D3	7.4	1156.25	$1.29*10^4$
1105D1	6.4	1000	$1.11*10^4$
1105D2	37.8	5906.25	$6.58*10^4$
1108D1	12.6	1968.75	$2.19*10^4$
1108D2	408.6	63843.75	$7.12*10^5$
1112D1	26	4062.5	$4.53*10^4$
1112D2	23.4	3656.25	$4.07*10^4$
1112D3	33.2	5187.5	$5.78*10^4$
Average	57.76	9025	$1.01*10^5$

Additionally, standard descriptive statistics results for the dirty-series reaerosolization trials are presented in Table 11. It is of particular interest that the standard deviation is greater than average itself, indicating significant variation in the data set.

Table 11: Dirty-Series Reaerosolization Concentrations of PSL Spheres

Attribute	Value (particles/m^3)
Average (x)	$1.01*10^5$
Sample Size (n)	10
Standard Deviation (s)	$2.16*10^5$
Minimum	$1.11*10^4$
Median	$3.41*10^4$
Maximum	$7.12*10^5$

Decontaminated Clean (Water-Series) Results

Once ten trials were completed for the clean and contaminated fabric, another ten trials were collected - this time using the decontamination procedure. Trials were again conducted in the alternating order of "control, experimental, control, experimental," and converted into units of concentration (part/m^3).

A small selection of representative photographs taken from the analysis of the Decontaminated-clean (water-series) filters is presented in Figure 26. During analysis, it was observed that there was a significant increase in yellow-ish marks on the sample filters, which were likely due to the effects of the water droplets on the PVC filter, as shown in Figure 26.A. While from a distance it appears as though there is contamination on the sample filter, these yellow-ish water particles are visually distinct from the characteristic PSL-sphere-representing particles, and were not counted as such. There were also a number of new phenomena observed on the sample filters that were likely the result of water droplets. For example, as shown in the center image of Figure 26.B, the black ink used to designate analysis locations was bled into a

pink-orange shade. Additionally, some filters included large yellow spots, most likely the result of a large water droplet being captured on the PVC filter during sampling, as shown in Figure 26.C.

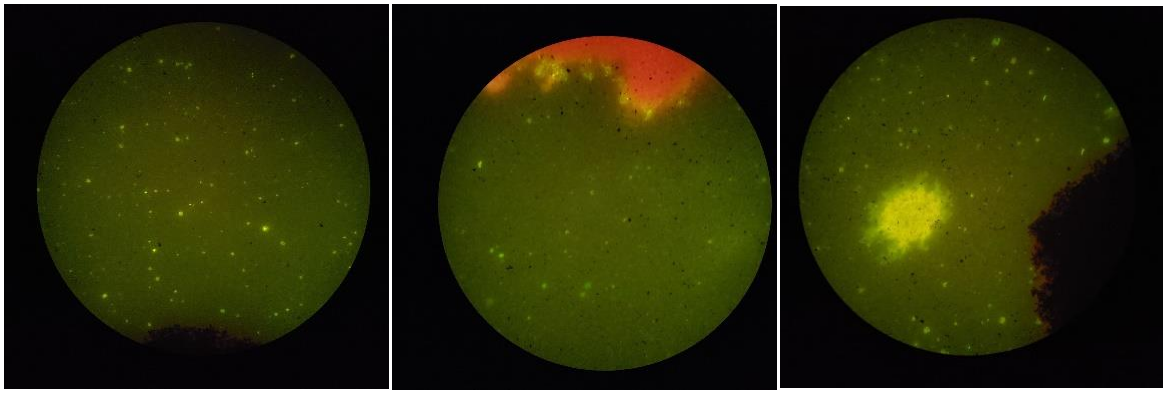

A. High Droplet Concentration (no PSL spheres)

B. Water Altering PVC Filter Colors

C. Large Water Droplet

Figure 26: Representative Photographs of Water-Series Trials

The average particle counts for each sample in the decontaminated-clean (water-series) trials is also presented in Table 12, with the average count per filter calculated using Equation 3, and the average airborne concentration calculated using Equation 5.

Table 12: Water-series Clean Fabric Reaerosolization Trials Filter Particle Counts

Sample ID	Average Count per 5 Images (part/image)	Average Count per Whole Filter (part/filter)	Average Concentration of Reaerosolized PSL Spheres (part/m^3)
1116W1	0.4	62.5	$6.97*10^2$
1117W1	0.2	31.25	$3.48*10^2$
1117W2	0.4	62.5	$6.97*10^2$
1117W3	0.2	31.25	$3.48*10^2$
1118W1	1.2	187.5	$2.09E*10^3$
1118W2	0.4	62.5	$6.97*10^2$
1118W3	1	156.25	$1.74*10^3$
1119W1	0.8	125	$1.39*10^3$
1119W2	0.4	62.5	$6.97*10^2$
1119W3	1.2	187.5	$2.09*10^3$
Average	0.62	96.875	$1.08*10^3$

Additionally, standard descriptive statistics results for the water-series reaerosolization trials are presented in Table 13.

Table 13: Water-Series Reaerosolization Concentrations of PSL Spheres

Attribute	Value (particles/m^3)
Average (x)	$1.08*10^3$
Sample Size (n)	10
Standard Deviation (s)	$6.86*10^2$
Minimum	$3.48*10^2$
Median	$6.97*10^2$
Maximum	$2.09*10^3$

Decontaminated Dirty (Post-decontamination-Series) Results

As with the other trials, a small selection of representative photographs taken from the analysis of the decontaminated-dirty (post-decontamination-series) filters is presented in Figure 27. There are several interesting phenomena that appeared in the post-decontamination series of trials. The majority of sample locations analyzed visually appeared very similar to those in the water-series trials, with the addition of sparse green PSL sphere-representing particles, as shown in the leftmost image of Figure 27.A. Additionally, unlike the dry reaerosolization dirty-series trials, particle counts at the different analysis locations across a single sample filter were not consistent. To illustrate, all three images in Figure 27 were taken from a single sample filter. Three analysis locations looked like the leftmost image, with only 3-5 PSL spheres-representing particles. However, the last analysis locations, shown in Figure 27 B and C, contained large droplets and showed a significantly higher concentration of PSL spheres-representing particles — concentrated entirely within the droplets. This trend was present in other post-decontamination trials as well: if the sample contained large droplets, it contained many PSL spheres; if the sample contained no large droplets, it contained little to no PSL spheres.

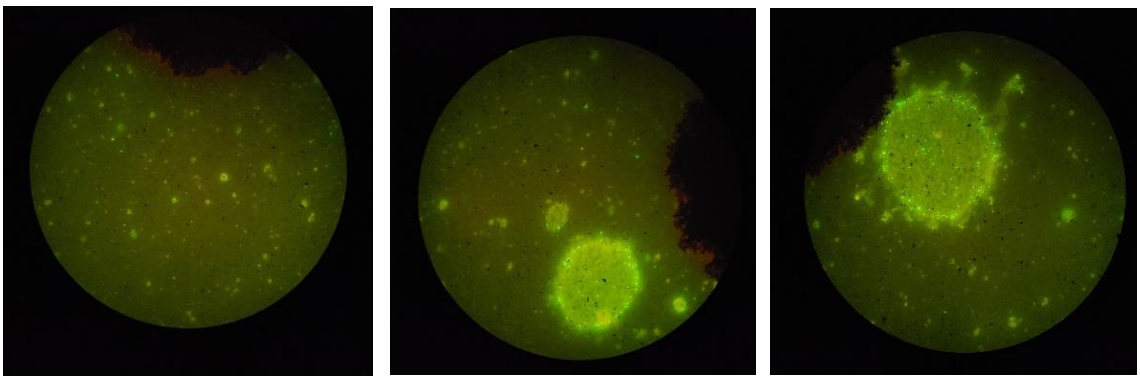

A. High concentration of yellow-drops; very few green PSL Spheres

B. Multiple large droplets carrying PSL Spheres

C. Very Large Water Droplet filled with PSL spheres

Figure 27: Representative Photographs of Post-Decontamination-Series Trials

The average particle counts for each sample in the decontaminated-dirty (post-decontamination-series) trials is also presented in Table 14, with the average count per filter calculated using Equation 3, and the average airborne concentration calculated using Equation 5. The same trend described above may be seen numerically in Table 14, where samples 1117P3 and 1118P3 exhibited large droplets, and likewise have a much higher average count per image.

Table 14: Post-Decontamination-series Fabric Reaerosolization Trials Filter Particle Counts

Sample ID	Average Count per 5 Images (part/image)	Average Count per Whole Filter (part/filter)	Average Concentration of Reaerosolized PSL Spheres (part/m^3)
1116P1	7	1093.75	$1.22*10^4$
1117P1	4	625	$6.97*10^3$
1117P2	1.2	187.5	$2.09*10^3$
1117P3	44.8	7000	$7.80*10^4$
1118P1	4.8	750	$8.36*10^3$
1118P2	9.4	1468.75	$1.64*10^4$
1118P3	19.2	3000	$3.34*10^4$
1119P1	5.4	843.75	$9.40*10^3$
1119P2	3.6	562.5	$6.27*10^3$
1119P3	4.4	687.5	$7.66*10^3$
Average	10.4	1621.88	$1.81*10^4$

Additionally, standard descriptive statistics results for the post-decontamination-series reaerosolization trials are presented in Table 15.

Table 15: Post-Decontamination-Series Reaerosolization Concentrations of PSL Spheres

Attribute	Value (particles/m^3)
Average (x)	$1.81*10^4$
Sample Size (n)	10
Standard Deviation (s)	$2.28*10^4$
Minimum	$2.09*10^3$
Median	$8.88*10^3$
Maximum	$7.80*10^4$

Statistical Comparison of Trials

The relationship between the four separate reaerosolization series is also presented graphically in Figure 28. Note that the standard error bars represent the standard deviation, divided by the square-root of the sample size, respectively, for each series.

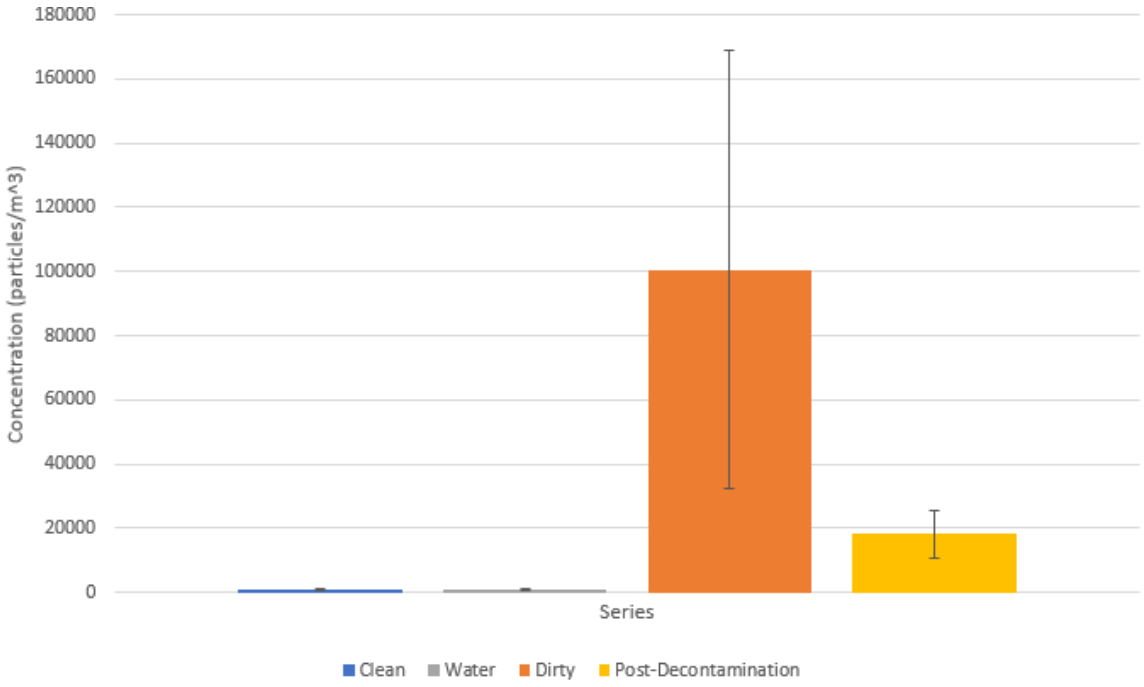

Figure 28: Concentration of Reaerosolized 1 µm PSL Spheres Across Series with Standard Error Bars

As both experimental group series contained wide standard error bars, and standard deviations greater than their means, there was a concern for outliers affecting the data sets. Each series was analyzed using the software JMP (SAS Institute, Cary, NC) by constructing a histogram and box-and-whisker plot, followed by testing each series for normality and lognormality. The produced analyses are presented below in Figure 29.

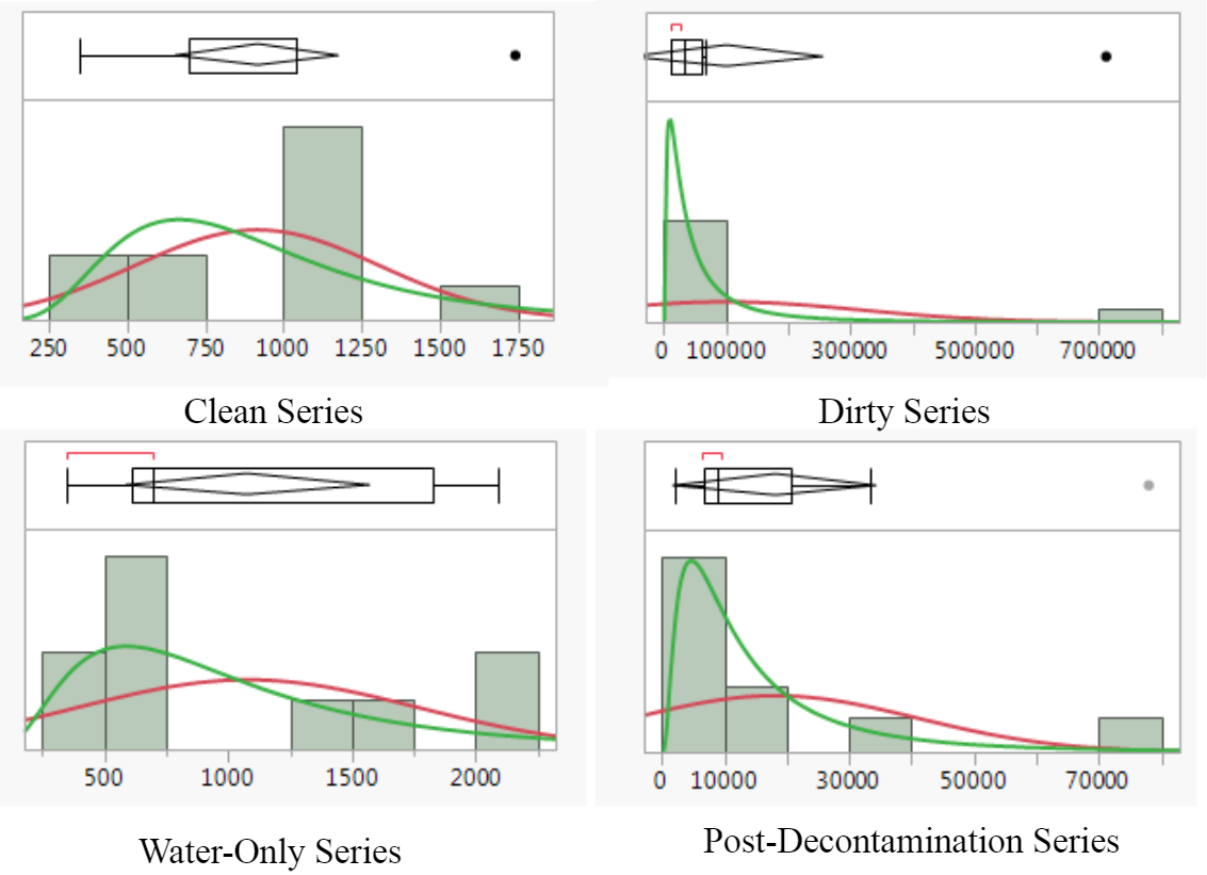

*Note: The red line represents the fitted normal distribution curve, and the green line represents the fitted lognormal distribution curve.

Figure 29: Distribution Analysis of the Four Reaerosolization Series Trials

As seen in Figure 29, three of the four series appear to include an outlier value, which is represented by a black dot in the box-and-whisker plot above each histogram. These outliers were further confirmed in JMP using the Dixon outlier Q-Test, where the clean and dirty series contained one identified outlier each, and the post-decontamination series contained two outlier values.

Additionally, all distributions were tested using the Shapiro-Wilks W-Test for normality, and the Kolmogorov's D-Test for lognormality. At a 95% confidence level ($\alpha = .05$), all four series rejected the W-Test for normality, whereas the dirty, water, and post-decontamination

series failed to reject the D-test, with a slight indication of lognormality. The results of the W-Test and D-Test are displayed below in Table 16.

Table 16: W-Test for Normality and D-Test for Lognormality Results for all Series

Series Name	W-Test (Prob>W)*	Normal? (Y/N)	D-Test (Prob>D)*	Lognormal? (Y/N)
Clean	0.0462	No	0.0100	No
Dirty	0.0001	No	0.1500	Yes**
Water	0.0401	No	0.0836	Yes**
Post-decontamination	0.0002	No	0.1500	Yes**

*Note: H_0: The data is from the Normal/Lognormal distribution. p-value below $\alpha = .05$ rejects H_0.
** These fail to reject H_0 at 95% confidence, but would reject H_0 at the 85% confidence level.

To further evaluate the effects of outliers, the outlier values from the clean, dirty, and post-decontamination series were removed from their respective data sets and summary statistics for each set were calculated again. The updated summary statistics are presented in Table 17.

Table 17: Reaerosolization Concentrations of PSL Spheres Summary Statistics (Outliers Removed)

Attribute	Value (particles/m^3)			
	Clean	**Dirty**	**Water**	**Post-Decon**
Average (x)	$8.33*10^2$	$3.26*10^4$	$1.08*10^3$	$8.67*10^3$
Sample Size (n)	10	9	10	8
Standard Deviation (s)	$2.91*10^2$	$2.07*10^4$	$6.86*10^2$	$4.24*10^3$
Minimum	$3.48*10^2$	$1.11*10^4$	$3.48*10^2$	$2.09*10^3$
Median	$1.04*10^3$	$2.75*10^4$	$6.97*10^2$	$8.01*10^3$
Maximum	$1.04*10^3$	$6.58*10^4$	$2.09*10^3$	$1.64*10^4$

Additionally, the same analyses as before were conducted on the amended data sets, with histograms, box-and-whisker plots, and tests for normality and lognormality. The updated distribution analysis for all four series is shown in Figure 30 and Table 18. Of particular note is that with the outliers removed, both the dirty and post-decontamination series can statistically be treated as falling in the normal distribution.

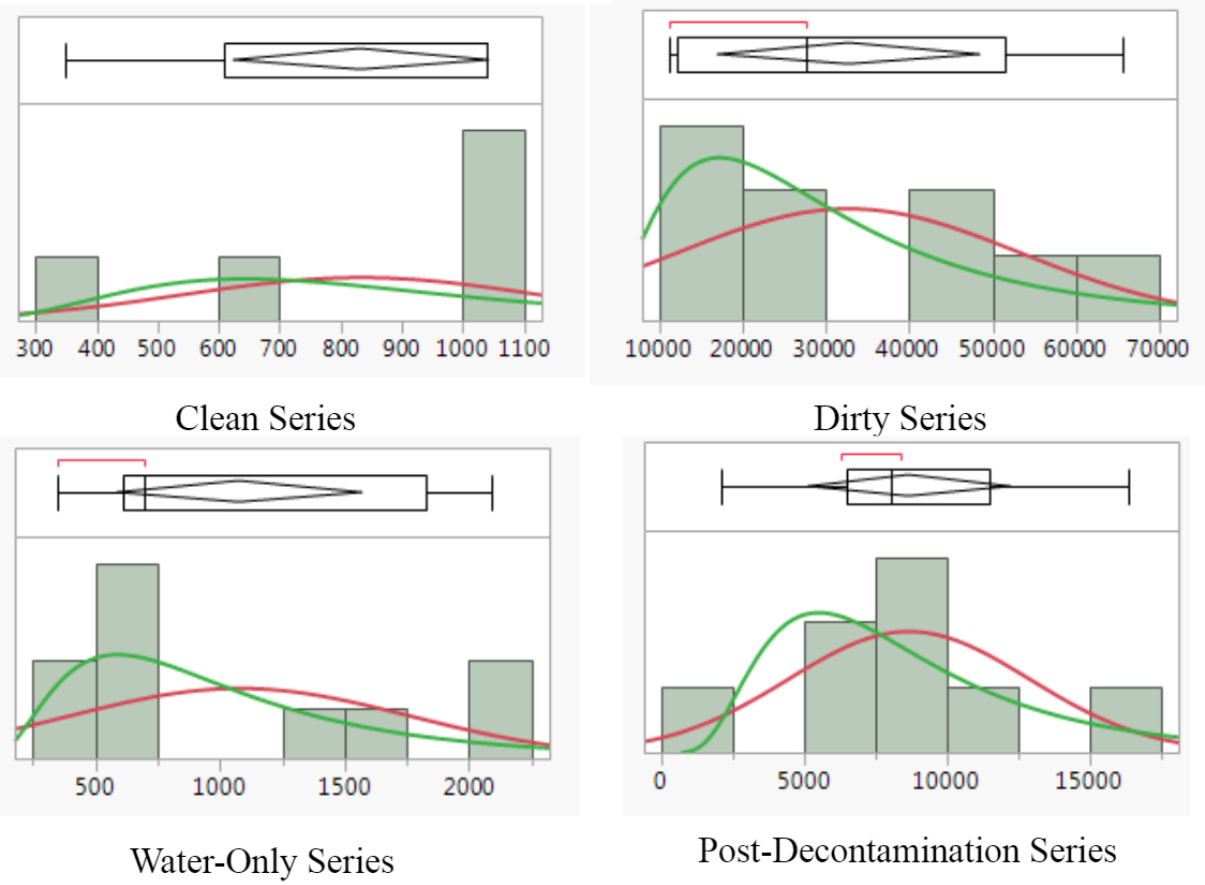

Figure 30: Distribution Analysis of the Four Reaerosolization Series Trials (Outliers Removed)

Table 18: W-Test for Normality and D-Test for Lognormality Results for all Series (Outliers Removed)

Series Name	W-Test (Prob>W)*	Normal? (Y/N)	D-Test (Prob>D)*	Lognormal? (Y/N)
Clean	0.001	No	0.01	No
Dirty	0.271	Yes	0.15	Yes**
Water	0.0401	No	0.0836	Yes**
Post-decontamination	0.825	Yes	0.15	Yes**

*Note: H_0: The data is from the Normal/Lognormal distribution. p-value below $\alpha = .05$ rejects H_0.
** These fail to reject H_0 at 95% confidence, but would reject H_0 at the 85% confidence level.

Following the distribution analysis, the averages of the four series were also compared again graphically, shown in Figure 31. Here it can be seen that although the extent of relationship has decreased, the dirty-series still has significantly higher levels of reaerosolization compared to either the control groups (clean and water series) and the post-decontamination group.

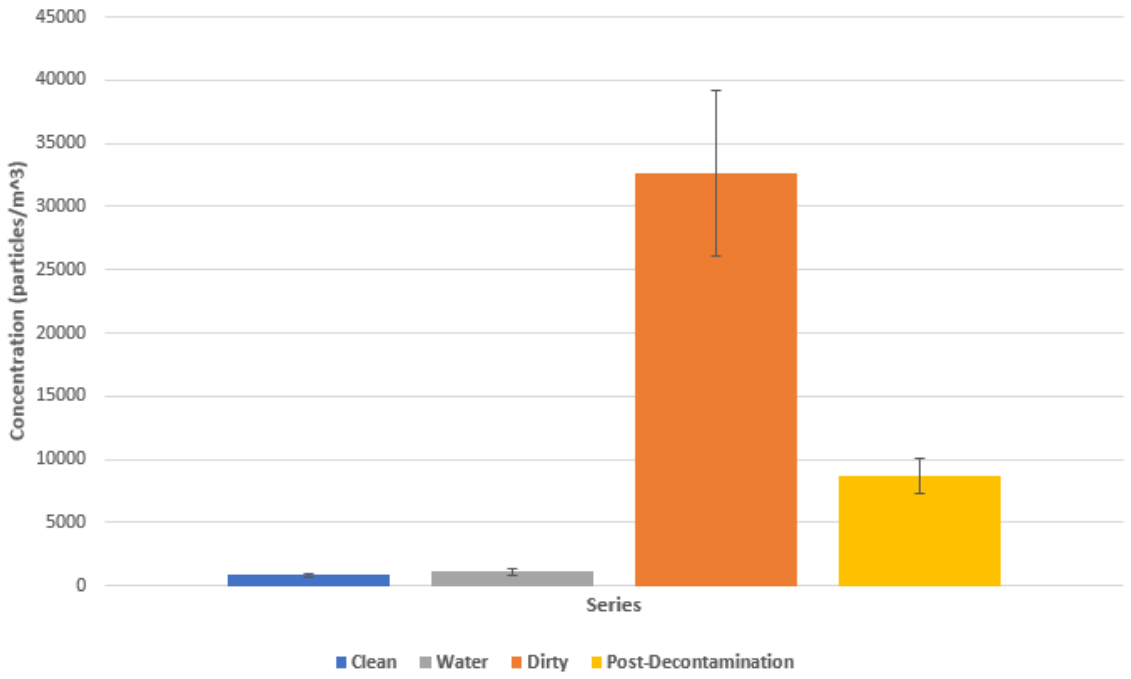

Figure 31: Concentration of Reaerosolized 1 µm PSL Spheres Across Series with Standard Error Bars (Outliers Removed)

In the above figure, it is evident that the uncontaminated, control groups (clean and water) have little to no reaerosolization of 1 µm green fluorescent spheres. This supports the result that the reaerosolization concentrations of the experimental groups (dirty and post-decontamination) are due to reaerosolized PSL spheres and not naturally occurring particles on the ABU fabric.

To verify the observations made above and to answer Research Objective #1, it needed to be confirmed whether reaerosolization could be quantified at statistically significant levels. For

this reason, a non-parametric Wilcoxon Rank Sums test was applied to each pair of control and experimental groups (clean/dirty and water/post-decontamination). For these tests, the null hypothesis was considered to be that "there is no difference between the two distributions." Additionally, it should be noted that as these tests are non-parametric, the full distribution – including outliers – was utilized. For the clean/dirty group comparison, the Wilcoxon Rank Sums test returned a p-value of 0.0002, rejecting the null hypothesis at the 99% confidence level. This may be seen below in Table 19.

Table 19: Wilcoxon Rank Sums Test Comparing Control Group #1 (Clean) and Experimental Group #1 (Dirty)

Wilcoxon / Kruskal-Wallis Tests (Rank Sums)

Level	Count	Score Sum	Expected Score	Score Mean	(Mean-Mean0)/Std0
Clean	10	55.000	105.000	5.5000	-3.775
Dirty	10	155.000	105.000	15.5000	3.775

2-Sample Test, Normal Approximation

S	Z	Prob>|Z|
155	3.77463	0.0002*

1-way Test, ChiSquare Approximation

ChiSquare	DF	Prob>ChiSq
14.5371	1	0.0001*

Additionally, the Wilcoxon Rank Sums test was also applied to Control Group #2 (water) and Experimental Group #2 (post-decontamination). For the water/post-decontamination series comparison, the Wilcoxon Rank Sums test also returned a p-value of 0.0002, rejecting the null hypothesis at the 99% confidence level. This may be seen below in Table 20.

Table 20: Wilcoxon Rank Sums Test Comparing Control Group #2 (Water) and Experimental Group #2 (Post-decontamination)

Wilcoxon / Kruskal-Wallis Tests (Rank Sums)

Level	Count	Score Sum	Expected Score	Score Mean	(Mean-Mean0)/Std0
Post	10	154.000	105.000	15.4000	3.687
Water	10	56.000	105.000	5.6000	-3.687

2-Sample Test, Normal Approximation

S	Z	Prob>|Z|
56	-3.68711	0.0002*

1-way Test, ChiSquare Approximation

ChiSquare	DF	Prob>ChiSq
13.8765	1	0.0002*

Next, in order to determine whether the difference between the reaerosolization concentrations for the dirty and post-decontamination series was statistically significant, both a non-parametric Wilcoxon Rank Sums test was used to evaluate the original distributions, and a two-tailed t-test was conducted to evaluate the distributions with the outliers removed. For the full-distribution dirty/post-decontamination series comparison, the Wilcoxon Rank Sums test also returned a p-value of 0.0211, rejecting the null hypothesis at the 95% confidence level. This may be seen below in Table 21.

Table 21: Wilcoxon Rank Sums Test Comparing Experimental Group #1 (Dirty) and Experimental Group #2 (Post-decontamination)

Wilcoxon / Kruskal-Wallis Tests (Rank Sums)

Level	Count	Score Sum	Expected Score	Score Mean	(Mean-Mean0)/Std0
Dirty	10	136.000	105.000	13.6000	2.306
Post	10	74.000	105.000	7.4000	-2.306

2-Sample Test, Normal Approximation

S	Z	Prob>|Z|
74	-2.30645	0.0211*

1-way Test, ChiSquare Approximation

ChiSquare	DF	Prob>ChiSq
5.4956	1	0.0191*

After removing the outlier values, in order to conduct the small-sample, two-tailed t test for samples with unequal variance, the sample sets themselves must be assumed to be approximately normal. Based upon the results shown in Table 18, the distributions of the dirty and post-decontamination series with outliers removed will be considered approximately normal. Although the control groups (clean-series and water-series) failed the null hypothesis of the W-test and thus cannot be considered approximately normal, they were not used in the t-test and thus do not impact statistical analysis between the dirty-series and post-decontamination-series.

Additionally, to ensure a large enough sample size was collected for each series, a power analysis was conducted. Given the sample standard deviation for the control groups and the sample means for each series, to achieve a power of 0.9 a sample size of 5 was calculated to be required. As 10 samples were collected for each trial, it was determined that the sample sizes were large enough to be considered statistically significant for analysis.

Next, for the comparison of means, a null hypothesis must be established. As before, the null hypothesis (H_o) is that "there is NO difference between the population means of reaerosolization concentrations of the dirty and post-decontamination groups," or that "(1-2) = 0." The mathematical process used to evaluate this hypothesis using a two-tailed t-test is shown in Equation 6.

Equation 6: Small-Sample Difference of Means for Dirty and Post-Decontamination Series

$$H_0: (\mu_1 - \mu_2) = 0$$

$$t = \frac{x_1 - x_2}{\sqrt{\left(\frac{s_1^2}{n_1}\right) + \left(\frac{s_2^2}{n_2}\right)}}$$

Where t is based on v degrees of freedom equal to $$v = \frac{\left(\left(\frac{s_1^2}{n_1}\right)+\left(\frac{s_2^2}{n_2}\right)\right)^2}{\left(\frac{\left(\frac{s_1^2}{n_1}\right)^2}{n_1-1}+\frac{\left(\frac{s_2^2}{n_2}\right)^2}{n_2-1}\right)}$$

Where:

1= Population mean of dirty reaerosolization trials
2= Population mean of post-decontamination reaerosolization trials
x1= Sample mean of dirty reaerosolization trials
x2= Sample mean of post-decontamination trials
s1= Sample standard deviation of dirty reaerosolization trials
s1= Sample standard deviation of post-decontamination reaerosolization trials
H0= Null hypothesis
t = Test statistic
v = Degrees of freedom

Following this equation, the dirty and post-decontamination groups were compared in the JMP software, producing the following one-way analysis comparison and t-test results, shown in Figure 32 and Table 22.

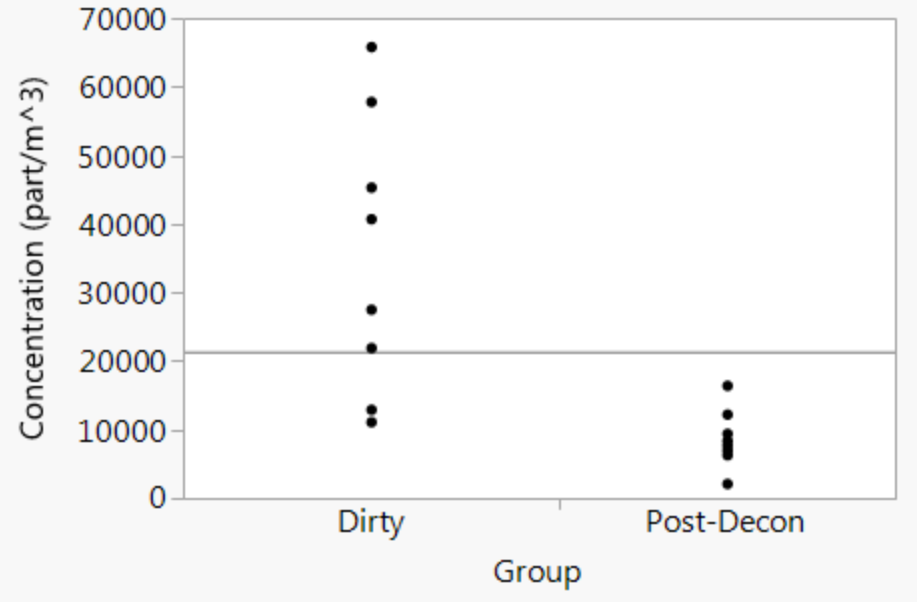

Figure 32: Analysis of Concentration by Group (Outliers Removed)

Table 22: Two Directional t-Test for Difference of Means Between Dirty and Post-Decontamination Groups (Outliers Removed), 99% Confidence

Assuming unequal variances			
Difference	-24009	t Ratio	-3.40535
Std Err Dif	7050	DF	8.752876
Upper CL Dif	-932	Prob > |t|	0.0081*
Lower CL Dif	-47086	Prob > t	0.9959
Confidence	0.99	Prob < t	0.0041*

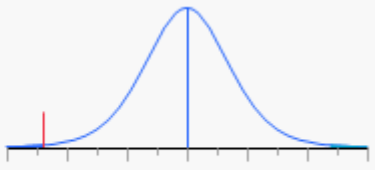

From the above table, a p-value of 0.0081 was attained. Assuming a desired confidence level of 99% (or an α of 0.01), the calculated p-value is *less* than alpha. Therefore, it can be said with 99% confidence that the null hypothesis that "there is NO difference between the population means of reaerosolization concentrations of the dirty and post-decontamination groups" may be rejected in favor of the alternative.

Summary of Results

All samples of fabric contained PSL spheres in numbers TNTC following contamination, but prior to reaerosolization trials. The clean-series and water-series (control) samples showed little to no presence of PSL spheres following reaerosolization trials. The dirty-series and post-decontamination-series (experimental) samples exhibited evidence of significant reaerosolization of PSL spheres following reaerosolization trials, supported by the Wilcoxon Ranked Sums test at the 99% confidence level. Three series' data sets failed the Q-test for outliers, so these values were removed before statistical analysis. After removing outlier values, the dirty-series and post-decontamination series' distributions were approximately normal according to the W-Test. An average ~70% reduction was observed following decontamination between the dirty-series and post-decontamination series' concentrations, statistically significant at the 99% confidence level according to a two-directional t-test for difference of means, with a p-value of 0.0081.

V. Conclusions and Recommendations

Chapter Overview

This chapter summarizes the conclusions of this study, as well as makes recommendations for future research based upon this study.

Research Objective #1: To develop a methodology to quantify the reaerosolization of a dry-biological surrogate aerosol from clothing during a medical evacuation.

The primary goal of this thesis was to develop a repeatable method that could be used to quantify secondary aerosolization of biological particles, with a specific focus on fabric as the contaminated surface, and vibration as mode of reaerosolization. To that end, through a rigorous trial-and-error process, a repeatable methodology was built.

Regarding the contamination and reaerosolization procedures, all materials that were used are standard products that are readily available for purchase. Reaerosolization via vibration is also an easily repeatable method; as an alternative to the standard laboratory shaker, a vibration calibration table with variable frequency settings could also be used to repeat this methodology. Additionally, the reaerosolized particles were captured using standard air sampling techniques. The use of the IOM sampler, air pump, and PVC filter is a standard technique that can be seen in many National Institute of Occupational Safety and Health (NIOSH) Manual of Methods (NMAM) procedures.

Furthermore, a standardized counting methodology with two separate particle counting techniques was developed. For samples with a very low concentration of particles, the human eye method proved the most efficient and the most accurate way to count contamination. On the other hand, for repeated samples with high, very high, and TNTC levels of contamination, the

computer counting method using the Image J software proved significantly more efficient, while maintaining a consistent level of accuracy. Additionally, although there is room for human and computer error in the "Counting Rules" used to guide particle counting, this rule-based technique is very similar to the industry standard method for counting fibers, such as asbestos in NMAM Method 7400 (NIOSH, 2019).

Using the counting rules and a UV microscope, a clear distinction was visible between clean/uncontaminated and dirty/contaminated swatches of ABU fabric, validating the "Contamination" procedure. Furthermore, after applying the "Reaerosolization" procedure and counting via the same process, a clear distinction was visible between the PVC filter samples from the clean and dirty trials, where the clean/control trials showed little to no green fluorescent particles, and the dirty/experimental trials showed significant presence of particles. These results indicate that fluorescent bright green particles are not naturally present on PVC filters, and that 1 µm particles can be reaerosolized off of ABU fabric and captured onto a PVC filter – validating both the "Reaerosolization" and "Microscopy" procedures.

As the methodology developed in this thesis was able to repeatedly contaminate, reaerosolize, and quantify microscopic biological surrogate particles from fabric under potential conditions in a medical evacuation, Research Objective #1 can be considered achieved.

Research Objective #2: To use the developed methodology to test the effectiveness of existing biological decontamination procedures in regards to bioaerosols.

The second aim of this study was to use the methods described above to measure the effectiveness of decontamination present in current literature. As it is the most cited and most applied method in practice, the "high-volume, low-pressure shower" was chosen to be tested

using the developed methodology. Additionally, although a full mass-casualty decontamination line was not used for this experiment, an approximation of the decontamination method was constructed using a gravity-fed water shower.

The results from the dirty series trials compared to the post-decontamination series trials show a distinct reduction in the concentration of particles captured during reaerosolization after the water-based decontamination. The results were statistically significant at a 99% confidence level, rejecting the null hypothesis that "there is no difference between reaerosolization concentrations of the dirty post-decontamination groups." This would indicate that using high-volume, low-pressure water is potentially an effective method to control biological particle reaerosolization off clothing.

As the methodology developed in this thesis was able to repeatedly decontaminate, quantify, and compare the reaerosolized microscopic biological surrogate particles from dirty fabric and fabric that was decontaminated via a prescribed method, Research Objective #2 can be considered achieved.

Applicability of Results to Real-World Scenarios

Laboratory versus real-world conditions

This study was developed with a real-world target in mind; however, as this experiment was designed in a controlled laboratory setting, there are numerous factors that must be considered before comparing the results to a real-world situation. For example, the number of particles that were reaerosolized came from 10 x 10 cm swatches of ABU fabric. The concentration results cannot be considered truly analogous to a real-world scenario, as a real-world scenario would involve full body clothing, clothing of different sizes, different materials,

and so on. In addition, the biological surrogate PSL spheres are an appropriate model, but may still not behave exactly like all biological particles; likewise, the miniaturized high-volume, low-pressure water decontamination method was an appropriate model, but may not behave exactly the same as a large scale mass casualty decontamination line. Furthermore, this experiment was conducted in a sealed chamber with stagnant air; in a real-world scenario, the chamber may be an entire aircraft, there may be cross-drafts, and a second individual may not remain in the breathing zone of the contaminated casualty. Nevertheless, while this study is not a one-to-one model of real-world conditions, it remains valuable as a proof of concept in quantifying biological particle reaerosolization.

Outlier values' importance in laboratory and real-world settings

Similarly, the outlier value results may not be treated the same way in a laboratory or a real-world setting, whereupon analyzing the distribution of the results from the four tested series and applying the Dixon outlier Q-Test, outliers were identified in the clean, dirty, and post-decontamination series. For the sake of statistical analysis, these outliers were removed, after which the dirty and post-decontamination series could be treated as normally distributed. By doing so, a statistically significant comparison could be made showing the effectiveness of water as a decontamination method; however, in a real-world scenario, the actual impact of these outlier results must be considered and cannot be discarded.

Military doctrine is often constructed with the "worst-case scenario" in mind. In the case of this study, this would mean that although the median reaerosolization concentration for the dirty series was 34,000 particles/m^3, the "worst-case" sample was the outlier with a concentration of 712,000 particles/m^3 – more than twenty times the median value. In practice, while a contaminated casualty may most likely be near the median value, emergency response

workers must be prepared to treat every casualty as though they might be the "worst-case" level of contamination.

The outlier reaerosolization concentrations reached 712,000 particle/m^3 in a laboratory setting off a 10 x 10 cm swatch of fabric, while the primary target biological particle for the surrogate, *Bacillus anthracis*, has an infectious dose of less than 600 particles, and potential lethal doses as low as 2,500 particles. As described above, this number cannot be considered a one-to-one risk value to emergency response workers; however, these results do establish a precedent for concern regarding the reaerosolization of biological particles.

Aerosol Versus Droplet Deposition Patterns Before and After Water Decontamination

An additional unexpected observation during this study was the change in deposition patterns of reaerosolized particles before and after decontamination using water. In the dirty-series trials, regardless if the contamination levels were low, high, very high, or TNTC, the deposition pattern was consistent throughout each image and over the five images taken from each filter. This is present above in Figure 25 where in each image the PSL spheres are distributed relatively evenly and randomly throughout the filter. This is characteristic of "aerosol" behavior, where each 1 μm particle moves independently of all other particles.

Conversely, after the contaminated swatches were decontaminated with water, the deposition pattern changed significantly. As seen in Figure 27, the number of particles per image was not at all consistent over the surface of a single filter. Each image could be roughly placed into one of two categories: those without droplets, that contained little to no PSL spheres; and those with droplets, that contained a high concentration of PSL spheres. In a similar way, an

emergency responder exposed to droplets may not inhale any, and thus have no exposure; however, if they inhale even a few large droplets filled with spores they may receive a high dose.

The change from "aerosol" behavior of the particles to "droplet" behavior of the particles can have significant implications for how emergency responders must protect themselves. For example, using the settling time equation shown in Equation 2, the significantly larger diameter of a water droplet compared to the diameter of a 1 µm spore would cause the droplet to deposit out of the atmosphere much more quickly, as well as be less susceptible to the effects of diffusion and cross-drafts (Hinds, 1999). Additionally, the degree of protection required differs between droplets and aerosols. According to guidance from the Food and Drug Administration (FDA), an N95 respirator is required to protect against the inhalation of aerosols, but a surgical mask is designed to help "block large-particle droplets" that may contain viruses or bacteria (FDA, 2021).

Limitations and Recommendations for Future Research

There were a number of sources of error and limitations present throughout the development of this study. As described previously, one limitation was the inability to quantify the amount of contamination present on each swatch of fabric after initial contamination. Under the UV microscope, PSL spheres were present on every sample that was in the aerosol chamber during the contamination process. However, due to the many layers of interwoven fibers in the ABU fabric, a full cross-section of fabric could not be completely brought into focus at a single time, preventing accurate quantification of initial contamination. For this reason, all swatches used in the dirty-series and post-decontamination-series were simply considered "contaminated," without a specific value. This is potentially a source of error, as when the results of the dirty-

series and post-decontamination-series were mapped onto the original layout of the swatches during contamination, the distribution of low, medium, and high concentration samples was not spread evenly throughout the chamber. This mapping is shown below in Figure 33.

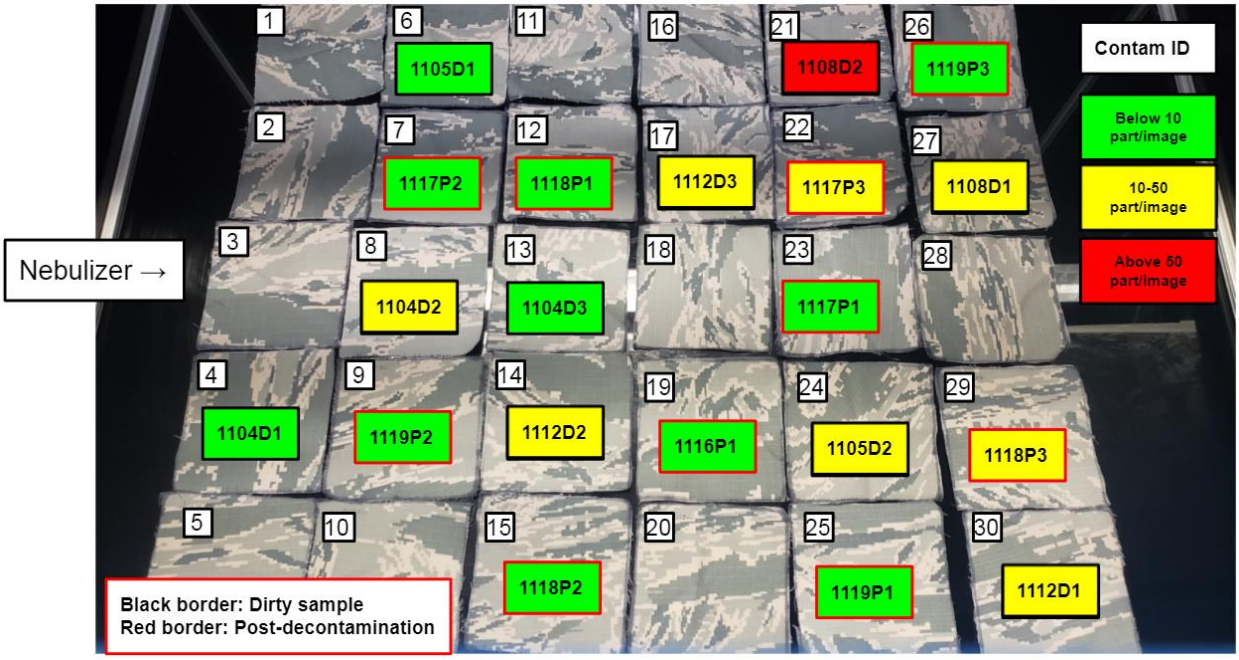

Figure 33: Distribution of Results of Dirty-Series and Post-Decontamination-Series over Swatch Contamination Layout

It can be seen above that the "near" side of the chamber has predominantly low-concentration results, while the "far" side of the chamber contains more medium and high-concentration results. Additionally, the outlier values for both the dirty-series and post-decontamination-series all come from the "far" side of the chamber. These results indicate that the aerosolized PSL sphere concentration during initial contamination may not have been consistent throughout the small aerosol chamber. If initial contamination was not consistent, then the swatch starting contamination may not have been consistent between trials, potentially affecting reaerosolization. To counteract this concern, samples were deliberately chosen to have

a roughly equal spread of selected samples for the dirty-series and post-decontamination series, as shown by the balance of red and black bordered samples in Figure 33. Regardless, to fully characterize the contamination process and its effect on reaerosolization contamination, further iterations of contamination followed by reaerosolization sampling would be required.

One limitation that does not affect this study itself, but rather its applicability to a real-world scenario, is the use of the vortex mixer for reaerosolization. As previously mentioned, vibration is generally presented as a function of both frequency and acceleration. The vortex mixer was chosen for its ability to produce vibrations at a consistent frequency, which it achieved by producing a consistent 50 Hz; however, the vortex mixer exhibited a much higher acceleration than present on the modeled aircraft. The C-130H showed body vibrations around 2 m/s^2, whereas the vortex mixer was considerably higher, at 150 m/s^2. That being said, as the same mixer was used throughout all trials, its use does not impact the statistical significance of the comparisons between the dirty-series and post-decontamination-series trials. Additionally, as there are many conditions contaminated clothing may be subjected to during a medical evacuation, such as running or shaking, the higher acceleration of the fabric is not outside the realm of real-world possibilities. That being said, this is another reason that the results of this study should not be considered a one-to-one model of a real-world scenario. For future studies, the use of a dedicated vibration calibration table for reaerosolization may provide a more accurate depiction of human body vibration while lying down in an aircraft.

For future studies, it is important to note the amount of time that was required to develop this methodology, and the amount of time it will take to perform this methodology in future trials. As the goal of this thesis was to develop a methodology, a significant amount of time was spent in a trial-and-error process exploring methods that ultimately were not used in the final

iteration of the methodology. Each time an experimental variable would be changed – such as pump flow rate, sample time length, clips used, vibration setting used, and so on – all trials using the previous settings needed to be discarded. Additionally, in the final version of the methodology, a significant amount of time is required to capture each sample. The sampling time for each trial was 30 minutes; however, there was an average of an additional 30 minutes required for each sample between trials to run the MURPHEE's exhaust system, clean the aerosol chamber, bag and label the finished sample, and prepare a new filter and sample for the next trial. Additionally, each filter took an average of 10 minutes to analyze and photograph under the UV microscope, and between 3 and 30 minutes to count particles. Thus, assuming an average of 75 minutes per sample, it would take 9,000 minutes, or 150 hours of sample collection with no complications, if one were to collect 30 samples per series, with 4 series of trials. This is not undoable, but important to note for future planning purposes.

The methodologies developed in this study are applicable to a number of potential future studies. First, this study only evaluated a single decontamination method for the biological surrogate off of the ABU fabric – the use of a water shower. In addition, the reaerosolization trials immediately followed the water shower decontamination; however, due to the evaporative effect of water, the efficacy of the method may decrease if a wait time were to be added and the samples were allowed to dry out first. Furthermore, future studies could attempt to apply different decontamination methods, such as the use of a HEPA vacuum, adjusting the amount or pressure of applied water, scrubbing the clothing with a soapy brush, or any other decontamination method described in literature. By doing so, a comparison can be made across all modes of decontamination for biological particles under the same set of conditions. In a similar vein, only ABU fabric was used during this study, although early-stage pilot studies also

include the use of Tyvek (Dupont, Wilmington, DE). By applying the same methodologies used in this study, but changing the type of contaminated fabric to denim, Tyvek, wool, and so on, an understanding of the relative risk of each fabric type to contamination and reaerosolization can be achieved.

Lastly, this study only involved the use of a biological surrogate, as opposed to a live biological agent. Repeating the methodologies used in this study with a biological agent, such as *Bacillus thuringiensis*, would give a more accurate depiction of the risk to reaerosolization from specific biological hazards. However, to repeat this study's methodologies with a live agent, a number of modifications to the sampling process would need to be made. First, biological safety levels would need to be adhered to in order to test with a live agent, the specifics of which would depend on the agent in question. Second, depending on the agent, a live agent may not be able to be preserved on ABU fabric for as long as PSL spheres can, so contamination and reaerosolization sampling may need to happen in a much shorter span of time. Third, instead of a PVC filter, reaerosolization samples may need to be captured on a gelatin filter, or plated onto an agar plate to be cultured before analyses. Lastly, unless specific strains of UV luminescent agents are used, they may not be able to be quantified under a microscope. Other counting methods, such as counting plate cultures or plaques may be required depending on the agent. Nevertheless, the methodologies developed in this study serve as a solid starting point for reaerosolization quantification studies using live biological agents.

Significance of Research

In this thesis, methodologies were successfully developed to contaminate, reaerosolize, decontaminate, and quantify a biological particle surrogate off fabric. Through this methodology, it was shown that high-volume, low-pressure water is an effective means at controlling reaerosolization risks, with a ~70% reduction in reaerosolization justified at the 99% confidence level. Most importantly, the methodologies established in this thesis lay the groundwork for the quantification of novel decontamination methods for biological particle control in the future.

APPENDIX I

Table I.1 Uncontaminated "Clean" Fabric Reaerosolization Trials Sample Photographs

Sample	Position 1	Position 2	Position 3	Position 4	Position 5
1104C1	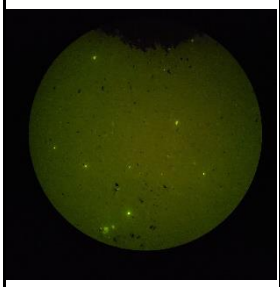	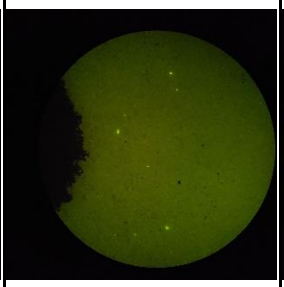	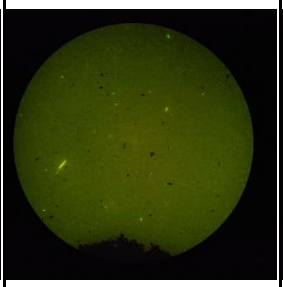	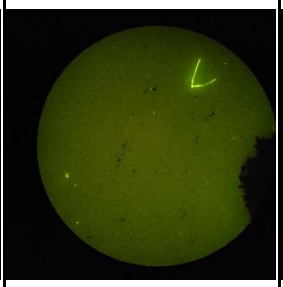	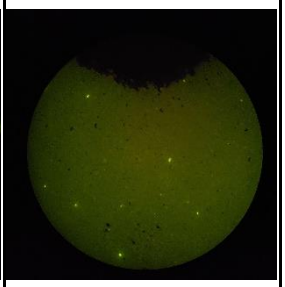
1104C2	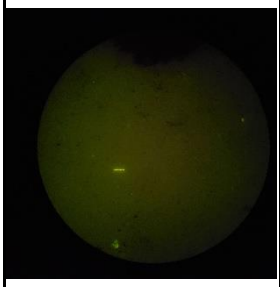	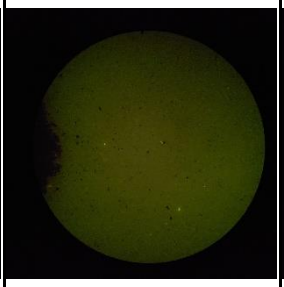	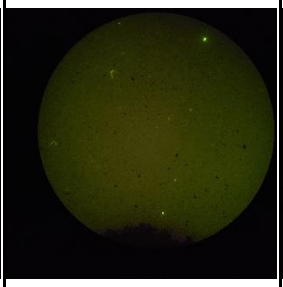	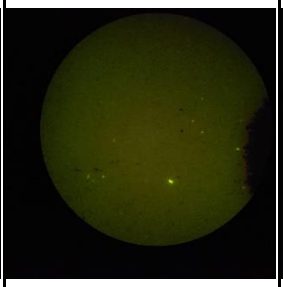	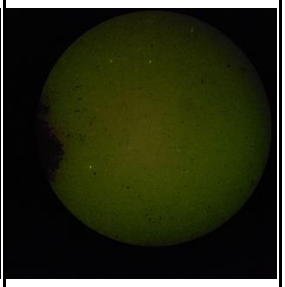
1104C3	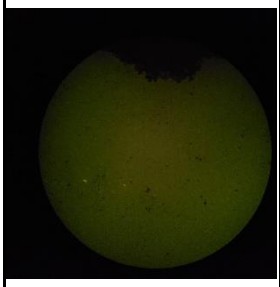	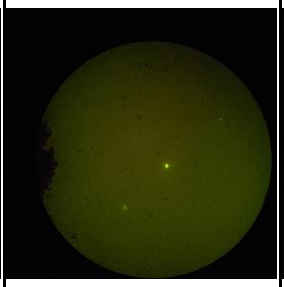	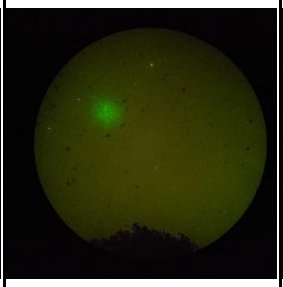	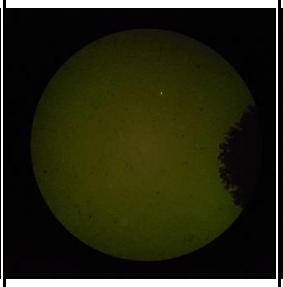	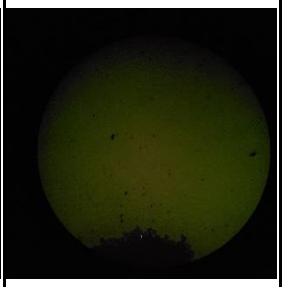
1105C1	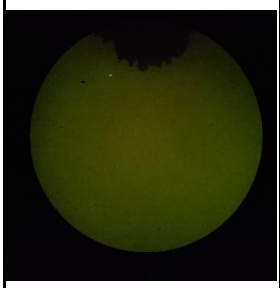	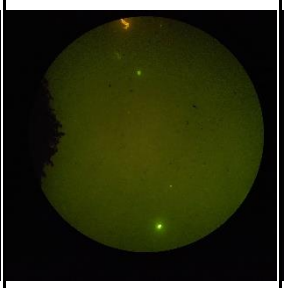	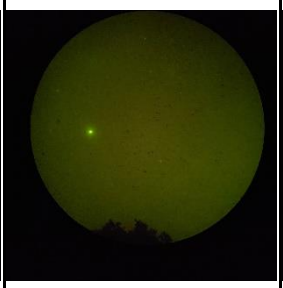	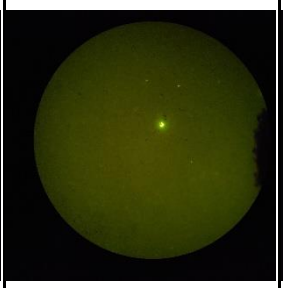	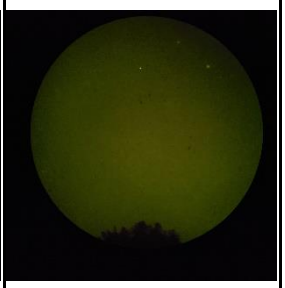
1105C2	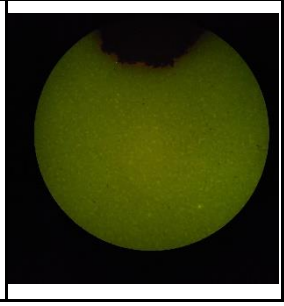	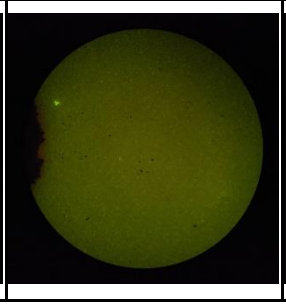	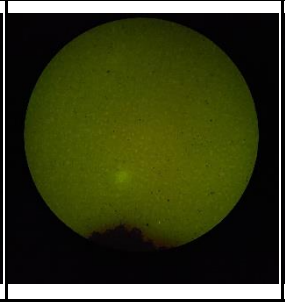	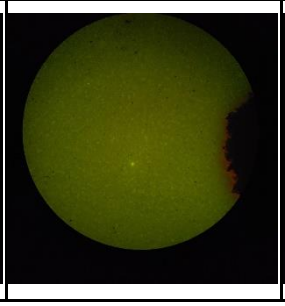	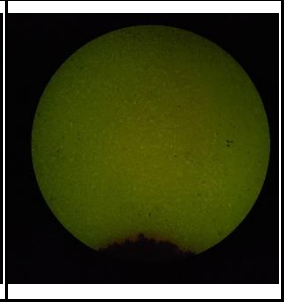

1105C3	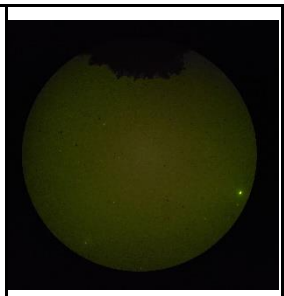	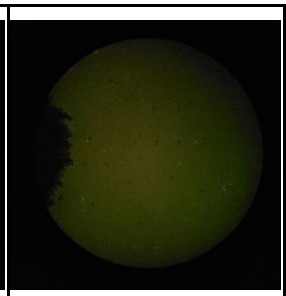	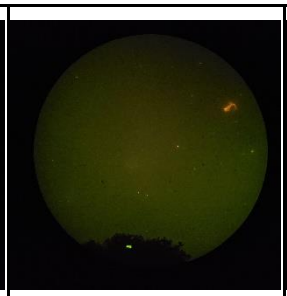	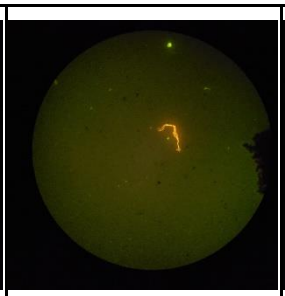	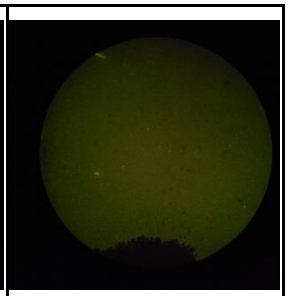
1108C1	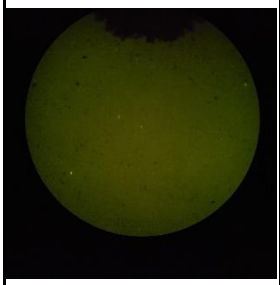	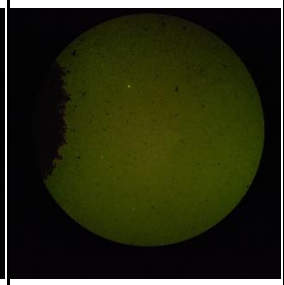	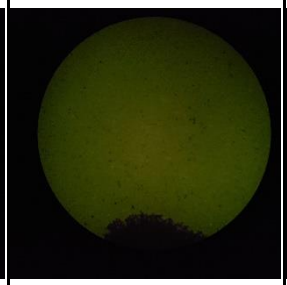	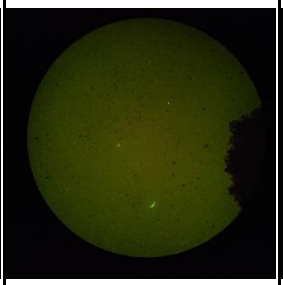	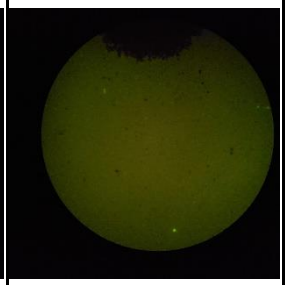
1108C2	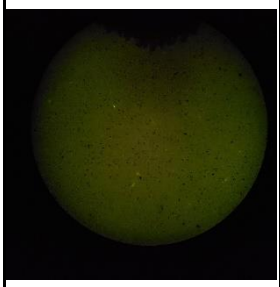	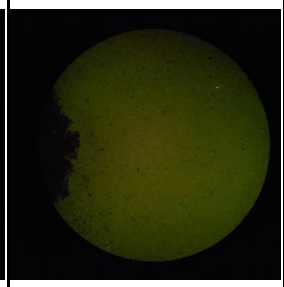	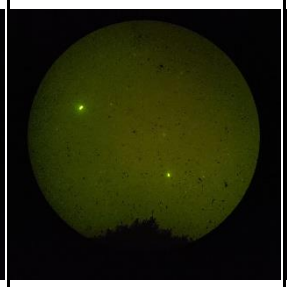	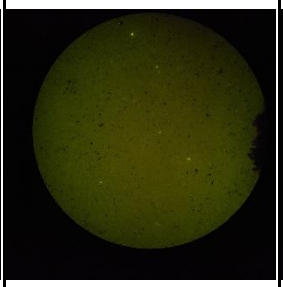	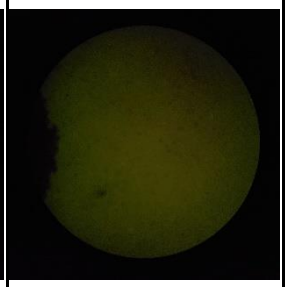
1112C1	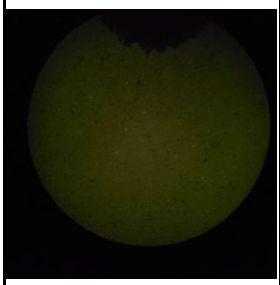	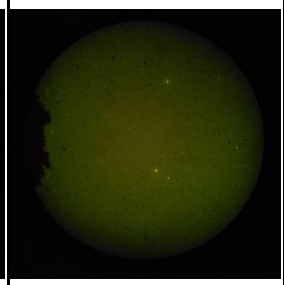	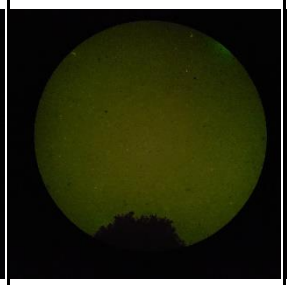	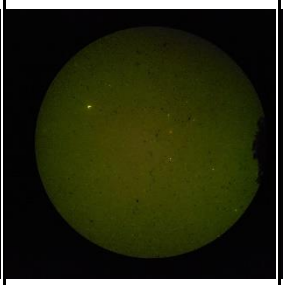	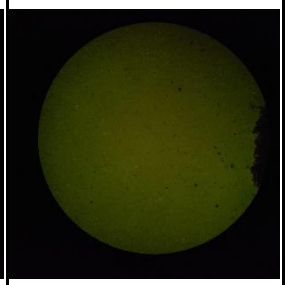
1112C2	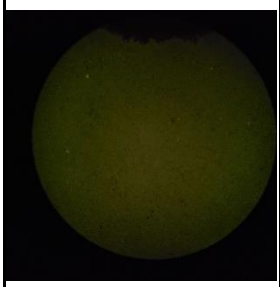	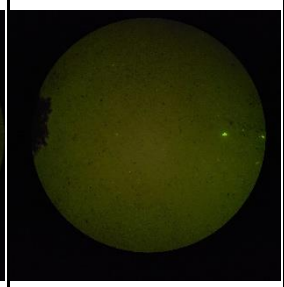	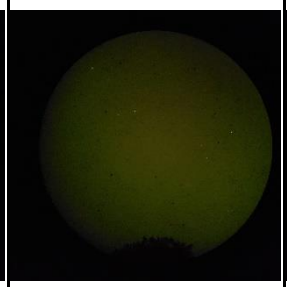	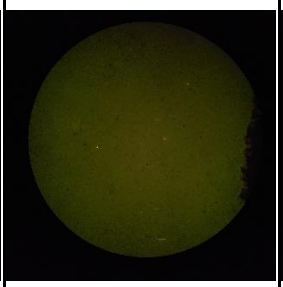	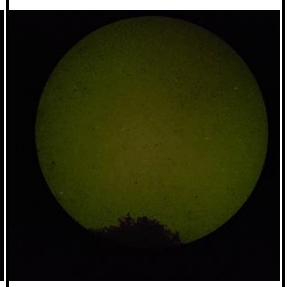
1112C3	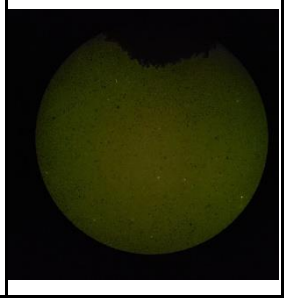	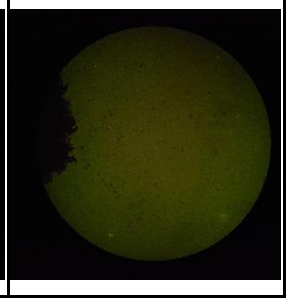	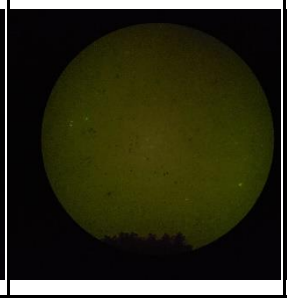	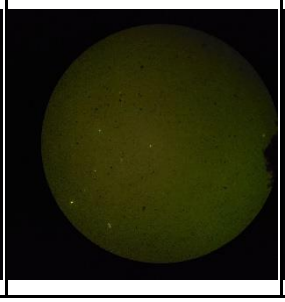	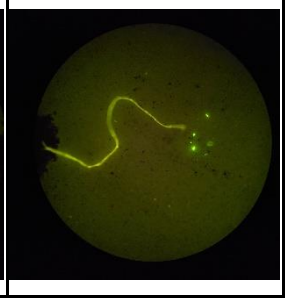

Table I.2 Contaminated “Dirty” Fabric Reaerosolization Trials Sample Photographs

Samp ID	Position 1	Position 2	Position 3	Position 4	Position 5
1104D1	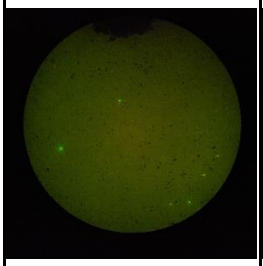	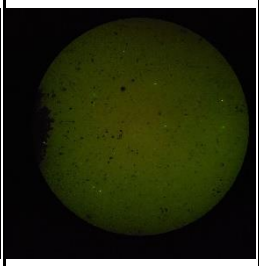	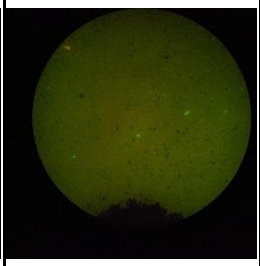	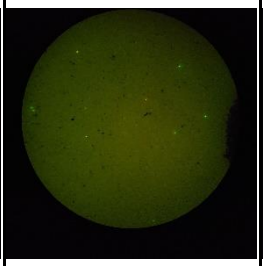	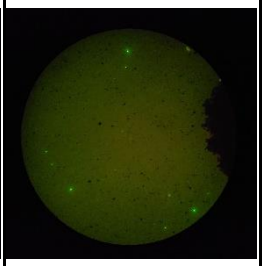
1104D2	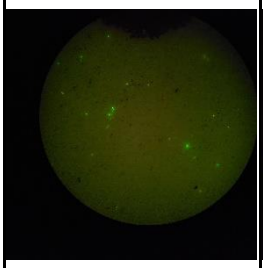	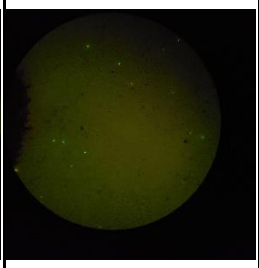	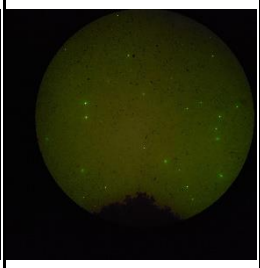	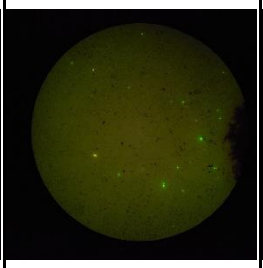	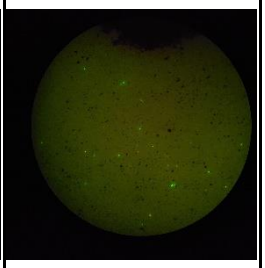
1104D3	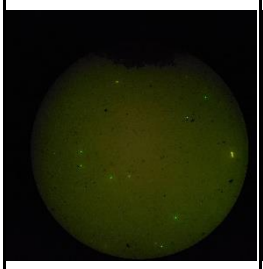	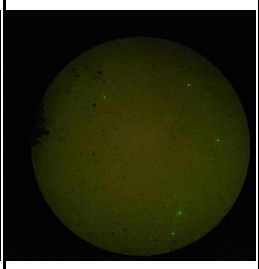	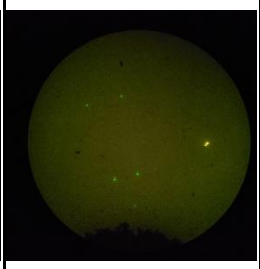	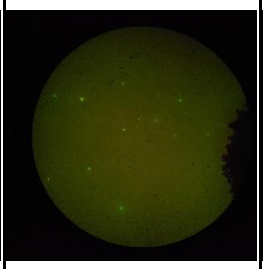	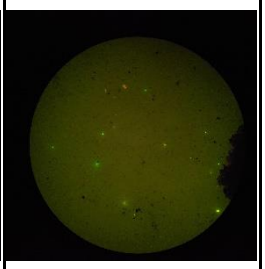
1105D1	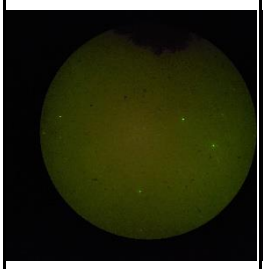	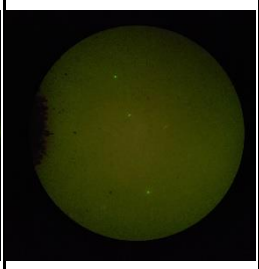	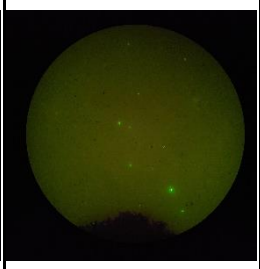	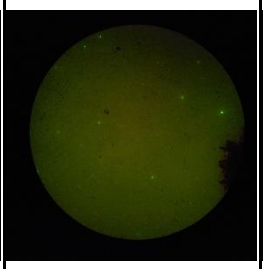	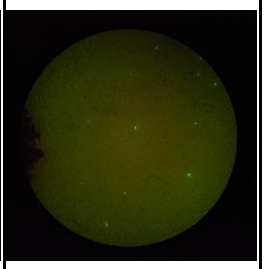
1105D2	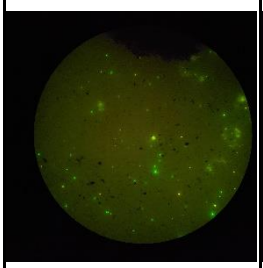	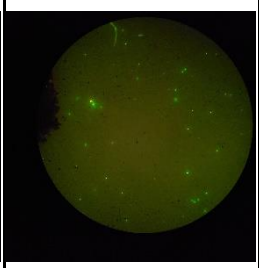	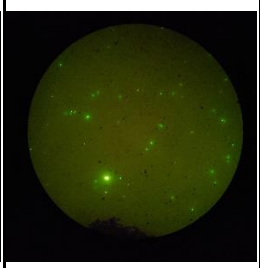	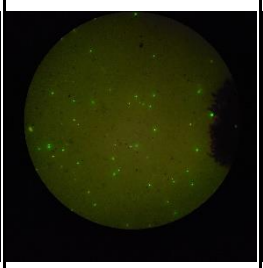	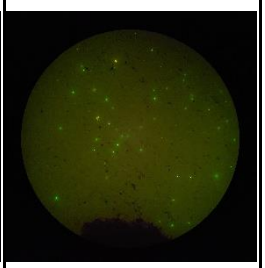
1108D1	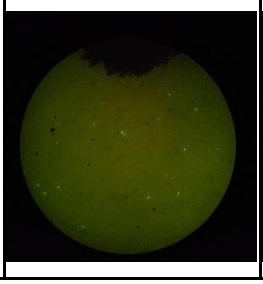	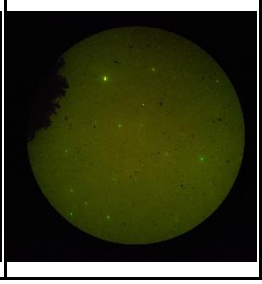	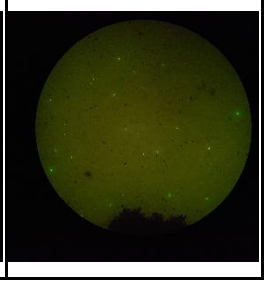	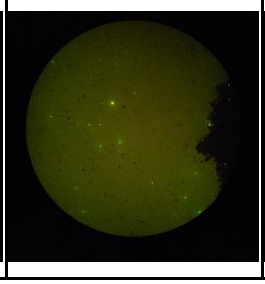	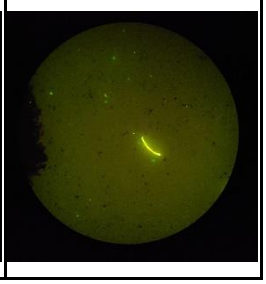

1108D2	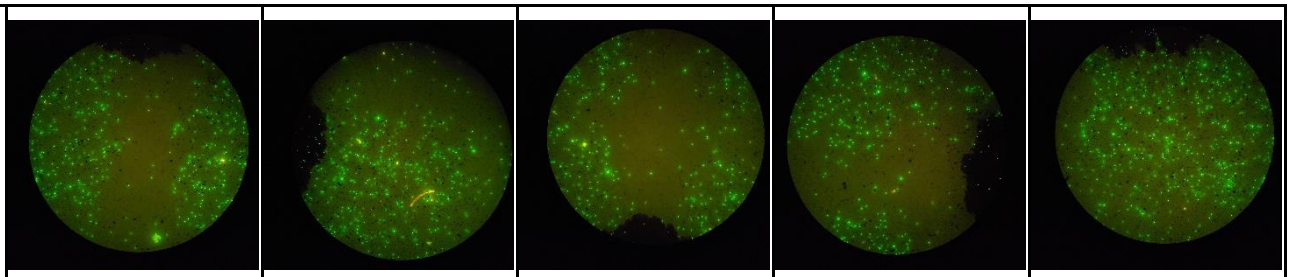				
1112D1	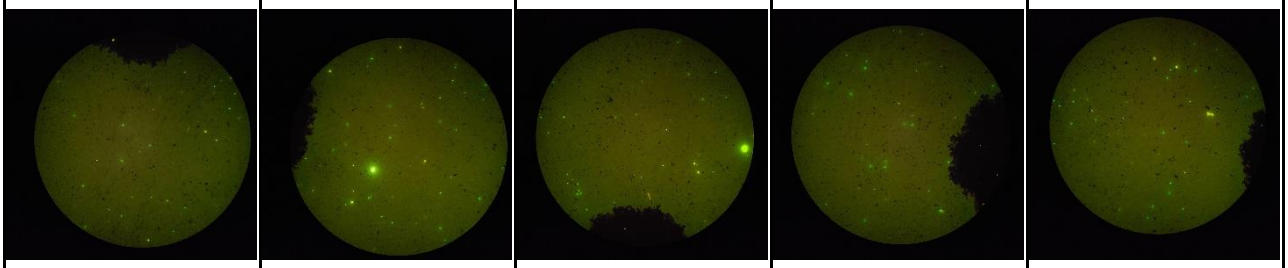				
1112D2	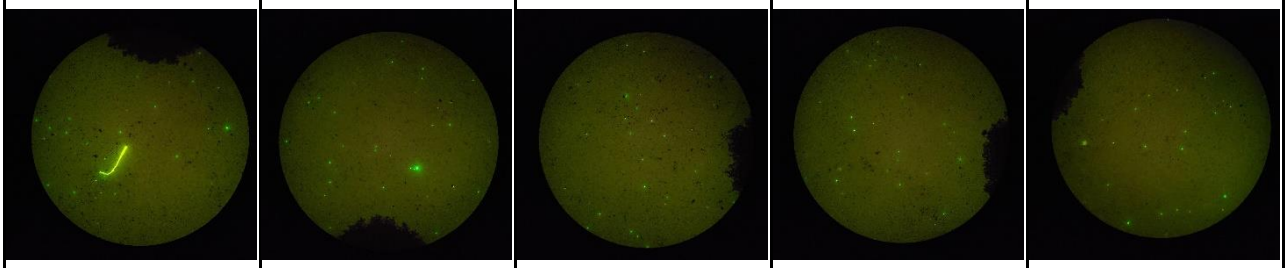				
1112D3	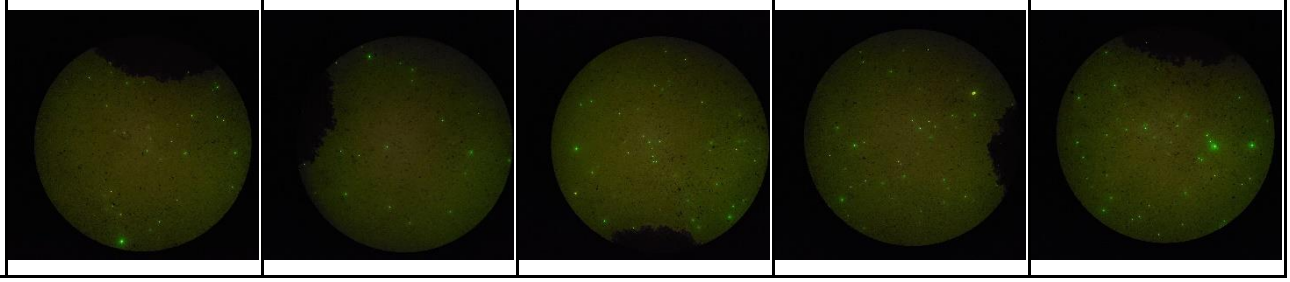				

Table I.3 Post-Decontamination-Clean “Water-Series” Fabric Reaerosolization Trials Sample Photographs

Samp ID	Position 1	Position 2	Position 3	Position 4	Position 5
1116W1	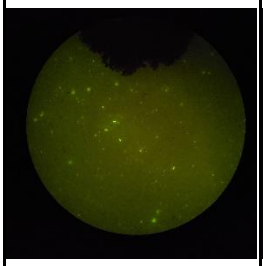	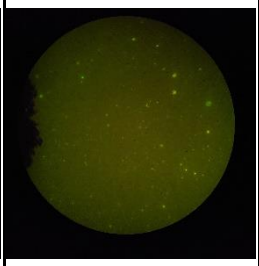	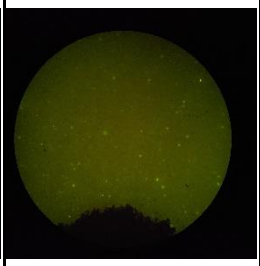	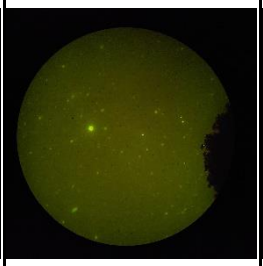	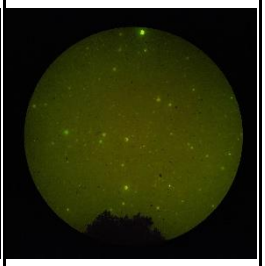
1117W1	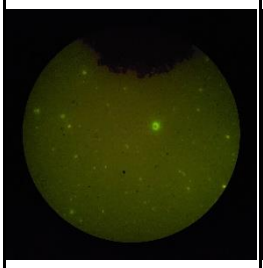	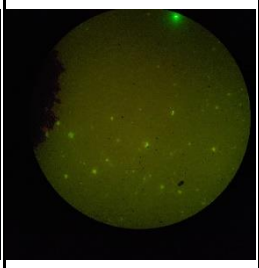	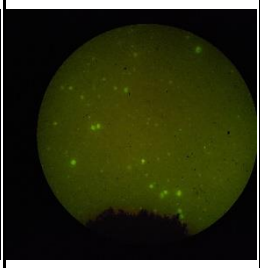	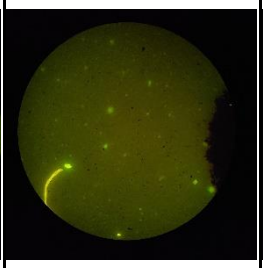	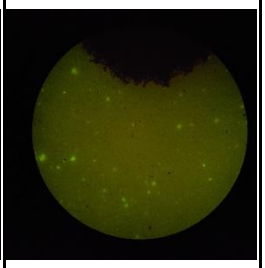
1117W2	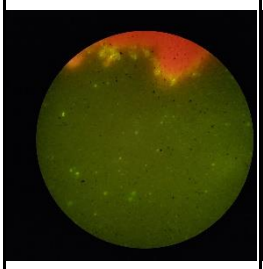	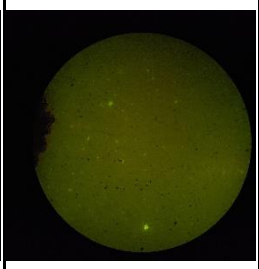	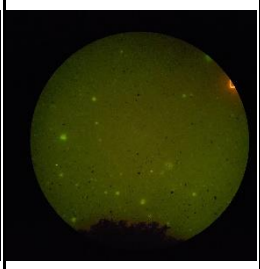	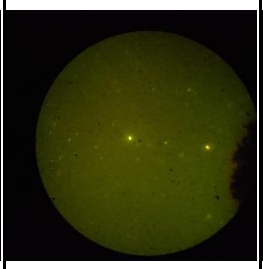	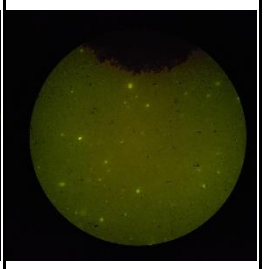
1117W3	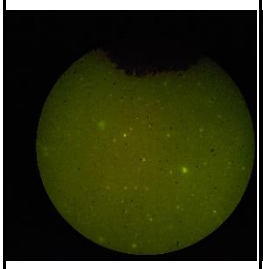	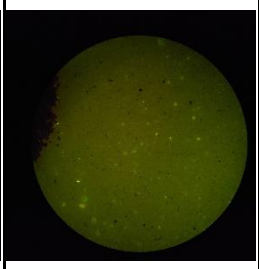	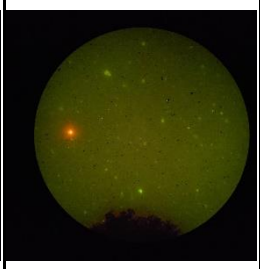	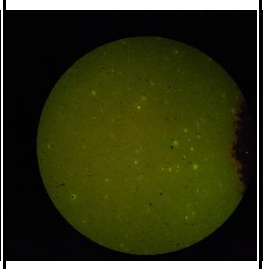	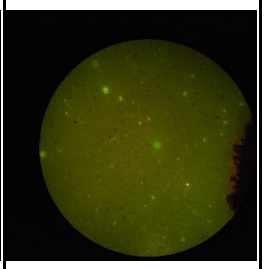
1118W1	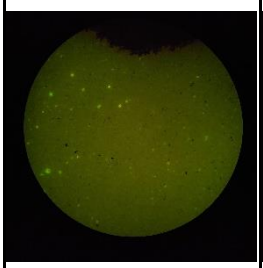	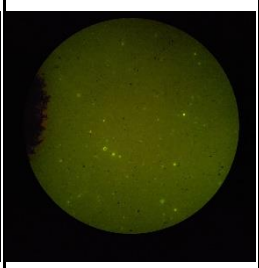	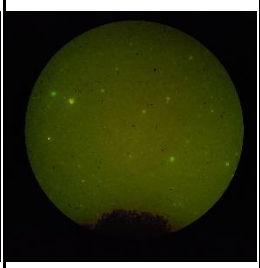	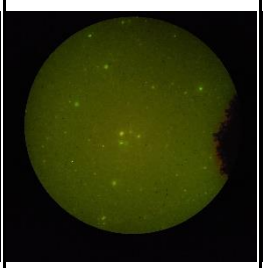	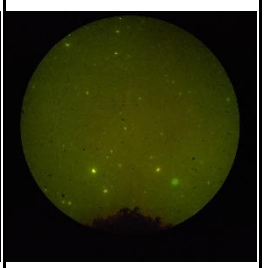
1118W2	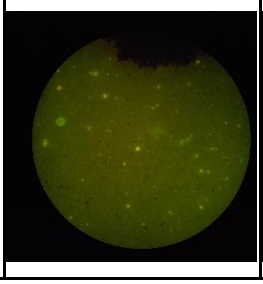	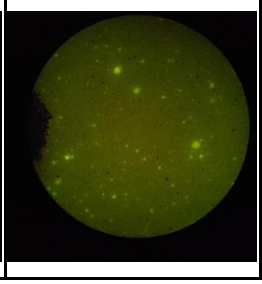	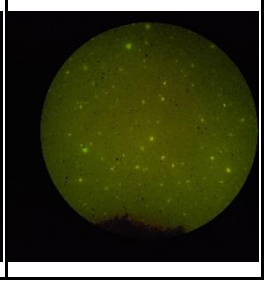	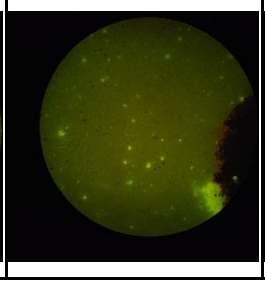	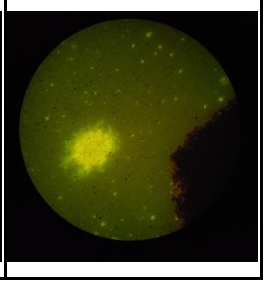

1118W3	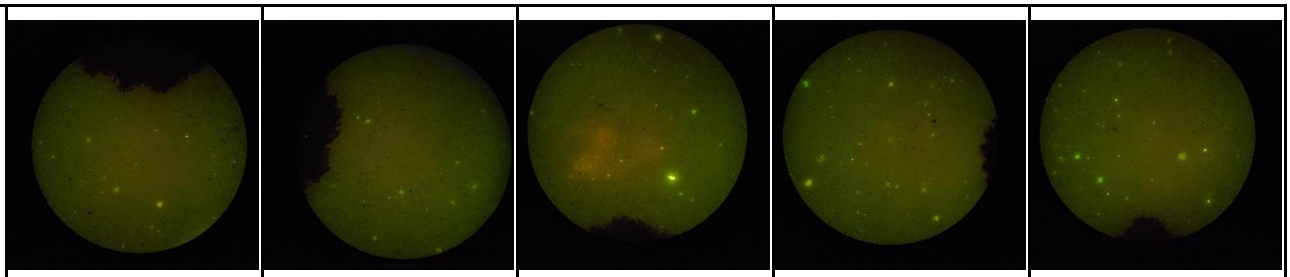				
1119W1	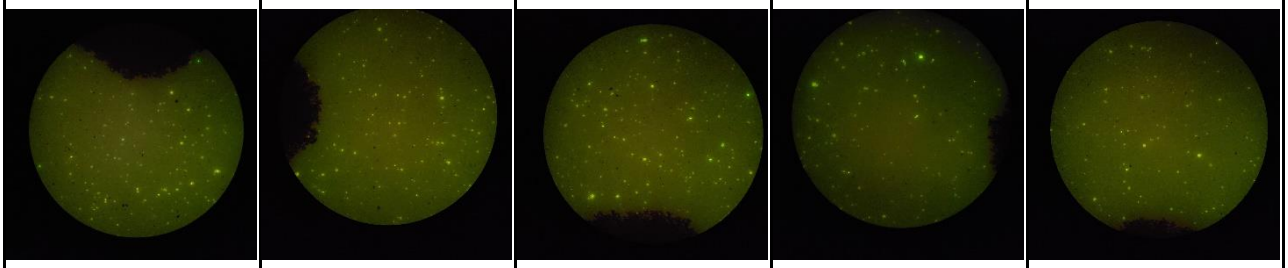				
1119W2	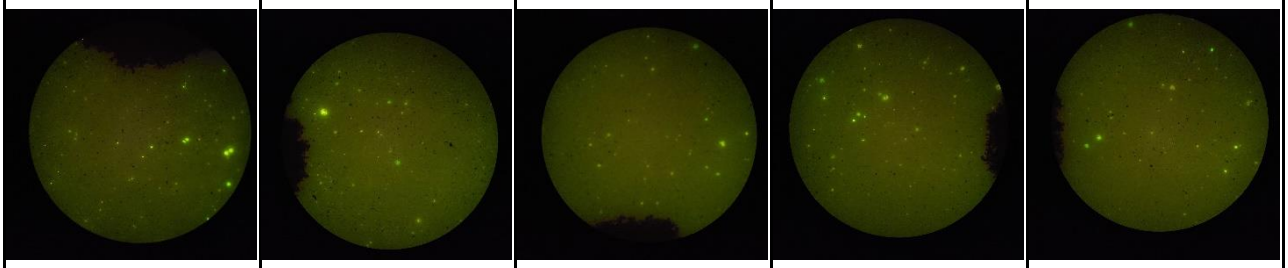				
1119W3	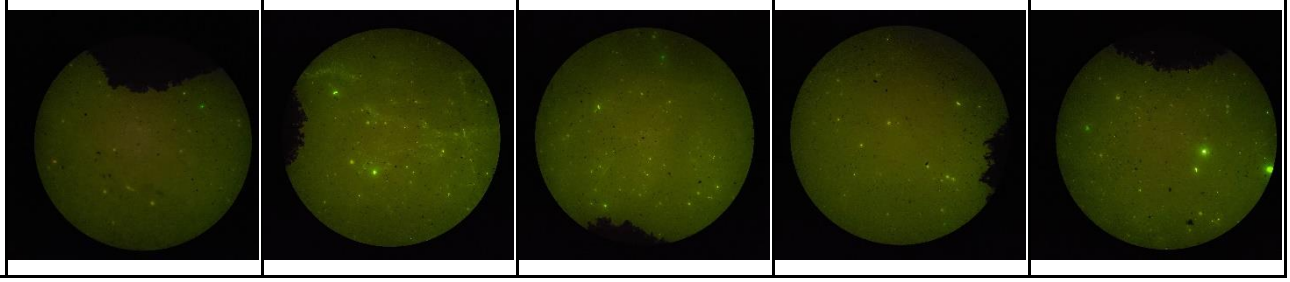				

Table I.4 Post-Decontamination “Dirty” Fabric Reaerosolization Trials Sample Photographs

Samp ID	Position 1	Position 2	Position 3	Position 4	Position 5
1116P1	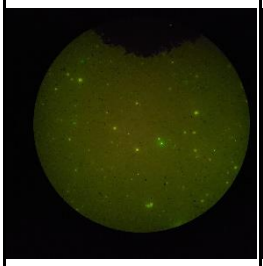	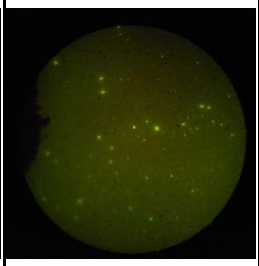	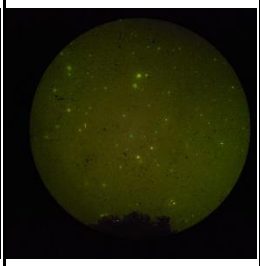	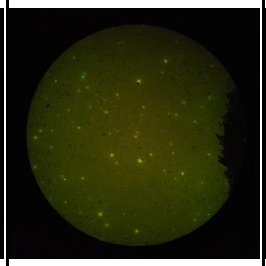	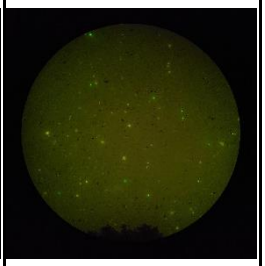
1117P1	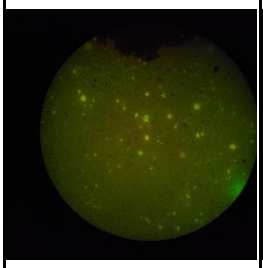	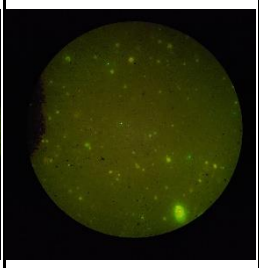	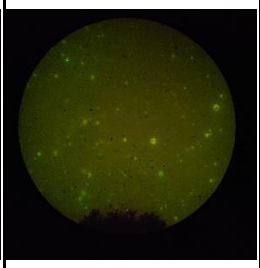	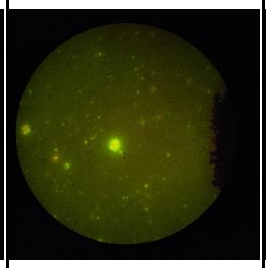	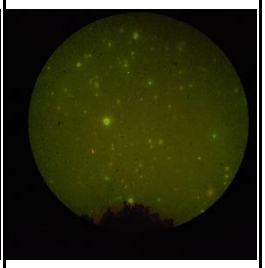
1117P2	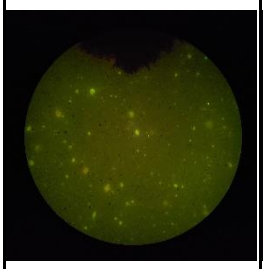	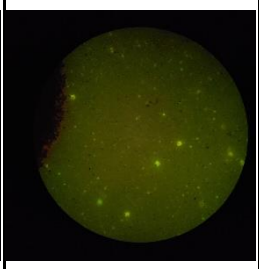	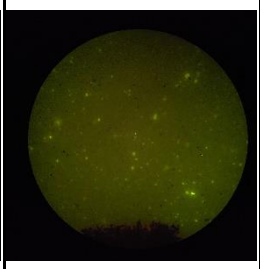	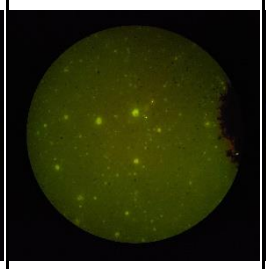	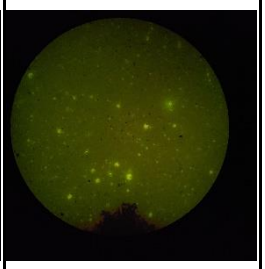
1117P3	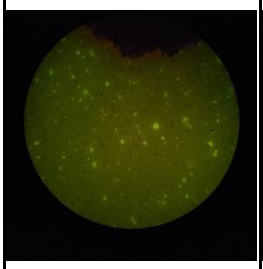	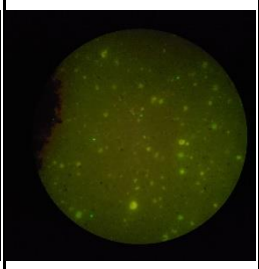	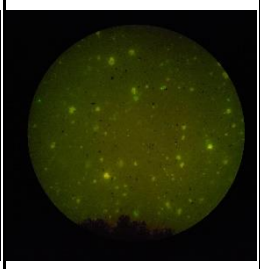	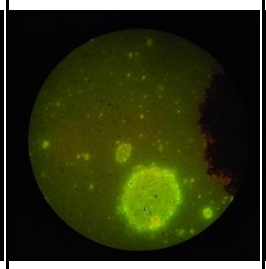	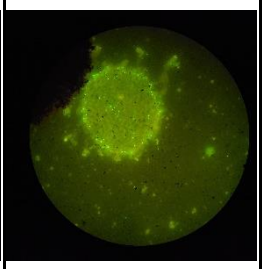
1118P1	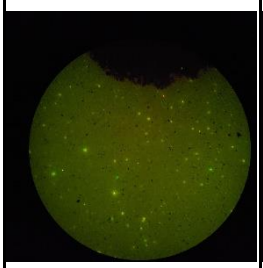	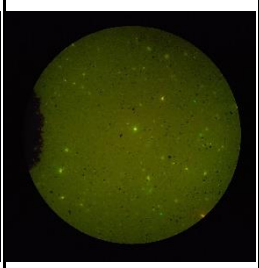	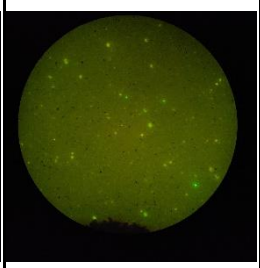	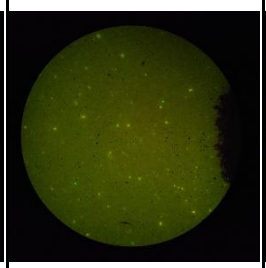	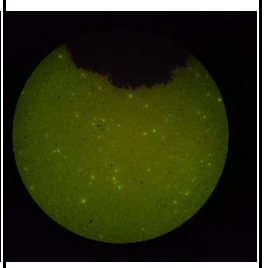
1118P2	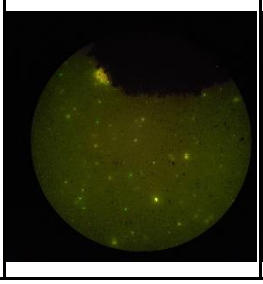	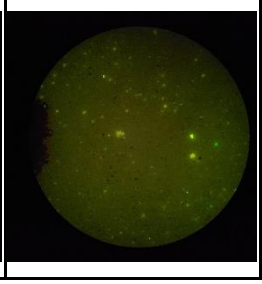	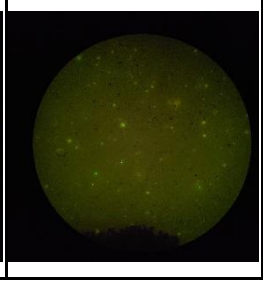	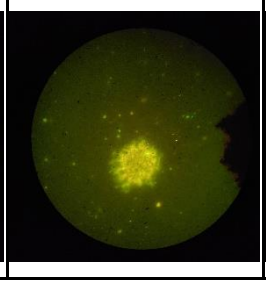	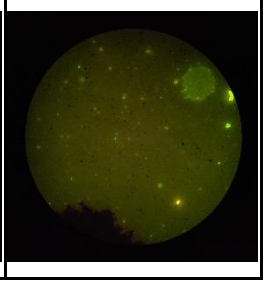

1118P3	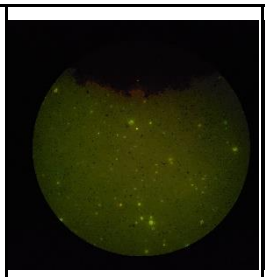	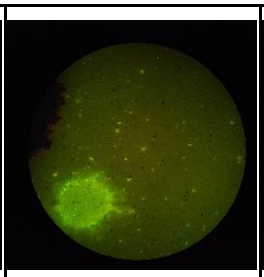	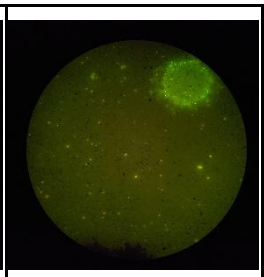	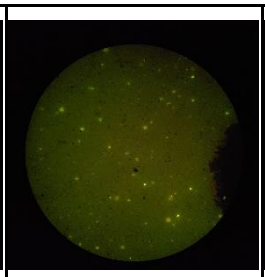	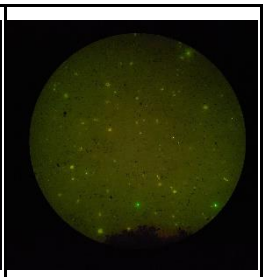
1119P1	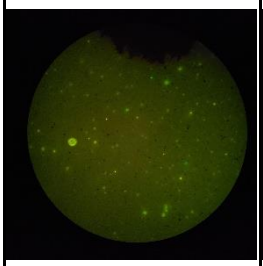	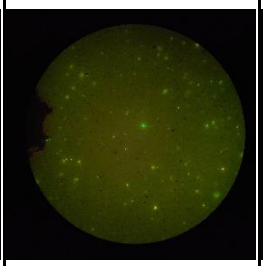	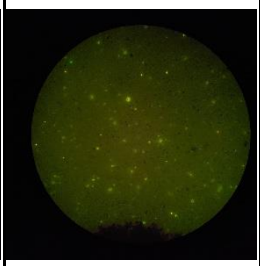	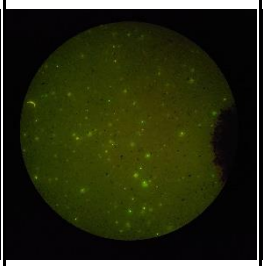	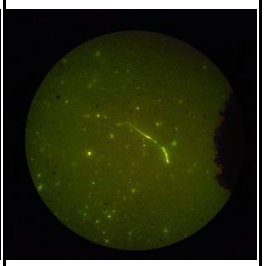
1119P2	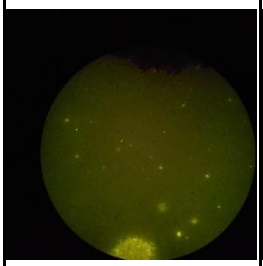	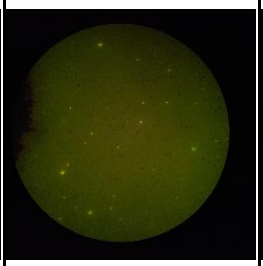	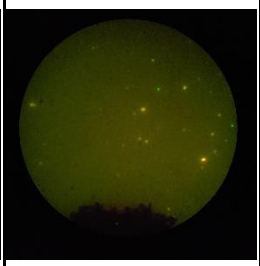	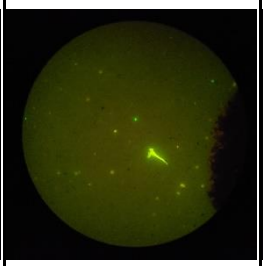	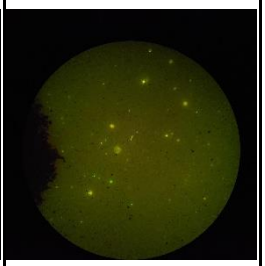
1119P3	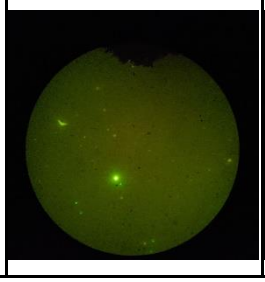	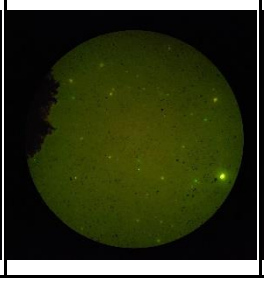	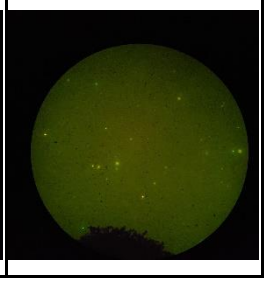	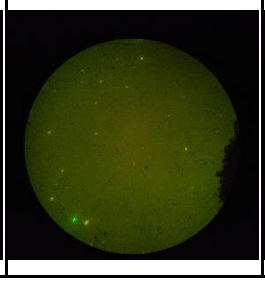	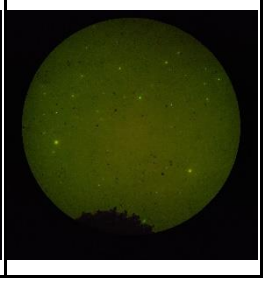

Table I.5 Clean-series Fabric Reaerosolization Trials Raw Filter Particle Counts

Sample ID	L1	L2	L3	L4	L5	Sample Avg
1104C1	2	0	1	0	2	1
1104C2	0	0	0	0	2	0.4
1104C3	0	0	1	0	0	0.2
1105C1	0	0	0	1	1	0.4
1105C2	1	0	0	0	0	0.2
1105C3	1	0	2	0	0	0.6
1108C1	1	1	0	0	1	0.6
1108C2	0	2	0	1	0	0.6
1112C1	0	2	0	1	0	0.6
1112C2	0	1	1	1	0	0.6
1112C3	0	0	2	1	0	0.6
					Total Average	0.527

Table I.6 Dirty-series Fabric Reaerosolization Trials Raw Filter Particle Counts

Sample ID	L1	L2	L3	L4	L5	Sample Avg
1104D1	4	6	6	7	9	6.4
1104D2	18	11	18	16	16	15.8
1104D3	9	6	5	8	9	7.4
1105D1	4	3	7	9	9	6.4
1105D2	42	30	38	37	42	37.8
1108D1	13	11	15	15	9	12.6
1108D2	397	437	288	360	561	408.6
1112D1	23	29	19	32	27	26
1112D2	24	26	26	22	19	23.4
1112D3	19	32	37	38	40	33.2
1104D1	4	6	6	7	9	6.4
					Total Average	57.76

Table I.7 Water-series Fabric Reaerosolization Trials Raw Filter Particle Counts

Sample ID	L1	L2	L3	L4	L5	Sample Avg
1116W1	1	1	0	0	0	0.4
1117W1	0	1	0	0	0	0.2
1117W2	0	0	1	0	1	0.4
1117W3	0	1	0	0	0	0.2
1118W1	1	1	2	1	1	1.2
1118W2	0	0	0	0	2	0.4
1118W3	0	0	1	2	2	1
1119W1	1	1	2	0	0	0.8
1119W2	0	0	0	0	2	0.4
1119W3	1	2	1	1	1	1.2
1116W1	1	1	0	0	0	0.4
					Total Average	0.62

Table I.8 Post-Decontamination-series Fabric Reaerosolization Trials Raw Filter Particle Counts

Sample ID	L1	L2	L3	L4	L5	Sample Avg
1116P1	6	4	6	7	12	7
1117P1	3	7	4	3	3	4
1117P2	2	2	1	0	1	1.2
1117P3	5	5	3	71	140	44.8
1118P1	7	4	5	4	4	4.8
1118P2	9	9	4	13	12	9.4
1118P3	5	44	41	0	6	19.2
1119P1	4	9	2	8	4	5.4
1119P2	5	2	3	3	5	3.6
1119P3	4	7	6	1	4	4.4
1116P1	6	4	6	7	12	7
					Total Average	10.38

APPENDIX II: Additional Methodology Explored in the Development of this Thesis

There was a different approach that was explored during the development of this study, that was ultimately not utilized in its final version. For the sake of documentation for future studies, this approach will be briefly described here.

Use of Optical Particle Counter to Count Reaerosolized Particles

One of the main approaches that were explored for a long time was the use of the optical particle counter (OPC) to count the amount of reaerosolized particles above the contaminated swatch. The basic setup was very similar to the one pictured in Figure 9. During pilot studies, trials were conducted filling the Collison nebulizer with deionized (DI) water, as well as the PSL solution. The results from these trials showed a clear difference in the concentration of 1 µm particles per minute between DI water and the PSL solution trials, shown below in Figure II.1, where the DI water line (in blue) stays near zero, and the PSL solution line (in orange) shows a drastic increase in particle count over time.

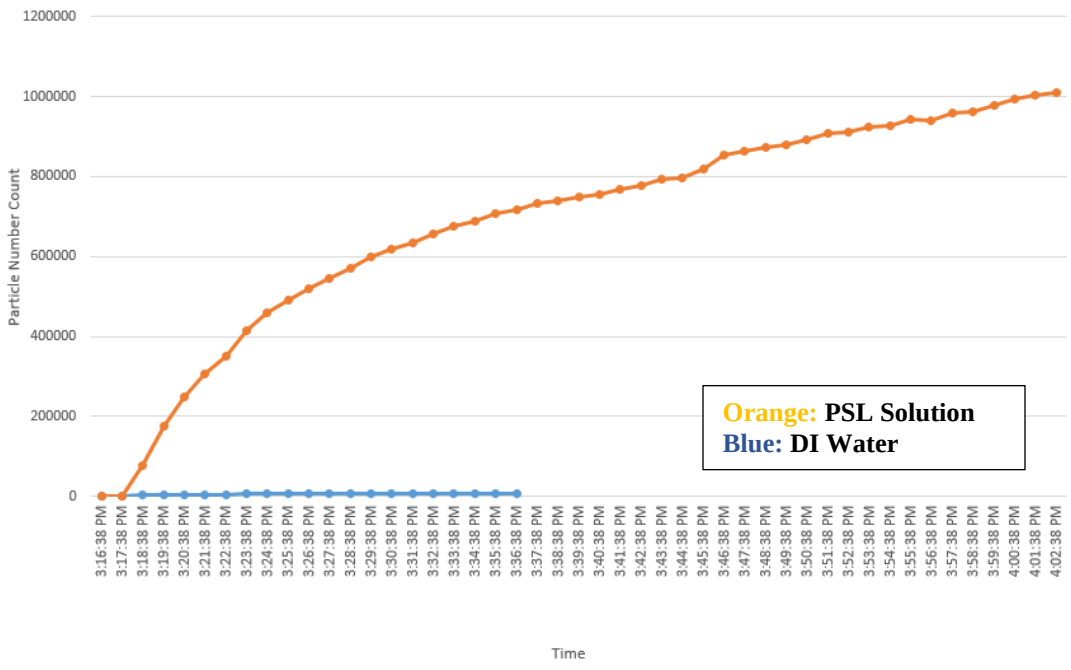

Figure II.1: Pilot Study #3, OPC 1 µm Count vs Time (DI water vs PSL Solution)

For reaerosolization trials, the setup was the same, except that the Collison nebulizer would not be attached to the aerosol chamber. The OPC was set to sample the air inside the chamber for 1 minute intervals, at a flow rate of 2.82 L/min. Meanwhile, the reaerosolization methodology was largely the same as described in this study, where the swatch (clean or contaminated) was placed on the laboratory shaker and vibrated for 30 minutes. In early trials, there appeared to be a difference between control and experimental trials. However, the variability was significant between trials – even for control samples. As shown below in Figure II.2, samples using only clean trials showed a variation after 30 minutes from as low as ~1000 particles per minute, to as high as ~4000 particles per minute.

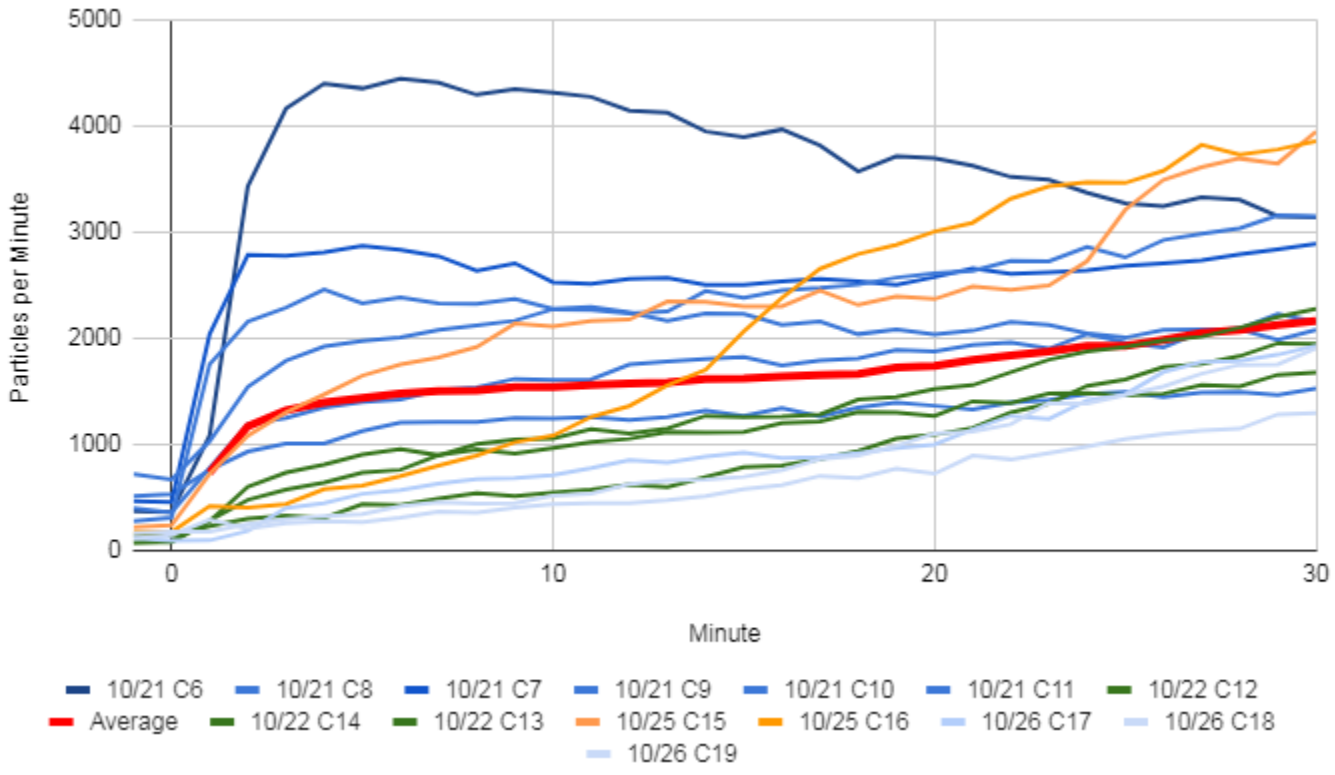

Figure II.2: Clean Swatch Results, Particles per Minute vs. Time.

In the above figure, the legend represents the sample IDs, which are colored by day. It can also be observed that the trend lines are roughly clumped by color, ergo day. This trend indicated that perhaps the natural background level of 1 µm particles in the chamber varied day by day, even after evacuating the chamber using the MURPHEE exhaust ventilation system. This was further supported by reviewing laboratory observation notes, where on days other work was be conducted in the vicinity of the MURPHEE chamber – such as mechanical grinding, sawing, operating forklifts, opening the garage door for deliveries, etc. – the background level of 1 µm particles was also higher. This trend also exhibited itself in the experimental (or dirty) trials.

Ultimately, after collecting a large number of 30 minute trials for both clean and contaminated swatches, the particles per minute counted by the OPC were averaged, and compared over time. As shown below in Figure II.3, there was very little difference in the particle per minute counts for the dirty and clean trials over time.

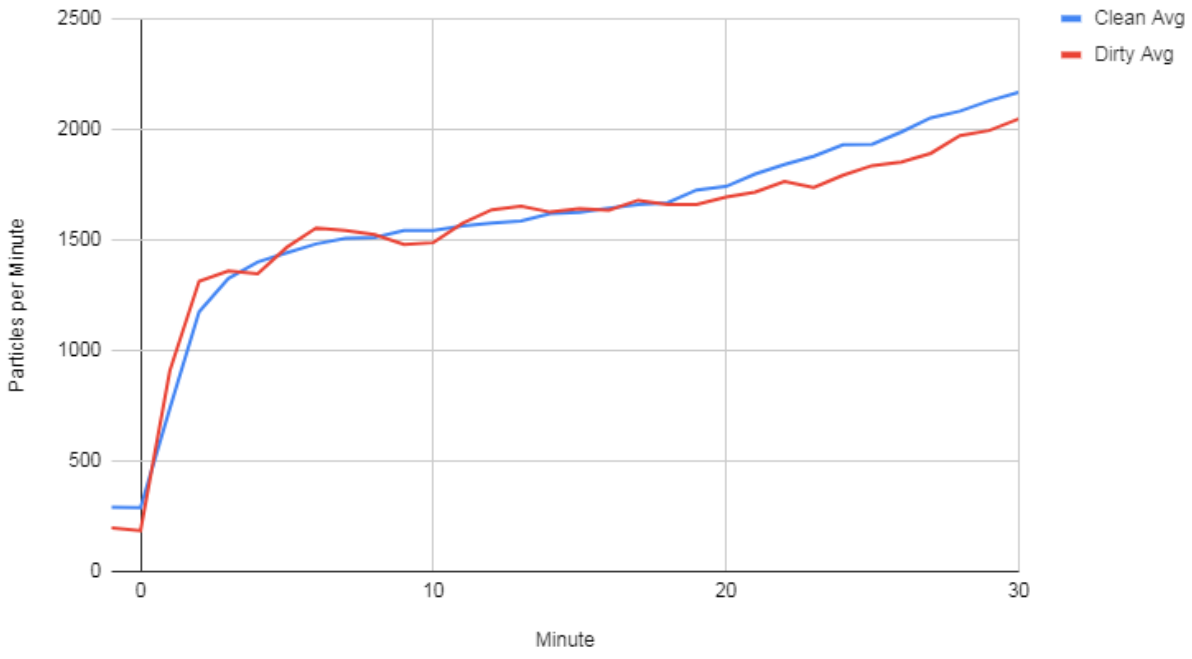

Figure II.3: Clean Average vs Dirty Average, Particles per Minute vs Time

The biggest issue with using the OPC as the means by which to count PSL spheres is that the OPC can only discern particle size; it cannot perform specific speciation of particles. That is to say, the trend observed in Figure II.3 did not mean that reaerosolization was *not* occurring, but rather that the background particles present in the chamber far outnumbered the amount of reaerosolized PSL spheres, such that the OPC was not able to provide an accurate count of reaerosolized PSL spheres.

Thus, the direct-reading OPC approach was rejected in favor of air sampling and visual microscopy counting techniques. Although sampling and using the microscope took longer, visual techniques provide a greater degree of confidence in confirming that the counted reaerosolized particles – be they surrogate PSL spheres or actual bioaerosol agents – are the target of the study, and not background noise.

Bibliography

Brown, M. J., Crockett, K., Daniel, W. B., Layshock, J. A., Pearson, B., Van Cuyk, S., & Omberg, K. M. (n.d.). Biological Reaerosolization: Material Threat or Myth? *5th National Biothreat Conference*.

Carrera, M., Zandomeni, R. O., Fitzgibbon, J., & Sagripanti, J.-L. (2007). Difference between the spore sizes of bacillus anthracis and other bacillus species. *Journal of Applied Microbiology*, 102(2). https://doi.org/10.1111/j.1365-2672.2006.03111.x

Carrera, M., Zandomeni, R. O., & Sagripanti, J.-L. (2008). Wet and dry density of bacillus Anthracis and other bacillus species. *Journal of Applied Microbiology*, *105*(1), 68–77. https://doi.org/10.1111/j.1365-2672.2008.03758.x

Chapman, J. M. (2021). Re-Aerosolization of Dense Metal Oxide Simulating Radiological Contamination from Military Clothing (thesis).

Chilcott, R. P., Larner, J., Durrant, A., Hughes, P., Mahalingam, D., Rivers, S., Thomas, E., Amer, N., Barrett, M., Matar, H., Pinhal, A., Jackson, T., McCarthy-Barnett, K., & Reppucci, J. (2019). Evaluation of US federal guidelines (primary response incident scene management [prism]) for mass decontamination of casualties during the initial operational response to a chemical incident. *Annals of Emergency Medicine*, 73(6), 671–684. https://doi.org/10.1016/j.annemergmed.2018.06.042

D'Amelio, E., Gentile, B., Lista, F., & D'Amelio, R. (2015). Historical evolution of human anthrax from occupational disease to potentially global threat as bioweapon. *Environment International*, *85*, 133–146. https://doi.org/10.1016/j.envint.2015.09.009

Davids, D. E., & Lejeune, A. R., Secondary Aerosol Hazard in the Field (U) (1981).

Dembek, Z. F. (2007). Medical aspects of biological warfare. Borden Institute, Walter Reed Army Medical Center.

Ellis, A., Edwards, R., Saunders, M., Chakrabarty, R. K., Subramanian, R., van Riessen, A., Smith, A. M., Lambrinidis, D., Nunes, L. J., Vallelonga, P., Goodwin, I. D., Moy, A. D., Curran, M. A., & van Ommen, T. D. (2015). Characterizing black carbon in rain and ice cores using coupled tangential flow filtration and transmission electron microscopy. *Atmospheric Measurement Techniques*, 8(9), 3959–3969. https://doi.org/10.5194/amt-8-3959-2015

Hinds, W. C. (1999). Aerosol technology: Properties, behavior, and measurement of airborne particles. Wiley.

Jernigan, D. B., Raghunathan, P. L., Bell, B. P., Brechner, R., Bresnitz, E. A., Butler, J. C., Cetron, M., Cohen, M., Doyle, T., Fischer, M., Greene, C., Griffith, K. S., Guarner, J., Hadler, J. L., Hayslett, J. A., Meyer, R., Petersen, L. R., Phillips, M., Pinner, R., … Gerberding, J. L. (2002). Investigation of bioterrorism-related anthrax, United States,

2001: Epidemiologic findings. *Emerging Infectious Diseases*, *8*(10), 1019–1028. https://doi.org/10.3201/eid0810.020353

Jończyk-Matysiak, E., Kłak, M., Weber-Dąbrowska, B., Borysowski, J., & Górski, A. (2014). Possible use of bacteriophages active Against bacillus Anthracis and other b. Cereus group members in the face of a bioterrorism threat. *BioMed Research International*, 2014, 1–14. https://doi.org/10.1155/2014/735413

J. Byers, R. (2013). Transfer and reaerosolization of biological contaminant following field technician servicing of an aerosol sampler. *Journal of Bioterrorism & Biodefense*, *01*(S3). https://doi.org/10.4172/2157-2526.s3-011

Keim, M., & Kaufmann, A. F. (1999). Principles for emergency response to bioterrorism. *Annals of Emergency Medicine*, *34*(2), 177–182. https://doi.org/10.1016/s0196-0644(99)70227-1

Koenig, K. L., Boatright, C. J., Hancock, J. A., Denny, F. J., Teeter, D. S., Kahn, C. A., & Schultz, C. H. (2008). Health Care Facility-based decontamination of victims exposed to chemical, biological, and Radiological Materials. *The American Journal of Emergency Medicine*, *26*(1), 71–80. https://doi.org/10.1016/j.ajem.2007.07.004

Lake, W., Divarco, S., & Schulze, P. (2013). Guidelines for Mass Casualty Decontamination During an HAZMAT/Weapon of Mass Destruction Incident: Volumes I and II. *U.S. Army Chemical Biological, Radiological and Nuclear School*.

Layshock, J. A., Pearson, B., Crockett, K., Brown, M. J., Van Cuyk, S., Daniel, W. B., & Omberg, K. M. (2012). Reaerosolization of bacillus spp. in outdoor environments: A review of the experimental literature. *Biosecurity and Bioterrorism: Biodefense Strategy, Practice, and Science*, *10*(3), 299–303. https://doi.org/10.1089/bsp.2012.0026

Lemmer, G. P. (2020). Survey of Airflow Around a Heated Manikin as a Simulated Aeromedical Evacuation Patient on a Litter With Computational Fluid Dynamics Models (thesis).

Paton, S., Thompson, K.-A., Parks, S. R., & Bennett, A. M. (2015). Reaerosolization of spores from flooring surfaces to assess the risk of dissemination and transmission of infections. *Applied and Environmental Microbiology*, *81*(15), 4914–4919. https://doi.org/10.1128/aem.00412-15

Parkhomchuk, E. V., Gulevich, D. G., Taratayko, A. I., Baklanov, A. M., Selivanova, A. V., Trubitsyna, T. A., Voronova, I. V., Kalinkin, P. N., Okunev, A. G., Rastigeev, S. A., Reznikov, V. A., Semeykina, V. S., Sashkina, K. A., & Parkhomchuk, V. V. (2016). Ultrasensitive detection of inhaled organic aerosol particles by accelerator mass spectrometry. *Chemosphere*, 159, 80–88. https://doi.org/10.1016/j.chemosphere.2016.05.078

Pottage, T., Goode, E., Wyke, S., & Bennett, A. M. (2014). Responding to biological incidents — what are the current issues in remediation of the contaminated environment? *Environment International*, *72*, 133–139. https://doi.org/10.1016/j.envint.2014.01.018

Latex bead technical overview. Thermo Fisher Scientific - US. (n.d.). Retrieved January 16, 2022, from https://www.thermofisher.com/us/en/home/life-science/cell-analysis/qdots-microspheres-nanospheres/idc-surfactant-free-latex-beads/latex-bead-technical-overview.html

Schulze, P., & Lake, W., Guidelines for mass casualty decontamination during a hazmat/weapon of mass destruction incident. volumes 1 and 2 (2008). Aberdeen Proving Ground, MD; U.S. Army Chemical Biological, Radiological and Nuclear School and U.S. Army Edgewood Chemical Biological Center.

Smith, S. D., Burch, D. S., & Fouts, B.L. AFRL-RH-WP-TR-2019-0086: Quantifying Patient Vibration Patterns During Aeromedical Evacuation Aboard the C-130H (2019).

Smith, S. D., Dooley, C. J, AFRL-RH-WP-TR-2020-0057: Quantifying Patient Vibration Patterns During Ambulance Bus (AMBUS) Ground Transport (2020).

Smith, S. D., Dooley, C. J., & Burch, D. S., AFRL-RH-WP-TR-2021-0016: Quantifying Patient Vibration Patterns During C-130J Aeromedical Evacuation (AE) (2021).

Stanek, S., Saunders, D., Alves, D., Burke, C., Cardile, A., Cieslak, T., Erwin, C., Gibson, K.c Kortepeter, M., Okwesili, A., Person, B., Poli, M., Shaecher, K., & Taylor, C. (2020). *Medical Management of Biological Casualties: Handbook* (9th ed.). U.S. Army Medical Research Institute of Infectious Diseases.

Thornbury, D., Goray, M., & van Oorschot, R. A. H. (2021). Transfer of DNA without contact from used clothing, pillowcases and towels by shaking agitation. Science & *Justice*, 61(6), 797–805. https://doi.org/10.1016/j.scijus.2021.10.005

Titus, BS, E., Lemmer, BS, G., Slagley, PhD, J., & Eninger, PhD, R. (2019). A review of CBRN topics related to military and civilian patient exposure and decontamination. *American Journal of Disaster Medicine*, *14*(2), 137–149. https://doi.org/10.5055/ajdm.2019.0324

Toth, D. J., Gundlapalli, A. V., Schell, W. A., Bulmahn, K., Walton, T. E., Woods, C. W., Coghill, C., Gallegos, F., Samore, M. H., & Adler, F. R. (2013). Quantitative models of the dose-response and time course of inhalational anthrax in humans. *PLoS Pathogens*, 9(8). https://doi.org/10.1371/journal.ppat.1003555

United States, F. B. of I. (2016, May 17). *Amerithrax or anthrax investigation*. Federal Bureau of Investigations Government Website. Retrieved November 21, 2021, from https://www.fbi.gov/history/famous-cases/amerithrax-or-anthrax-investigation.

United States, Department of Defense, ATP 4-02.7: Multi-Service Tactics, Techniques, and Procedures for Treatment of Biological Warfare Agent Casualties (2016).

United States, Department of Defense, ATP 4-02.84: Multi-Service Tactics, Techniques, and Procedures for Treatment of Biological Warfare Agent Casualties (2019). Retrieved from https://armypubs.army.mil/epubs/DR_pubs/DR_a/pdf/web/ARN19960_ATP%204-02x84%20FINAL%20WEB.pdf.

Villa, Mario & Hubert, Geneviève & Lima, Simone & Kauffer, Edmond & Héry, Michel. (1994). Occupational exposure during asbestos removal operations. *Journal of the international society for respiratory protection.* 12. 7-14.

REPORT DOCUMENTATION PAGE

Form Approved
OMB No. 074-0188

1. REPORT DATE *(DD-MM-YYYY)*	**2. REPORT TYPE**	
24-03-2022	Master's Thesis	August 2020 – March 2022

TITLE AND SUBTITLE

Development of a Methodology for the Quantification of Reaerosolization of a Biological Contaminate Surrogate Particle from Military Uniform Fabric

5a. CONTRACT NUMBER

5b. GRANT NUMBER
2020-055R

5c. PROGRAM ELEMENT NUMBER

6. AUTHOR(S)

Cooksey, George, D., Captain, USAF, BSC

5d. PROJECT NUMBER

5e. TASK NUMBER

5f. WORK UNIT NUMBER

7. PERFORMING ORGANIZATION NAMES(S) AND ADDRESS(S)

Air Force Institute of Technology
Graduate School of Engineering and Management (AFIT/EN)
2950 Hobson Way, Building 640
WPAFB OH 45433-7765

8. PERFORMING ORGANIZATION REPORT NUMBER

AFIT-ENV-MS-22-M-187

9. SPONSORING/MONITORING AGENCY NAME(S) AND ADDRESS(ES)

711 Human Performance Wing/RHBAF
2510 Fifth Street, Wright-Patterson AFB, OH 45433
(937) 938- 3761
ATTN: Maj Michael Horenziak; michael.horenziak@us.af.mil

10. SPONSOR/MONITOR'S ACRONYM(S)

711 HPW/RHBAF

11. SPONSOR/MONITOR'S REPORT NUMBER(S)

12. DISTRIBUTION/AVAILABILITY STATEMENT

DISTRUBTION STATEMENT A. APPROVED FOR PUBLIC RELEASE; DISTRIBUTION UNLIMITED.

13. SUPPLEMENTARY NOTES

14. ABSTRACT

During a mass casualty medical evacuation after a bioaerosol attack, a decontamination method is needed that is effective at both decontamination and preventing the secondary hazard of biological particles reaerosolizing from contaminated clothing. However, neither the efficacy of current decontamination methods nor the risk of biological particle reaerosolization is significantly explored in existing literature. The goals of this thesis were to develop a repeatable methodology to quantify the reaerosolization of a biological contaminate off Airman Battle Uniform (ABU) fabric swatches, and to test the efficacy of one decontamination method (high-volume, low-pressure water) using 1 µm polystyrene latex (PSL) spheres as a surrogate. Four major methodologies were developed: Contamination using a Collison Nebulizer; Reaerosolization using a laboratory mixer and collection using an air pump and inhalable air sampler with a polyvinyl chloride (PVC) filter; Decontamination using a gravity-fed water shower; and Quantification using ultraviolet (UV) microscopy techniques via both human eye and computer techniques. All results for control samples showed little to no presence of PSL sphere-like particles, while the experimental trials showed a ~73% reduction in reaerosolization before and after decontamination via water, at the 99% confidence level (p-value = 0.0081), along with a change in deposition patterns from aerosol-like (before decontamination) to droplet-like (after decontamination).

15. SUBJECT TERMS

CBRN, decontamination, bioaerosol, fluorescent, PSL, vibration, image analysis, method development

16. SECURITY CLASSIFICATION OF:			**17. LIMITATION OF ABSTRACT**	**18. NUMBER OF PAGES**	**19a. NAME OF RESPONSIBLE PERSON**
a. REPORT	**b. ABSTRACT**	**c. THIS PAGE**			Dr. Jeremy Slagley, AFIT/ENV
U	**U**	**U**	**UU**	121	**19b. TELEPHONE NUMBER** *(Include area code)* (937) 255-3636, ext 4632 (NOT DSN) (Jeremy.slagley@afit.edu)

Standard Form 298 (Rev. 8-98)
Prescribed by ANSI Std. Z39-18